Numerical Analysis of Two-Stroke Engine with Direct Injection and Jet Ignition

A thesis submitted in fulfilment of the requirements for the degree of

Master of Engineering by Research

Shuheng Jiang

Bachelor of Engineering

School of Aerospace Mechanical and Manufacturing Engineering

College of Science Engineering and Health

RMIT University

September 2015

ABSTRACT

This thesis is carried out to evaluate the combustion evolution and the engine performance parameters of a two-stroke engine with direct injection and jet ignition.

Two-stroke engines are lightweight, simple to construct, high power- to-weight ratios and offer low cost to manufacture. The main problems with two-stroke engines are emissions and low fuel-efficiency.

This research used a two-stroke engine with crankcase scavenging. It also adopted an exhaust reed valve and lamellar intake, accommodating a high pressure direct injector as used in the latest two-stroke gasoline engines. The jet ignition device is replacing traditional spark plug. The main chamber and jet ignition use hydrogen as fuel. The jet ignition instrument is a pre-chamber accommodating a high-pressure injector operated with hydrogen fuel, and an 8 mm racing spark plug. The pre-chamber inside the jet ignition device is connected to the main combustion chamber through calibrated orifices. Lubrication is performed by selective oil injection where needed, rather than oil mixed with fuel.

A two-stroke engine CAD model has been designed by using 3D CAD software SolidWorks. Included are a jet ignition device, fuel injector, gas exchange system, combustion systems, lubricating system and other major engine components. The CFD simulations were performed in Star CCM+ to analyse the combustion evolution with hydrogen fuel in the cylinder from exhaust port closure to exhaust port opening. The obtained combustion rate results from CFD simulation were transferred into 1D

software to investigate and analyse the performance of the two-stroke engine.

This research has shown good modelling results with efficiencies well in excess of 30% in the area of best engine operation, and reduced energy penalties when changing load and speed. The solution offers the opportunity to produce an efficient alternative to four- stroke engines with improved power density running an alternative fuel with better combustion properties and reduced pollution than traditional diesel and gasoline fuels.

DECLARATION

I certify that except where due acknowledgement has been made, the work is that of the author alone; the work has not been submitted previously, in whole or in part, to qualify for any other academic award; the content of the thesis/project is the result of work which has been carried out since the official commencement date of the approved research program; any editorial work, paid or unpaid, carried out by a third party is acknowledged; and, ethics procedures and guidelines have been followed.

Shuheng Jiang

September 2015

ACKNOWLEDGEMENTS

The author wishes to express sincere appreciation to his supervisor Professor Albert Parker and joint senior supervisor Professor Reza Nakhaie Jazar for the continuous support and assistance during this research.

Thanks also to my colleges Siti Khalijah and Bing Jie Zhang for their stimulating discussions and their valuable input.

Finally, the author would like to thank Peter Ewing for his professional advice and help regarding CFD simulation.

NOMENCLATURE

a	Thermal Diffusivity
λ	Relative Air-to-Fuel Ratio: Actual/Stoichiometric
φ	Equivalence Ratio ($1/\lambda$)
A	Surface area
AFR	Air-to-Fuel Ratio
AFR_s	Stoichiometric Air to Fuel Ratio
BTDC	Before Top Dead Centre
BSFC	Brake specific fuel consumption
BMEP	Brake Mean Effective Pressure
CA	Crank Angle
CAD	Computer aided design
CFD	Computational Fluid Dynamics
CH_4	Methane
CNG	Compressed Natural Gas
CO	Carbon Monoxide

CO_2	Carbon Dioxide
CR	Compression Ratio
DI	Direct Injection
EOI	End Of Injection
EPO	Exhaust port open
EPC	Exhaust port close
FEM	Finite Element Method
GDI	Gasoline Direct Injection
h_c	Heat Transfer Coefficient
H	Hydrogen Radical
H2	Hydrogen
HAJI	Hydrogen Assisted Jet Ignition
HC	Hydrocarbon
HCCI	Homogeneous Charge Compression Ignition
IC	Internal Combustion
IPO	Intake port open
IPC	Intake port close
IMEP	Indicated Mean Effective Pressure
ISFC	Indicated Specific Fuel Consumption

LPG	Liquefied Petroleum Gas
m	Mass
MAP	Manifold Absolute Pressure
MBR	Mass Burn Rate
MC	Main Chamber
MFB	Mass Fraction Burned
O_2	Oxygen
OH	Hydroxyl Radical
P	Pressure
PC	Prechamber
SI	Spark Ignition
SOI	Start Of Injection
ST	Spark Timing
t	Time
T	Temperature
TDC	Top Dead Centre
V	Volume
VVT	Variable Valve Timing

CONTENTS

LIST OF FIGURES

LIST OF TABLES

CHAPTER 1

1.INTRODUCTION

A two-stroke engine is a type of internal combustion (IC) engine that completes the power cycle in one crankshaft revolution, which is half that number in comparison with four-stroke engine.

Spark Ignition (SI) two-stroke engines are commonly found in the small power tools such as chain saw and scooter. While Compression Ignition (CI) engines are very commonly used in large machines such as marine propulsion and electricity generator. Spark ignition engine works on Otto cycle and uses gasoline as the fuel. It is smaller in size and has lower compression ratio than the CI engine. Compression ignition engine work on diesel cycle and uses diesel as the fuel. This thesis is mainly focus on the studying of small SI two-stroke engine.

Two-stroke engines are simple, lighter, higher power- to -weight ratio and offer a low manufacturing cost. It is able to generate a 1.6~1.7 times higher power than a same displacement four-stroke engine (Blair 1989). It is also possible to have lower rotating forces with a small number of cylinders.

The disadvantages of two- stroke engines are emissions and efficiency. A clear disadvantage of a two -stroke engine is the gas exchange process, especially in the cheapest design with crankcase scavenging. The intake process has low efficiency, mostly due to shortness in the effective-strokes. Mean effective pressure and efficiency are also low, mostly due to the long opening of the exhaust.

Pollution has also played a dominant role recently for the reduced popularity of small two- stroke engine with crankcase scavenging. This two -stroke engine mixes fuel and engine oil for lubrication, and this further increase the already higher emissions than a four-stroke engine. The main pollution of two- stroke engines with crank case scavenging comes from the lubrication oil and mainly from charge exchange period when exhaust and transfer port are opened. With this simple design, they do not have a dedicated lubricating system, and the oil burned in the combustion chamber causes exhaust pollution.

1.1 CHALLENGES OF TWO-STROKE ENGINES

Two-stroke engines have excellent power-to-weight ratio, simple design and are light weight in comparison with four-stroke engines. On the other hand, the disadvantages with traditional two-stroke engines are high pollutant emission, respectively high BSFC that limits these engines to be used only in applications where the appliance is not operated frequently and high power-to-weight ratio is necessary. Scavenging, lubrication and low-efficiency are the three main challenges for two-stroke engine.

1.1.1 Scavenging

Gupta (1999) conclude that the scavenging is a process of replacing the products of combustion out of the previous power stroke and charging fresh air or air/fuel mixture in the next cycle. This process must be accomplished in a very duration between the expansion stroke and exhaust stroke.

Scavenging process has an enormous effectiveness on two-stroke engine efficiency. Bad scavenging leads to low mean indicated pressure. If the scavenging is insufficient, it results in high specific fuel consumption. In addition, bad scavenging causes the lubricating oil to become more contaminated, and it generates more pollution and increased frazzle of

cylinder wall and piston ring. Moreover, poor scavenging process leads to higher mean temperatures and heat stresses inside cylinder bore (Thipse 2008). Therefore, every improvement in scavenging process is important to engine efficiency.

1.1.2 Efficiency

Traditional spark ignition two-stroke engines are not very efficient; because the exhaust port and intake port are always open at the same time, this allows up to 30% unburned air/fuel mixture(Thipse 2008) is escaping from the exhaust port during the scavenging process.

1.1.3 Lubrication

Two-stroke engines wear a lot faster than four- stroke engines. There is no dedicated lubrication system in traditional two-stroke engine. The oil is mixed with the fuel for lubrication. The oil is burned during combustion process with the air/fuel mixture.

1.2 CURRENT AND FUTURE TWO-STROKE ENGINE TECHNOLOGIES AND SOLUTIONS

Two-stroke engines were very prominent during 20th century in applications such as motorcycles, chainsaws, outboard motors and other small-engine devices. However, the two-stroke engine has faded out for several reasons. First, and foremost, is they could not meet the increasingly tightening exhaust emission standards in most of countries. Second, they have low engine efficiency. In other words, they had worse fuel economy, which is caused by the short circuiting, as the traditional two-stroke engine transfer and exhaust port open at the same time. There is always some flow escaping from the exhaust port. In comparison with four-stroke engines, it has approximately 25 percent lower efficiency

(Blair 1989), as short circuiting can be prevented by using mechanical valves in four-stroke engines.

There are several effective technologies to overcome the two-stroke emission and fuel economy issues. Direct Fuel Injection (DFI) allows fuel to be injected directly into the combustion chamber after the cylinder's exhaust port has closed. This eliminates the two-stroke fuel short-circuiting problem, and also reduces the exhaust emission.

Recently, the addition of direct injection and some refinement of the crank case scavenging with reed valve and lamellar intake, plus precise lubrication systems have produced more fuel efficiency and less pollution in outboard and snowmobile applications.

Outboard company Yamaha with HPDI technology and Snowmobile Company Bombardier with E-TEC technology meet all emission standards and producing remarkable fuel economy over most commonly used rpm range in the engine (Ski-doo 2014; Yamaha 2013).

Snowmobile industry leading company Ski-Doo's third generation of advanced two-stroke E-TEC and Power T.E.K technologies enable snowmobiles to deliver a cleaner and higher efficiency power (Ski-doo 2014). Similarly, Yamaha's High-Pressure Direct Injection (HPDI) technology utilised on some of its outboard motors and outboard marine. These engines meet EPA emission requirements and have been extensive tested to prove its reliability (Yamaha 2013).

In addition to DI system, homogeneous charge compression ignition (HCCI) technology reduces engine emissions while simultaneously increasing engine efficiency. This can be achieved by equipping a jet ignition device. Jet ignition is a pre-chamber combustion initiation system for conventional SI engines and is replacing the standard spark plug. The jet ignition option has the advantage of faster burn rate and lean mixture (Boretti 2012). In addition, it is easier to fit the jet ignition

on the two-stroke engine spark plugs as there are no valves or camshaft on the cylinder head.

1.3 RESEARCH QUESTIONS

The research questions for this research were:

- Is there any option to improve the brake thermal engine efficiencies of two-stroke engine for transport applications?

- Is there any option to improve the part load efficiency of two-stroke engine for transport applications?

- Is it possible to reduce the emissions of pollutants and the smoke of two-stroke engines for transport applications?

1.4 RESEARCH OBJECTIVES

The research objectives for this study were:

- Investigate the performance of two stroke IC engine with direct injection and jet ignition system.

- Conduct comparative study of using direct injection and jet ignition system for two-stroke IC engines instead of conventional fuel injection and ignition systems.

1.5 OUTLINE OF THESIS

The present chapter introduces two-stroke engine's principle of operation. Compression with four-strokes and their advantages of simple components, low-cost, high-power to weight ratio, disadvantages of low-efficiency, high fuel consumption. Direct injection and jet ignition are the potential solution to eliminate two-stroke engine efficiency issues.

Current and future technologies of two-stroke engine are briefly described in this chapter.

Chapter 2 covers a literature review of two-stroke engine history, followed by applications for motorbike and outboard motors. It discusses two different types of direct injection systems; air-assist direct injection and high pressure direct injection. Next is a literature review on jet ignition devices. Lastly, a description of current and future fuels for SI engines is discussed.

Chapter 3 describes the simulation framework, including details of CAD modelling of the two-stroke engine in SolidWorks, and the CFD model in Star CCM+. This chapter is followed by 1D and 3D modelling methodology, which includes details of modelling combustion, turbulence, flow rate calculation and engine specifications. Lastly, an overview of the injection strategies is provided.

Chapter 4 presents the simulation results from this research, including CFD results and 1D CAE results, and a discussion of each result is provided.

The final chapter summarizes the research and achievements, in addition to providing recommendations for future research regarding two-stroke engines with direct injection and jet ignition.

CHAPTER 2

2.LITERATURE REVIEW

Small spark ignition two-stroke engines have received much less investments in their development compare to four stroke engines. The two stroke engine was very common around 20th century in small displacement applications such as chain saws, outboard motors, lawn mowers, motorcycles, snowmobiles and snow blowers. Two stroke engines are still commonly used for portable, small and specialized engine applications such as, motorcycles, outboard motors, scooters, lawnmowers and dirt bikes, but their popularity has been largely reduced. The most relevant areas of development of two stroke engines for transport are non-symmetrical port timing, supercharging scavenging, dry sump, direct injection and throttle-less load control.

2.1 HISTORY

The two-stroke cycle engine is as old as the concept of the heat engine, which has served mankind for over 450 year. The two-stroke engine is mostly credited to Dugald Clark who invented it around 1880 (Inchley 2008). But the engine he designed had a separate charging cylinder. Although there were other engineers who accomplished the engine, such as creating the charging pump that is commonly attributed to Joseph Day and Frederick Cock is credited for invention of the inlet port that controlled by piston.

The environment has played a significant role for engine development and research in recent years. There were less investments and attention payed to two-stroke engines, rather than to the four-stroke engines, since they mix fuel with oil for lubrication which leads to higher emissions. Therefore, the environmental issues prevented the two-stroke engines to be developed before. However, nowadays though advanced innovative technologies the two-stroke engine emissions can be reduced and new design approaches can be developed.

2.2 DIFFERENT TWO-STROKE ENGINE DESIGN

Although the knowledge-based theory of the two-stroke engine remains the same, the construction specifics of the individual two-stroke engines differ depending on the type and applications. For example, designs can be different in a way of introducing the air/fuel mixture to the cylinder, like the cross-scavenged and loop-scavenged designs which are the basic types of two-stroke engines.

2.2.1 Cross-Scavenged Design

Alfred (2004; Roth 2004) concluded that the cross-scavenged engine has a convexity on top of the piston, which operates as a block to divert the fuel/air mixture charge upward in the cylinder as it shown in Figure 2.1. This prevents fuel to escape from the exhaust port as it is located directly across from the intake port.

Cross-scavenged engines usually come with reed valve or rotary valve, which is connected to the flywheel, as it is shown in Figure 2.2. The reed valve is a type of check valve commonly fitted in the intake track of the piston-controlled port. It has simple but highly efficient design which limits the intake flow to a single direction by opening and closing the valve's face under changing pressure. This design improves power and fuel economy and increases the power band. The rotary valve inlet port is

fixed in the crankcase which provides more space for the additional transfer port to achieve better scavenging and fuel transfer.

These valves hold the entering air/fuel mixture charge in the crankcase, so it is possible to compress the mixture when the piston moves down in the cylinder. This configuration allows piston to acts as a valve and to control the motion of charge in the exhaust, intake and transfer ports. The transfer port allows a part of the air/fuel mixture to transfer from the crankcase to the cylinder.

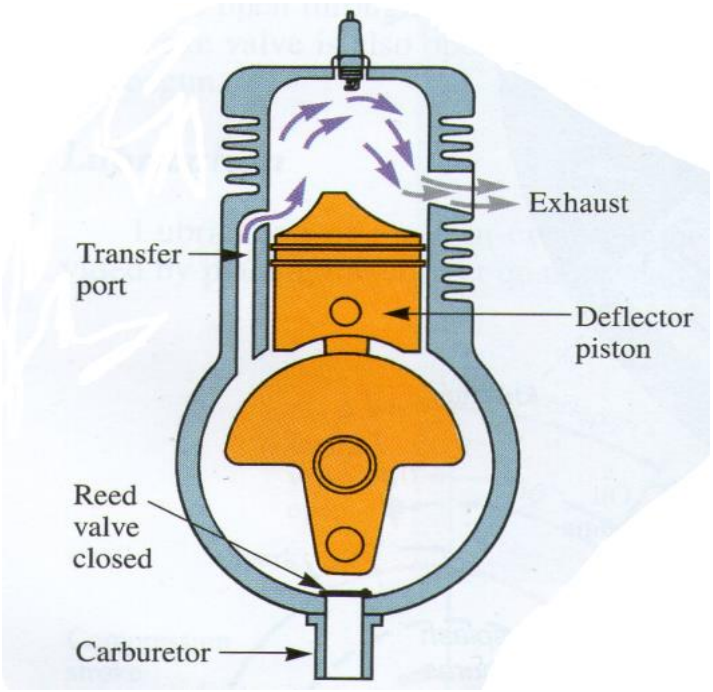

Figure 2.1 Cross Scavenged Reed Valve Design (Alfred, 2004)

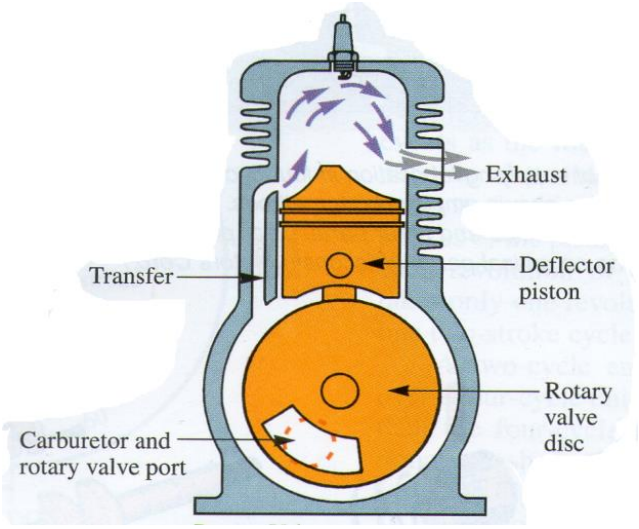

Figure 2.2 Rotary Vale Cross Scavenged (Alfred, 2004)

2.2.2 Loop Scavenged Design

Unlike cross scavenged design, loop-scavenged engine does not divert the incoming charge; it uses a slightly domed piston head to position the mixture, as it is shown in Figure 2.3. The fuel/air mixture enters the cylinder following the shape of the combustion chamber. This ordered flow helps to push out mixture from the exhaust port and allows a new charge of air/fuel mixture to access.

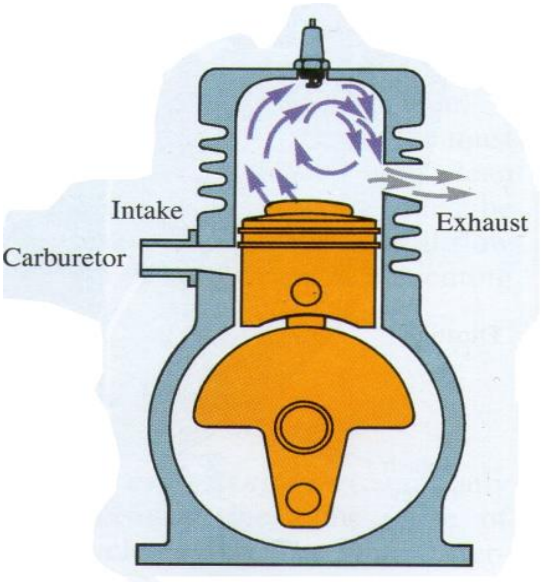

Figure 2.3 Loop Scavenged 3rd Port Design (Alfred, 2004)

2.3 APPLICATION

Two-stroke engines are relatively cheap to manufacture and operate in comparison with four-stroke engines. They have less moving components and higher power-to-weight ratio than four-stroke engines. The two-stroke engines were very common in small capacity engines around 20^{th} century. They are very suitable in applications such as lawn mowers, chain-saws, outboard motors, motor-cycles, marine propulsions and electricity generators. Two-stroke engines are much easier to start in low temperatures due to their low oil consumption and design. That is the reason why they are commonly used in snowmobiles and snow blowers. However, the main drawback of conventional two-stroke engines is that they are harmful to the environment and have louder radiated sound from exhaust pipe compare to four-stroke engines. EPA (US Environmental protection agency) has mandated and had been continuously tightening emission controls from 1978 to 2010. This policy largely impacted on traditional two-stroke engines production and the industry responded by switching to four-stroke engines which in its order reduced the amount of pollution (United States Environmental Protection Agency 2001).

The main reason of pollution from two-stroke engine is lubrication oil. Due to their simpler design, conventional two-stroke engines don't have an advanced lubricating system. Oil is mixed with fuel and burned in the combustion chamber which causes smoke and pollution problems. Consequently, four-stroke engines are replacing two-stroke engines in many applications.

Nonetheless, two-stroke engines are still commonly used for small, lightweight and specialized applications such as dirt bikes, outboard motors, high-performance racing engines and lawnmowers.

2.3.1 Motorbike

Two-stroke motorbikes are able to delivery wide range of the power band. Unfortunately, today's two-stroke motorbikes are on the wane and many models has been stopped from production because of the pollution that they cause. Yamaha, Husqvarna and KTM are the only three big companies that are still producing two-stroke motocross bikes. These dirt bikes are usually under 250cc, single cylinder, reed value. Figure 2.4 shows a typical two-stroke motorbike engine.

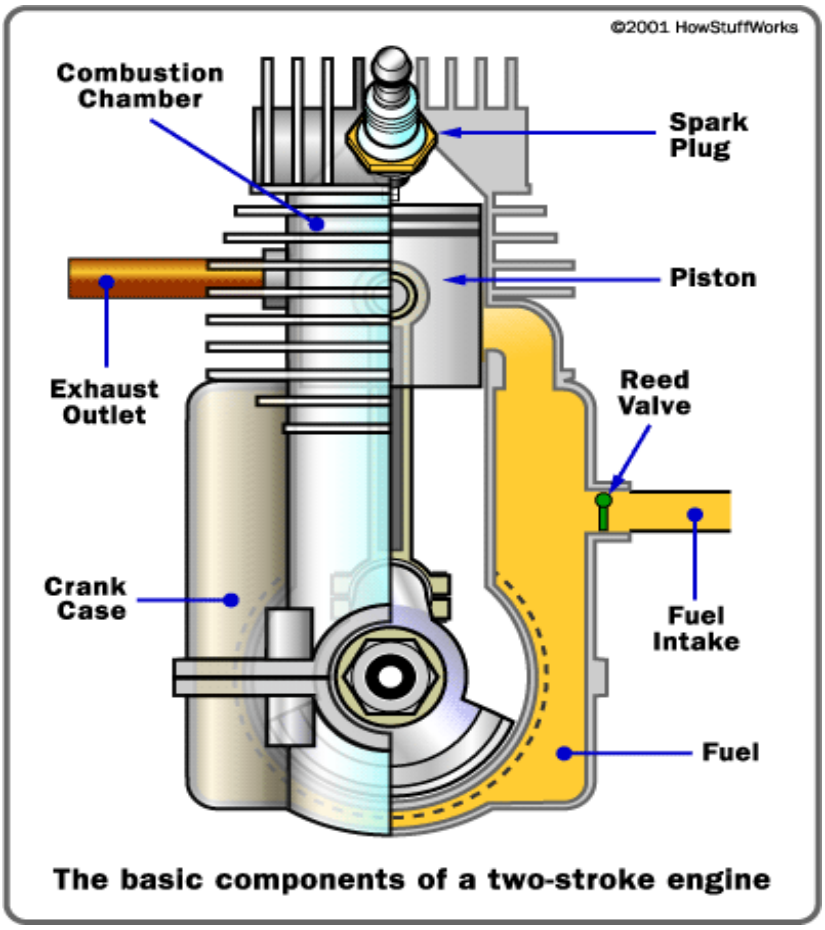

Figure 2.4 Two-stroke engine configuration (Alfred, 2004)

2.3.2 Outboard

Conventional two-stroke outboards are harmful to the environment and they are fuel inefficient. In recent years the outboards two-stroke engines have been changed: most of the conventional two-strokes engines were withdrawn and replaced by DI two-strokes engines (Marine Engine Digest 2013).

Yamaha is one of the many big outboard engine companies that offer a new generation of two-stroke engines. Yamaha has developed a two-stroke direct injection system, which utilizes a high-pressure direct injector. This system is used on the new V6 engines which helps to achieve fuel efficiency in the most commonly used speed range and meet all the emission requirements (Yamaha 2013).

Yamaha's high pressure direct injection (HPDI) features an engine control module (Figure 2.5), which regulates the HPDI System to provide greater power, fuel economy and reliability. In addition, the six individual sensors help the microcomputer to advance ignition timing and air/fuel mixture (Yamaha 2013).

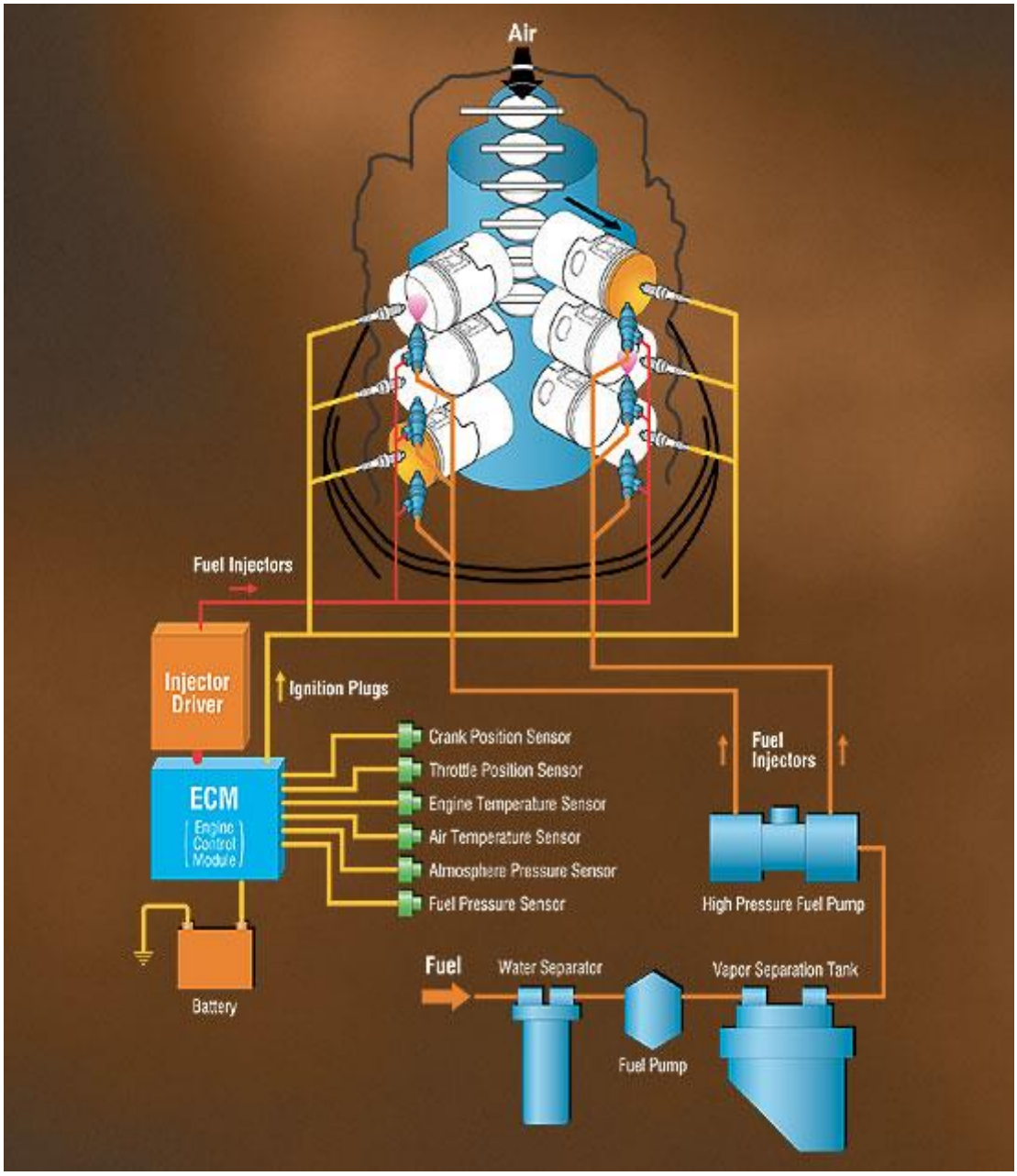

Figure 2.5 Yamaha HPDI components (2013)

The most important factor that helps Yamaha's HPDI system stands out from other outboard competitors is that the system utilizes high fuel pressure injectors that deliver up to 700 psi, while the other outboards companies use fuel injectors that can provide pressure from 90 to 250 psi. Higher pressure injectors generate better atomization and, as a result, the combustion process burns faster and the injector charges more power into the cylinder.

2.4 PORT TIMING

There are two types of port timing on two-stroke engines: symmetrical and asymmetrical ones. The timing of transfer and exhaust ports play an important role in two-stroke performance characteristics. Therefore understanding port timing is crucial to determine the power curve obtained by the engine.

2.4.1 Symmetrical port timing

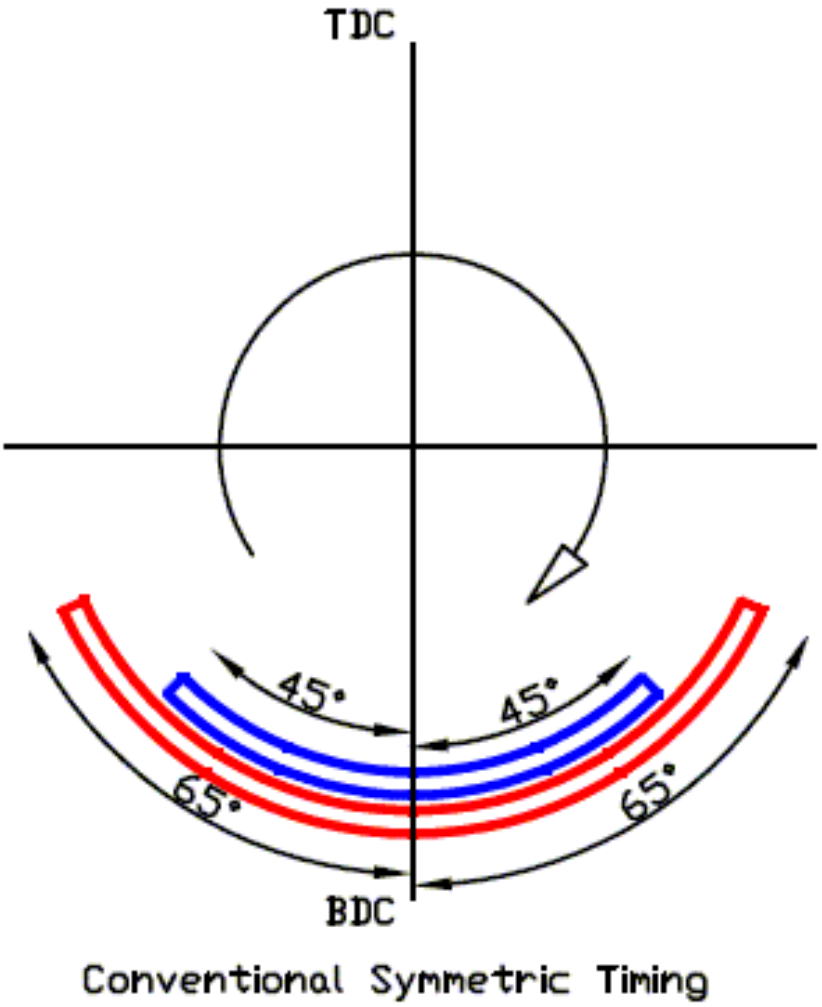

Figure 2.6 Symmetrical port timing diagram (Pattakon 2014)

Traditional two-stroke engine has symmetrical port timing where the exhaust port and the transfer port are controlled by the piston movement. The transfer port opens after the exhaust port and closes before the exhaust port. For instance, in Figure 2.6, the exhaust port opens at 65 degrees before the BDC and closes at 65 degrees after the BDC, while the transfer port opens at 20 degrees after the exhaust port and closes 20 degrees before the exhaust port.

In the classic symmetrical port timing theory, the port's opening and closing by the piston always happens at the same time. Cross-flow and loop-flow engine designs have symmetrical porting. The drawbacks of symmetrical port timing are short circuiting, translating in charge loss, poor intake and exhaust efficiency and impossibility to super charge.

The process of symmetrical port timing is as follow: the exhaust port opens; the intake port opens; the intake port closes; the exhaust port closes. This process must be accomplished in a very short duration between the expansion stroke and exhaust stroke. If the scavenging is insufficient, it results in high fuel consumption, lubricating oil contamination and large internal exhaust gas recirculation.

2.4.2 Asymmetrical port timing

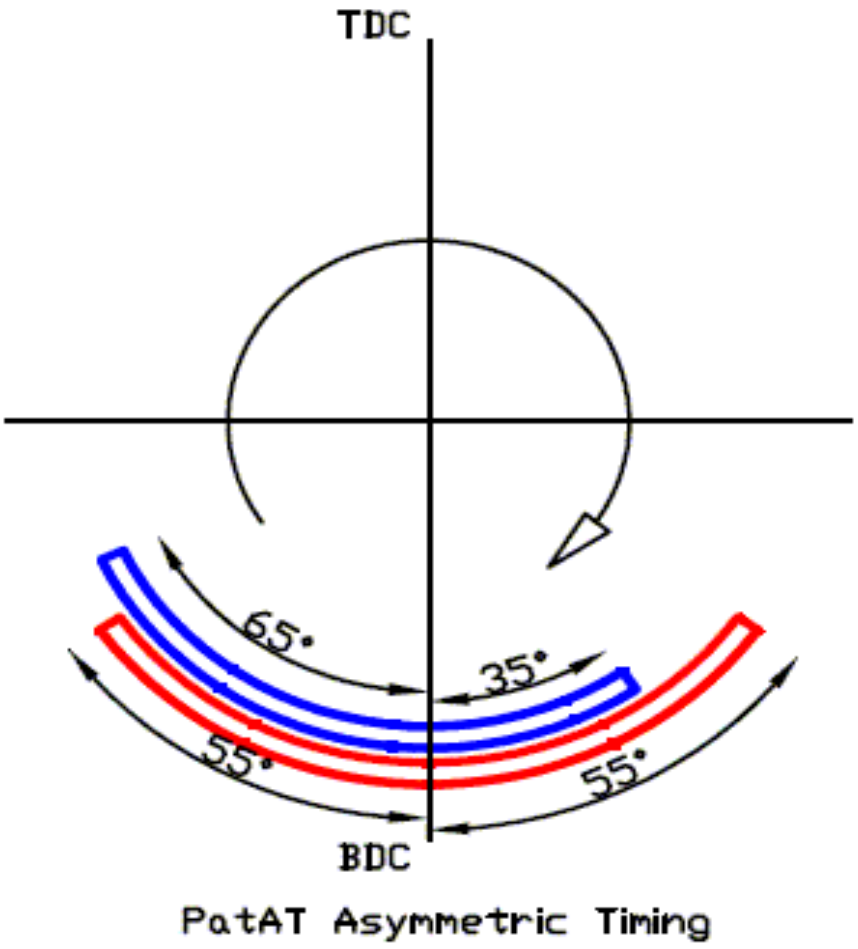

Figure 2.7 Asymmetric port timing diagram(Pattakon 2014)

In non-symmetrical port timing, the opening and closing of the intake and exhaust is not-symmetrical which leads to much more complex design.

The process of non-symmetrical port timing as follow: the exhaust port opens; the intake port opens; the exhaust port closes; the intake port closes as in a four-stroke engine. An advantage for non-symmetrical port timing is that the super charging is possible, and scavenging is more efficient (Gupta 1999).

In his paper, Pattakon (2014) describes an advanced design such as PartAT where the two-stroke operates in asymmetric port timing as shown in Figure 2.7. The exhaust port opens at 55 degrees before the BDC and closes at 55 degrees after the BDC, while the transfer starts at 35 degrees before the BDC and ends at 65 degrees after the BDC.

2.5 IGNITION TIMING

In SI engines the combustion pressure in the cylinder reaches maximum value and, therefore, efficiency when the crank angle passes about 10 degrees after TDC (Hannu Jääskeläinen 2014). This means the ignition should be timed accordingly.

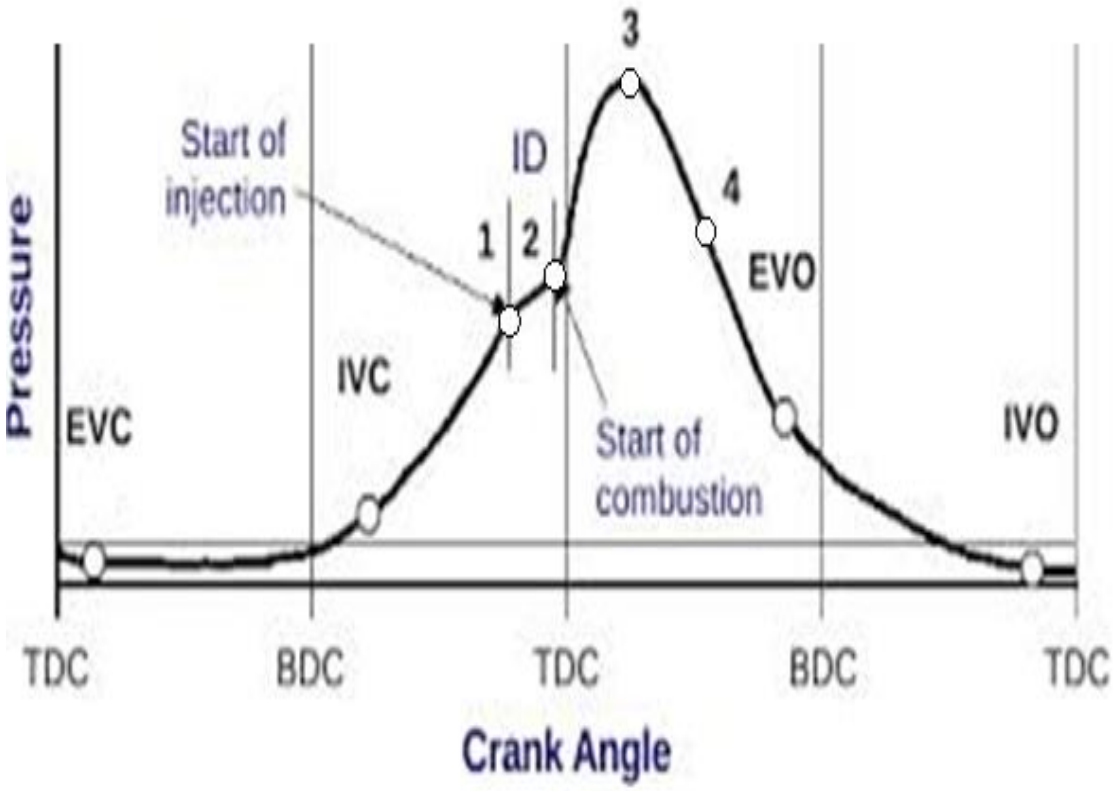

Figure 2.8 Pressure versus Crank Angle in a four-stroke SI engine (Hannu Jääskeläinen 2014)

Figure 2.8 shows the process of combustion in terms of the pressure changes inside the cylinder. Injection starts at point 1, but the combustion initiates with delay at point 2 where compression starts to increase. Compression reaches maximum value of pressure at point 3. Finally, after significant decrease of compression, combustion finishes at point 4. The period between points 1 and 2 is called the ignition delay time. For a given fuel this delay is fixed to some degree irrespective to the engine speed.

Let us consider the case when the engine speed increases. Because the ignition delay time between points 1 and 2 is constant, the angle through which the crank rotates is in the same period of time. The point at which maximum pressure is reached lags behind, so it is required to advance the ignition timing.

When the load on the engine increases, the volume of the fuel/air mixture and the compression pressure inside the cylinder increase, the temperature of the air fuel mixture goes up and so the mixture burns faster. As a result, the combustion time gets shorter and the ignition timing has to be retarded.

Therefore, the ignition timing should be adjusted according to the load, speed conditions and other factors which are listed in Table 2-1.

Table 2-1 Spark timing adjusting factor (MSD 2014)

Factor	Advance Timing for:	Retard Timing for:
Cylinder Pressure	Low	High
Combustion Chamber Shape	Open	Compact
Energy of Ignition	Low	High
Fuel Octane	High	Low
Mixture (Air/Fuel)	Rich	Lean
Temperature	Cool	Hot
Spark Plug Location	Offset	Center
Combustion Turbulence	Low	High
Load	Light	Heavy
Vacuum	High	Low

2.6 DIFFERENT TYPES OF FUEL INJECTION

Fuel injection is a system which optimizes air/fuel ratio and calibrates fuel in the IC engine. It began replacing carburettor in the 1980s and nowadays it is the primary fuel delivery system used in automotive engines.

The major difference between fuel injection and carburettors is that fuel injection uses a high pressure pump to atomize fuel while carburettor relies on suction created by air flow through a jet into a venturi (BOSCH 2015).

2.6.1 Single-point or throttle body injection

Single-point body injection is the earliest and simplest fuel injection system. It simply replaces the carburettor (it is positioned at the same location) with fuel-injector nozzle in the throttle body and combines with electrically controlled fuel injector valves. It was a low cost improvement because automotive manufacturers did not make much modifications to their engine design, therefore the number of the carburettor's supporting components could be reused (Crazymechanical 2015).

2.6.2 Port or multi-point fuel injection

Port fuel injection positions the injector in the intake manifold, close to the combustion chamber. If it is a four-cylinder engine, there would be four injectors placed at each cylinder of the intake manifold. Instead of delivering fuel in one place and distributed by the throttle body through air flow into the cylinder, fuel is injected just outside the combustion chamber. The main advantage of the multi-point fuel injection is to allow even distribution of fuel into each cylinder, to provide more precise fuel metering and quicker throttle response (BOSCH 2015).

2.6.3 Sequential fuel injection

Sequential fuel injection is more advanced fuel injection system and it is based on the multi-point fuel injection design. Sequential fuel injection places the injector at the same location as multi-port fuel injection, but it triggers each injector independently. Each injector sprays just before the intake valve opens for that particular cylinder. This design improves the engine efficiency and performance (BOSCH 2015).

2.6.4 Direct Injection

Direct injection cut down the amount of air/fuel mixture that may escape the combustion chamber. This is achieved by directly injecting the fuel into the combustion chamber and only when the exhaust port is closed. Direct injection may also provide more fuel rich areas surrounded by air (M. Badami 1999). The jet ignition is a pre-chamber device that may ignite the main chamber premixed fuel and air with very high energy all across the chamber or in a selected region as well. The direct injection and hot ignition carefully coupled may permit load control completely throttle-less having the main chamber fuel air mixture restricted to a selected area where the jet ignition would start combustion that will complete almost instantaneously. In the latest developments, jet ignition and direct injection are coupled together to modulate the amount of premixed and diffusion combustion to achieve the best trade off of fuel conversion efficiency and pollutant formation all over the load and speed range.

The potential of advanced two-stroke engines in future applications is indubitable. Several studies have discussed the advanced two-stroke engines. In their paper, Kumarappa and Prabhukumar (2008) received promising results on solving the crucial problems of fuel efficiency and lubrication system. Also, they showed that direct injection allows to avoid short-circuit scavenging and do not premix fuel with oil (S. Kumarappa a & Prabhukumar 2008).

In conventional two-stroke engines, the fuel and air are mixed in the carburettor and then drawn into the cylinder. Simultaneous opening of the intake and the exhaust ports causes some unburned mixture escape from the exhaust port. Direct injection do not have the carburettor to mix air and fuel. It delivers air only to the crank case while fuel is injected directly into the cylinder. The injection in the engines is precisely timed, so no fuel escapes out of the exhaust port. This dramatically increases fuel economy and reduces emissions. Direct injection models have all the

benefit of two-stroke engines and they are still equal to or greater in emissions and fuel efficient with compare to many four-stroke engines.

Another advantage of direct injection two-stroke engines is that they have much lower oil consumption than traditional two-stroke engines since fuel is no longer mix with oil. Instead, oil is only injected in the crankcase and then it is distributed to the bearing and the other moving components though the scavenging process.

Rotax 600 H.O. E-Tec Engine uses an external oil tank (Figure 2.9) that have an oil capacity of about 2 litters which is enough for about 50 hours of engine operation under the normal conditions. Oil is accurately injected to the places where required, such as crankshaft, bearings and cylinder wall. Unlike the conventional carburetted two-stroke engine, oil no longer mixes with air that getting pumped through the crankcase. There is only slight amount of oil gets burn during the combustion process that has no noticeable effect on emission. In addition, E-TEC oil is designed to be combusted and meets all the emission requirements(Ski-doo 2009).

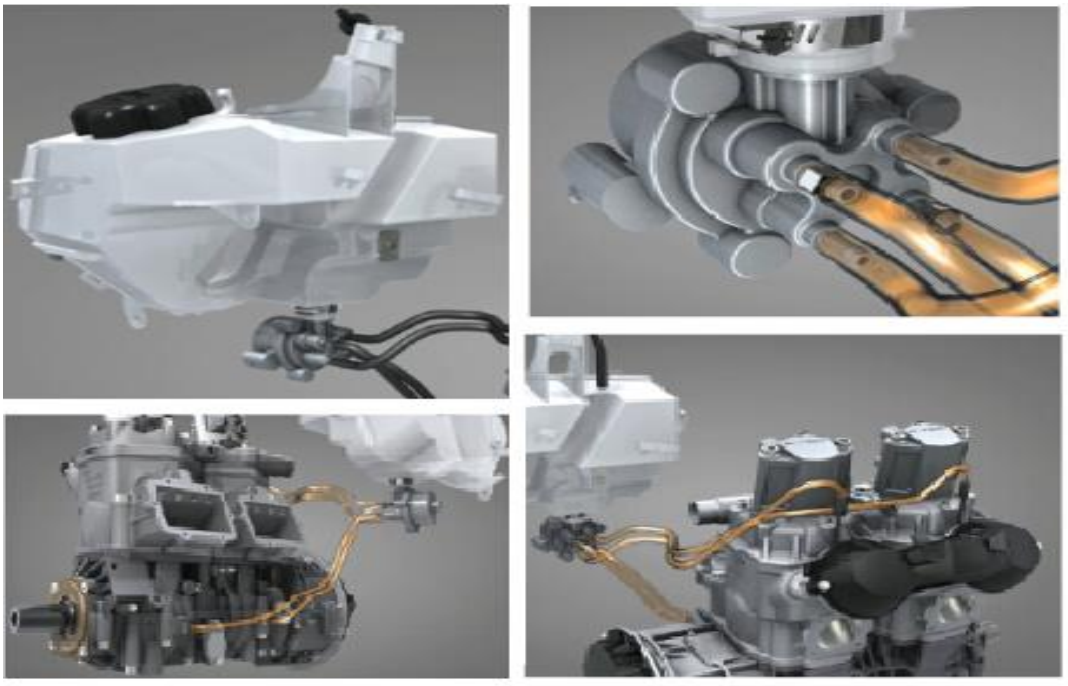

Figure 2.9 Rotax 600 H.O. E-TEC Engine Oil System (Ski-doo 2009)

Two commercial direct injection systems are used in modern two-stroke engines: air-assisted direct injection and high-pressure direct injection.

Figure 2.10 shows the low-pressure air-assisted direct injection system developed by Orbital Corporation. This system uses an injector to deliver fuel and compressed air into the cylinder. The benefits of this system are low power consumption and durability. The disadvantage is added complexity of supplying compressed air to the system. The Orbital system is used in outboard motors companies by Tohatsu and Mercury, in personal watercraft manufactured by Bombardier Recreational Products (BRP) and in motor scooter companies such as Aprilia, Kymco, Piaggio and Peugeot.

According to Leighton (Leighton & Ahern 2003), low-pressure air-assisted direct injection engine has the following characteristics:

- Low fuel pressure.
- Low fuel particle size.
- Fuel calibrating by a traditional automotive based port fuel injector.
- Fuel calibrating independent of the actual in-cylinder injection process.

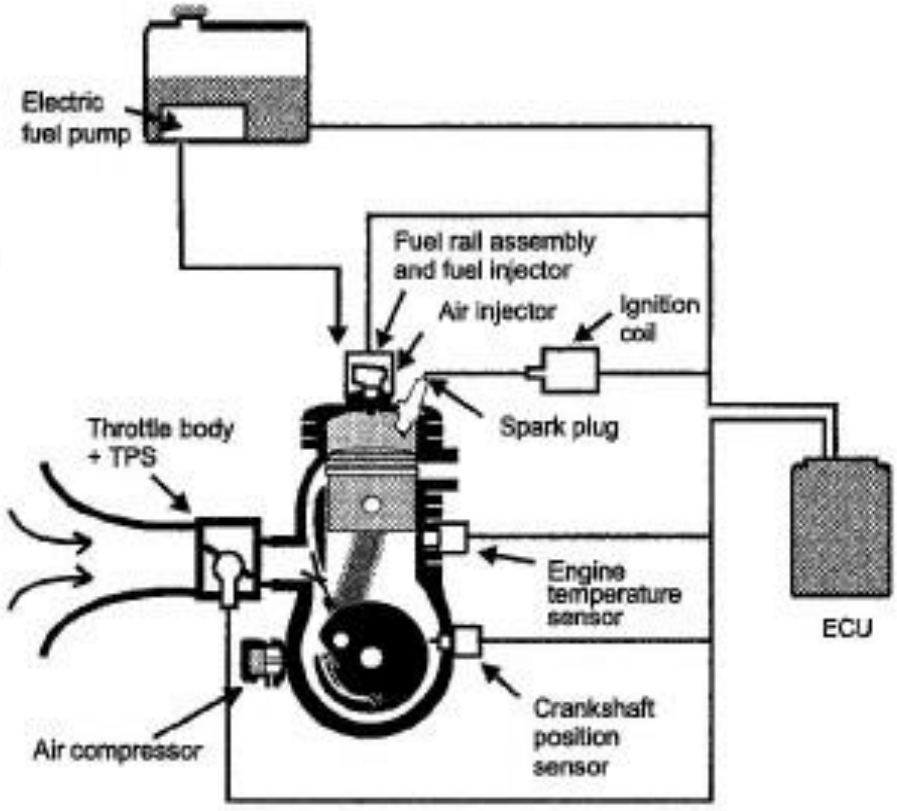

Figure 2.10 Schematic air assist direct injection in a two-stroke engine (Leighton & Ahern 2003)

The high-pressure direct injector system (Figure 2.11) was developed by Ficht GmbH of Kirchseeon Germany. This system utilizes a hammer injection system. Fuel enters the injector at low pressure, and then solenoid injector system immediately increases the fuel pressure and helps to atomize the fuel. The high-pressure direct injector has fewer parts compare with air-assistant direct injection system, but it requires higher voltage (between 38 and 43 volts) as compared to air-assistant direct injection system.

According to Leighton (Leighton & Ahern 2003), high pressure DI two-stroke engine has the following features and introduces some drawbacks:

- High fuel injection pressure and higher Fuel calibrating is done directly by the direct injector.
- Fuel calibrating is connected directly to the cylinder injection process (this may cause insufficient fuelling at high speed.).

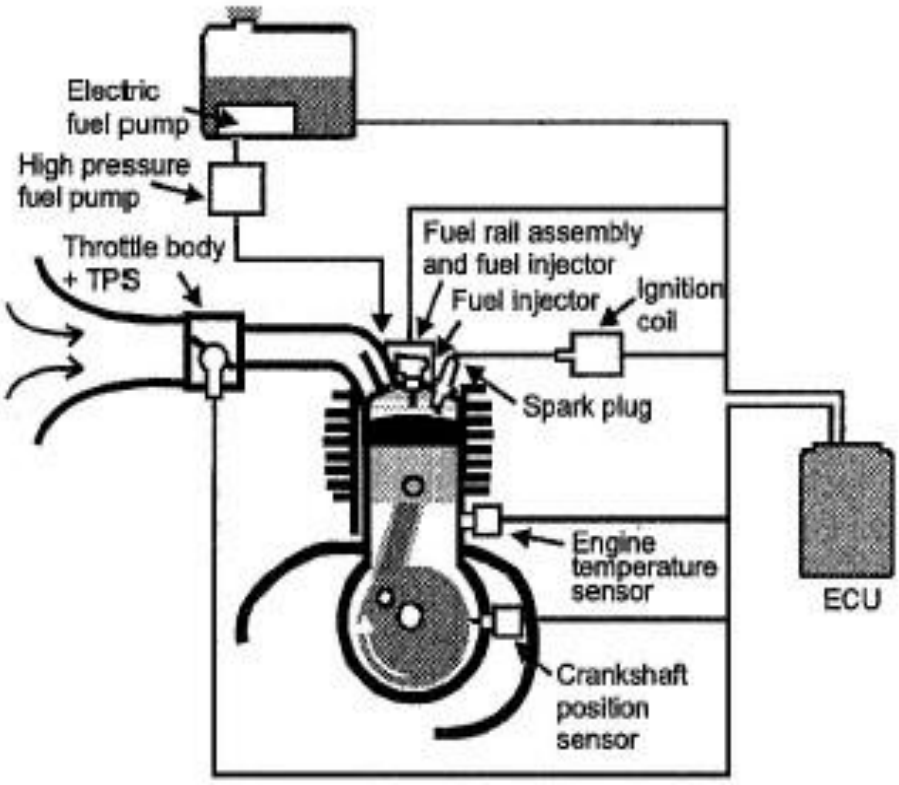

Figure 2.11 High pressure direct injection in a two-stroke Engine (Leighton & Ahern 2003)

According to Leighton's(2003) report, two-stroke direct injection is expected reduce emission from 25 to 35 precent inferior than those of a four-stroke engine. This system is now applied on marine engines and watercrafts and they surpassed the four-stroke standards. Table 2-2 presents the different type engine combustion gas chemical composition.

Table 2-2 Combustion gas chemical composition (United States Environmental Protection Agency 2001)

			grams/HP/Hour	
Engine	HC	CO	NO_X	MP
Two-Stroke	111	296	1	2,7
Four-Stroke	8	123	9	0,2
Two-Stroke DI	22	90	3	0,6

Recent study on direct fuel injection technology (Blair 1989) for two-stroke spark ignition engine in transport application shows the following evident advantages:

- High torque at low engine RPM
- Very low specific fuel consumption in comparison with the other types of engines; especially in the low B.M.E.P. range where the engines are used on short urban distances.
- Low CO emission with lean mixture feeding at full throttle.
- Low emission of NOx and high concentrations of O_2 at the exhaust.

However, direct injection systems developed in recent years introduce relatively complicated components regarding to the injector and lubrication systems. As a consequence, the high-cost systems are not likely to be widely applicable in the commercial applications.

In the other study Bartolini (Bartolini, Caresana & Vincenzi 2001) develops a new injection device, the "Water Hammer Gasoline Direct Injection" (WHGDI) system (Figure 2.12). It is equipped with a low-pressure fuel pump and it is provided with high injection pressure values while retains the simplicity of two-stroke engines. The proposed injection system is mounted on a 240 cm^3 single cylinder engine. The experimental data resulted from a first prototype had confirmed that the proposed concept is suitable for spark-ignition internal combustion engines but a more precise analysis is necessary to prove its effective capabilities.

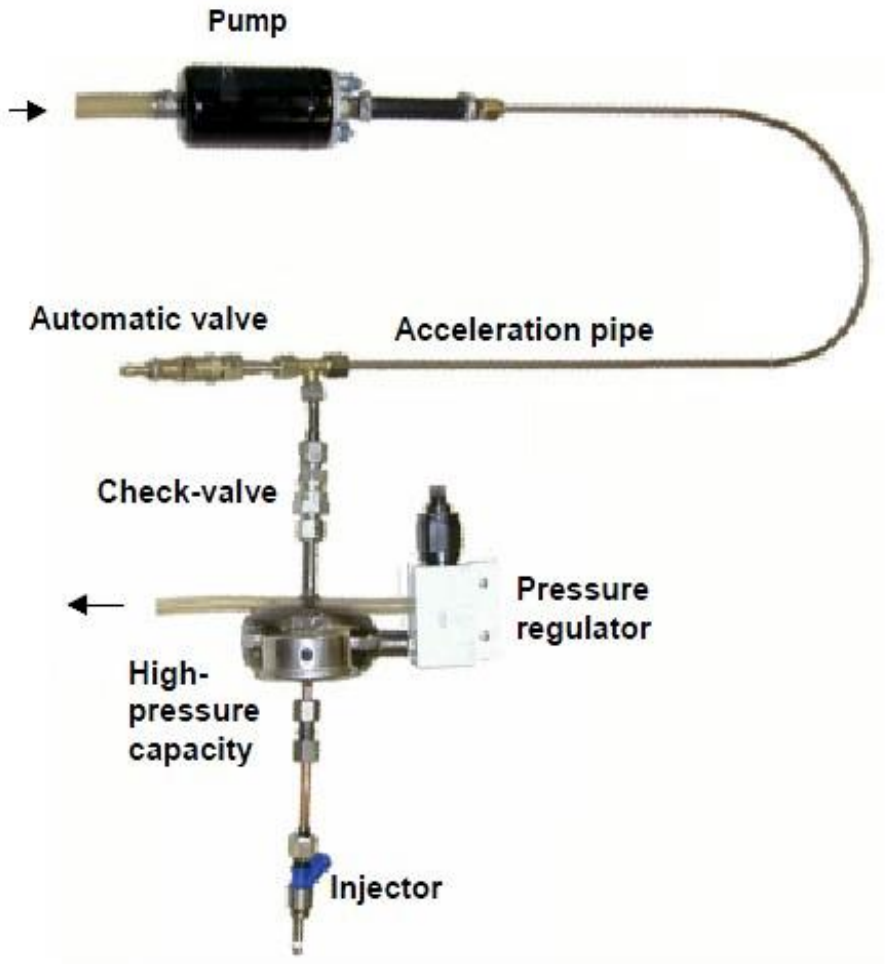

Figure 2.12 WH-GDIS injection plant (Bartolini, Caresana & Vincenzi 2001)

The Institute of Internal Combustion Engines and Thermodynamics at Fraz University of Technology has developed another direction injection device, a low pressure (5 bar) direct injection (LPDI) combustion system for 50 cm^3 two-stroke engines. The results show that the LPDI technology has the potential to compete with four-stroke engines. The high power to weight ratio, high engine efficiency and the low emissions system are especially practical in the India market as the urban pollution is high (Oswald, Ebner & Kirchberger 2010).

The other study on M. Badmi's (1999) report "Comparison Between Direct and Indirect Fuel Injection in an S.I. Two-Stroke Engine" highlights the potential of the direct injection strategy. The engine used for the experimental tests is a single cylinder two-stroke engine with

inlet, exhaust and transfer port governed by the piston movement. The comparison between direct injection and indirect injection has been performed at the full load engine condition, with a constant air to fuel ratio, which is equal to the stoichiometric value. A cutaway view of the engine is shown in Figure 2.13.

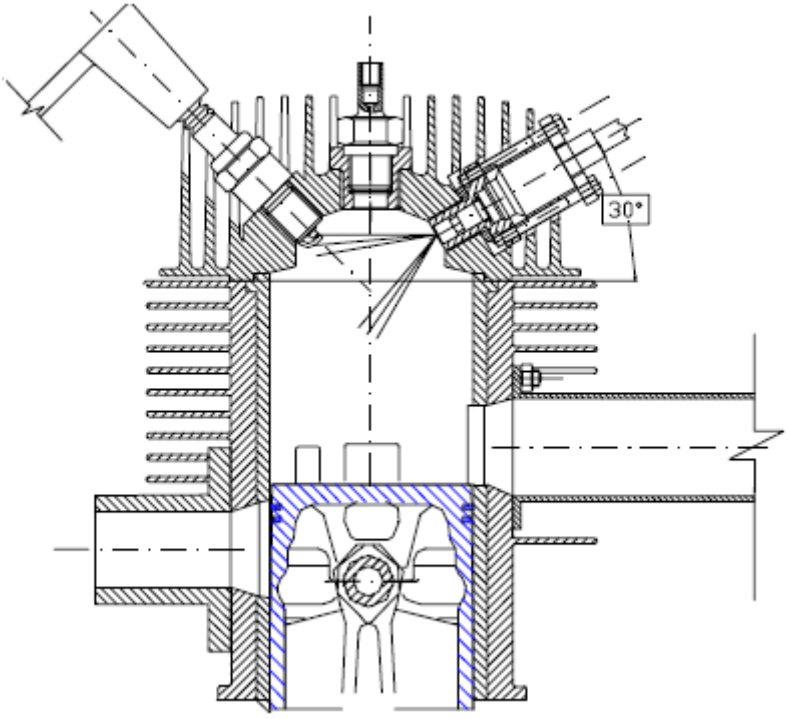

Figure 2.13 Cutaway view of the modified engine for gasoline direct injection (M. Badami 1999)

Results of gasoline DI engine has shown remarkable advantages compared to indirect injection. The accuracy of injection timing in DI system prevents fuel losses at the outlet during the scavenging process. With direct injection the scavenging charge is only made of air, instead of a pre-mixed air-fuel mixture. Therefore the actual air-fuel ratio inside the cylinder during the combustion process needs to be properly estimated.

Torque, power and bsfc versus revolution speed for both DI and ID system are shown in Figure 2.14. Results show that direct injection has higher torque and power than indirect injection, except for 5000 and 5500 rpm. Bsfc value of direct injection is lower than indirect injection over the whole

revolution speed range. There is about 39% bsfc improvement has been found at the minimum speed. However, at 5500 rpm the bsfc reduction is only about 3.5%

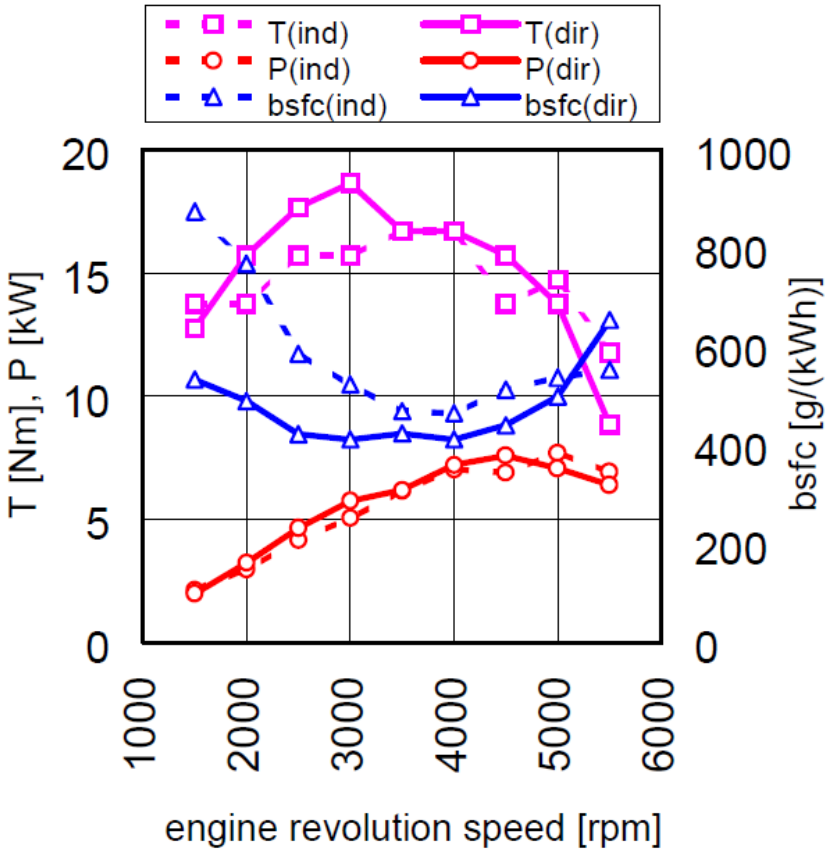

Figure 2.14 Comparison between direct and indirect fuel injection: torque, power and bsfc versus engine revolution speed at WOT. (M. Badami 1999)

Other study made on Balduzzi's (Balduzzi et al. 2015) report "Development of a Low Pressure Direct Injection System for a Small 2S Engine. Part I - CFD Analysis of the Injection Process" highlighted that the great potential of solving issues such as high specific fuel consumption and pollutant emissions in small two-stroke engines. This paper presents the results of a detailed study on the application of an innovative Low Pressure Direct Injection (LPDI) fuel supply system on an existing 300 cm3 2S cylinder. The engine was modified from a naturally aspirated SI two-stroke engine with carburettor.

The proposed solution is characterized by placing two injectors in the cylinder wall, opposite of the exhaust port and above all the cylinder ports in order to have an independent injection timing (see Figure 2.15). The benefit of this design is to reduce short-circuit under all the engine operation condition. The only constrain to the injection timing is related to the piston motion.

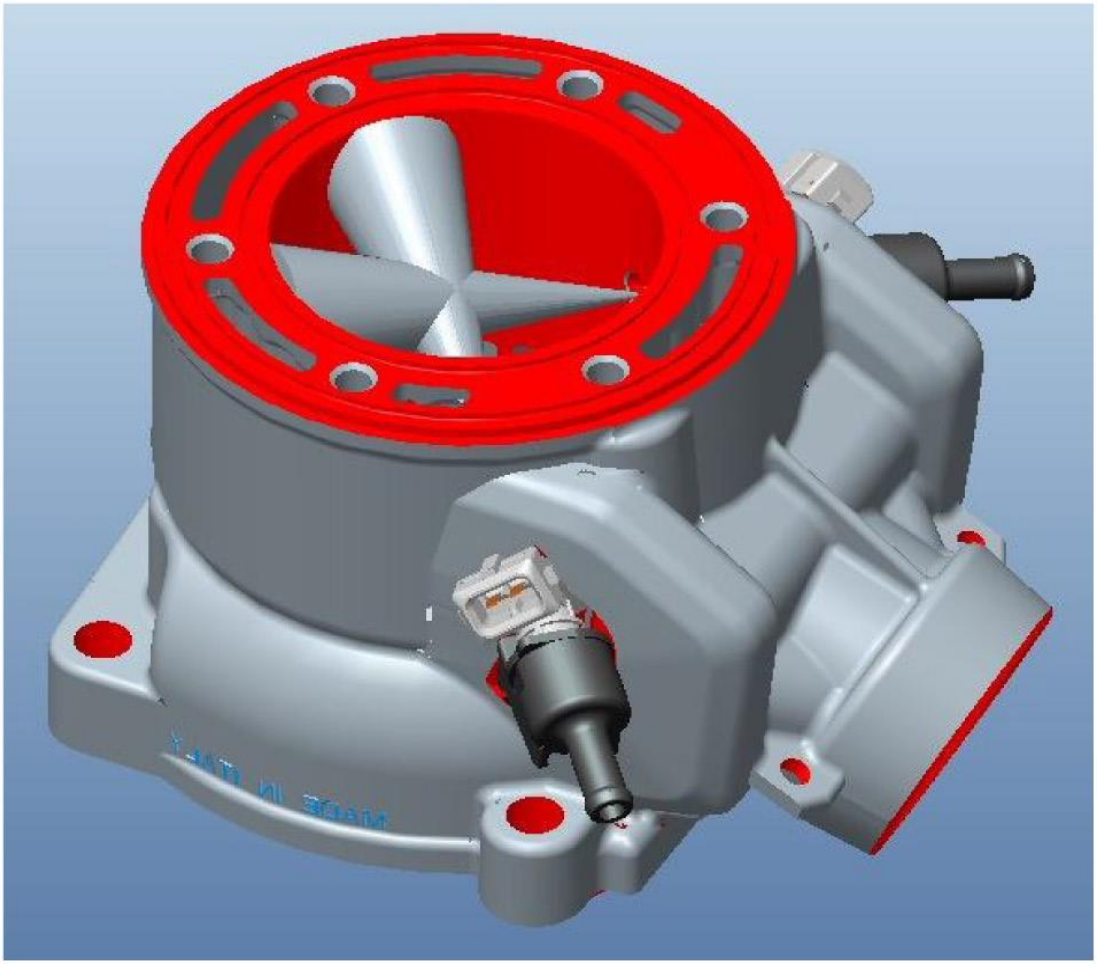

Figure 2.15 CAD model of the cylinder modified with the injectors' housings.(Balduzzi et al. 2015)

Figure 2.16 shows the evolution of the fuel vaporization and homogenization inside the cylinder at four different piston positions (from 210 °CA to 300 °CA). The injector nozzle is located on the opposite side of the exhaust port, the jet is deflected towards the cylinder head and then distributed in the entire cylinder. Simulation results show that the fuel short-circuit of LPDI system is at almost 4%, while the fuel

loss of the carburetted two-stroke engine is at almost 25% at the same operating condition. The proposed solution shows the great potential in term of solving the main issue of homogenously scavenged engines (Balduzzi et al. 2015).

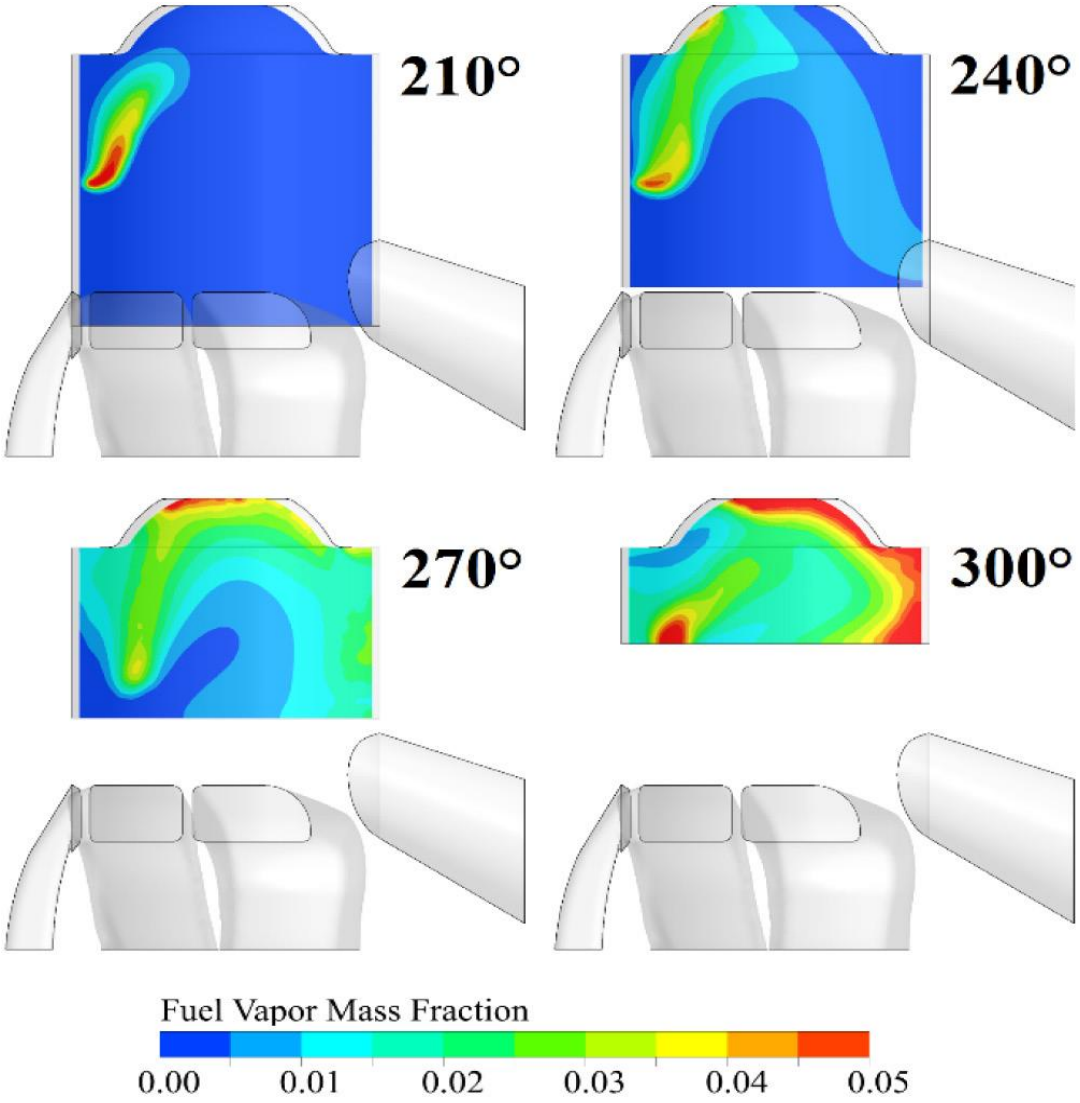

Figure 2.16 Evolution of fuel evaporation inside the cylinder for various piston positions. (Balduzzi et al. 2015)

The following table provides a comparison among the different types of fuel injection design and carburettor.

Table 2-3 Comparison of the different types of fuel injection design and carburettor (eBay 2014)

Fuel Delivery Method	Advantages	Disadvantages
Carburettor	It's easy and more directly to adjust the engine performance	Inefficient; and hard to tune economically
Throttle body injection	Computer-controlled fuel delivery	Inefficient; dumps fuel into intake similarly to carburettor
Multi-port injection	Even fuel distribution, more accurate fuel metering and quicker response	Fuel must still be drawn from intake into combustion chamber
Sequential injection	Independent injector fuelling; improves efficiency and economy	Still some incomplete fuel burn in intake and around valves
Direct injection	Fuel directly injected into combustion chamber; bypasses intake and valves; most efficient	More expensive to repair

2.7 SUPERCHARGING OF TWO-STROKE ENGINE

Supercharging involves increasing inlet air/change density and a corresponding increase in the flow rate. Supercharger increases an engine's power and efficiency by introducing extra air into the combustion chamber (Stone 1999).

Two-stroke engines can be supercharged. The arrangements possible to supercharge two-stroke engines are:

1) Retention of scavenging (pump) compressor and addition of exhaust driven turbocharger. The output of the turbocharger is fed to the scavenging pump.

2) Elimination of the scavenging compressor and addition of a high capacity turbo compressor driven by exhaust gases (Thipse 2008).

2.8 JET IGNITION

Through literature review it has been found that jet ignition has been extensively studied for use with 4-stroke IC engines. It is commonly considered with stationary or marine natural gas internal combustion engines (CIMAC 2006; TUM 2013) that have pre-chamber injection and use part of fuel together with jet ignition system. Jet ignition pre-chamber have also been proposed for transport engines with in-cylinder homogeneous mixtures (Boretti & Watson 2009a) or bulk, lean stratified (Boretti 2012; Boretti & Watson 2009b) produced by direct injection.

With the jet ignition, the main combustion chamber air/fuel mixture is ignited by multiple jets of hot reacting fuel issued by the jet ignition holes and crossing the main chamber at very high speed. The jet ignition device is a small-scale volume linked to the main combustion chamber volume through multiple orifices and coupled with a fuel injector and a smaller spark or glow plug. The dedicated injector delivers to the pre-

chamber volume also receiving air from the main combustion chamber during the compression produces a locally stoichiometric mixture.

Jet ignition has been traditionally coupled to lean premixed operation with port fuel injection. The coupling of jet ignition to direct injection permits to produce a confined near stoichiometric air fuel mixture ignited by the jet ignition streams in the centre of the combustion chamber (Boretti & Watson 2009b).

In addition, modulating the phasing of the injection and jet ignition events, it is possible to modulate the amount of premixed and diffusion combustion for operation gasoline-like, diesel-like and mixed to better optimize performances over the load and speed range (Boretti & Watson 2009a).

Recent study on a jet ignition (Boretti & Watson 2009c) system which uses hydrogen assisted jet ignition (HAJI) has shown the potentials of jet ignition to enhance combustion and allow control of load mostly by injected fuel quantity rather than throttling. The advantage of this system is to reduce pumping losses and improve outputs with cryogenic over gaseous PFI. The HAJI system is shown in Figure 2.17 and Figure 2.18. It presents the HAJI assembly compared with a standard spark plug and the HAJI pre-chamber, injector and reduced size spark plug.

Figure 2.17 Comparison between HAJI device and standard spark plug (Boretti & Watson 2009c)

Figure 2.18 HAJI pre-chamber assembly, injector and reduced size spark plug(Boretti & Watson 2009c).

Specifications of the HAJI system are presented in Table 2-4 HAJI system specifications. The overall size of the HAJI device that contains spark plug and pre-chamber is constructed to fit into the standard spark plug screwed hole (14mm).

Table 2-4 HAJI system specifications (Boretti & Watson 2009c)

No. of nozzles	6
Diameter of nozzles [mm]	1.25
Angle between nozzles [deg]	120
Pre chamber to Main chamber volume ratio [%]	1.47

Another study on MAHLE turbulent jet ignition system by Attard (William P. Attard 2011) reveals very promising fuel economy and emission results. The pre-chamber replaces the standard spark plug in a conventional SI engine, shown in Figure 2.19.

The system is able to operate on commercial fuels (gasoline, CNG, propane) and offer a new solution to previous jet ignition hurdles that use hydrogen assisted fuel in the pre-chamber.

The biggest advantage of the jet ignition is reduced the combustion duration that takes place when the nozzle inside the jet ignition device producing multiple, widely dispersed ignition sites which charge the main combustion chamber more rapidly. The fast burn rates allow lean burn combustion when compared to traditional spark ignition. With lean burn combustion it is achievable to implement homogeneous charge compression ignition (HCCI). In addition, jet ignition has combustion control, load and speed range advantages in contrast to HCCI, without changing the SI-HCCI combustion mode. The reduced combustion duration also allow operating at a higher compression ratio (CR) when compared to conventional spark ignition combustion. This is feasible due

to jet ignition system increase the flame propagation, and reduces the chance of engine knock due to the shorter residence time.

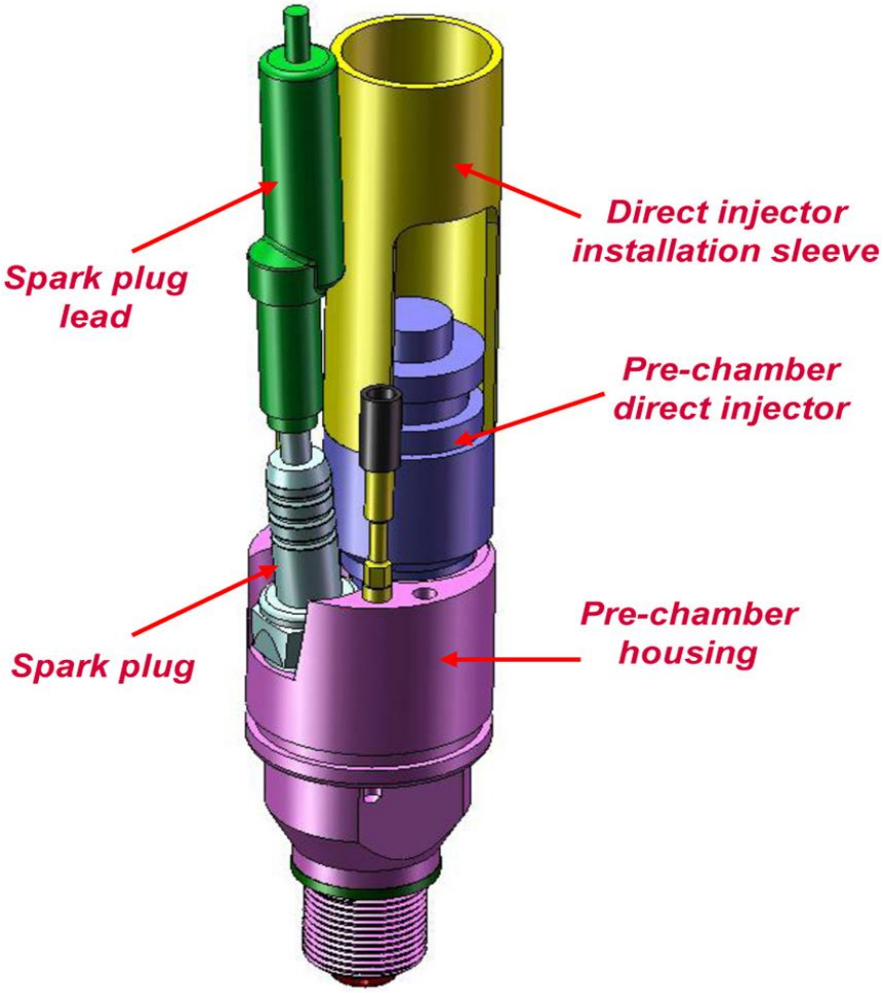

Figure 2.19 design of Turbulent Jet ignition device, replace the standard spark plug in a contemporary SI combustion system. (William P. Attard 2011)

2.9 CURRENT AND FUTURE TRANSPORT FUELS

At present, petrol is the major fuel source for transport vehicle throughout the world. Other alterative fossil fuels to petrol are compressed natural gas (CNG), diesel, liquid petroleum gas (LPG), ethers and other major non-fossil alternative fuels are hydrogen and ethanol. Figure 2.20 presents the world transportation fuel demand. Although there is an increasing number of vehicles are running on

mixture with alternative fuels, it is improbable that any one of these alternative fuels will reach to the global consumption of petrol in the near future, mainly due to the fact that alternative fuels are too costly.

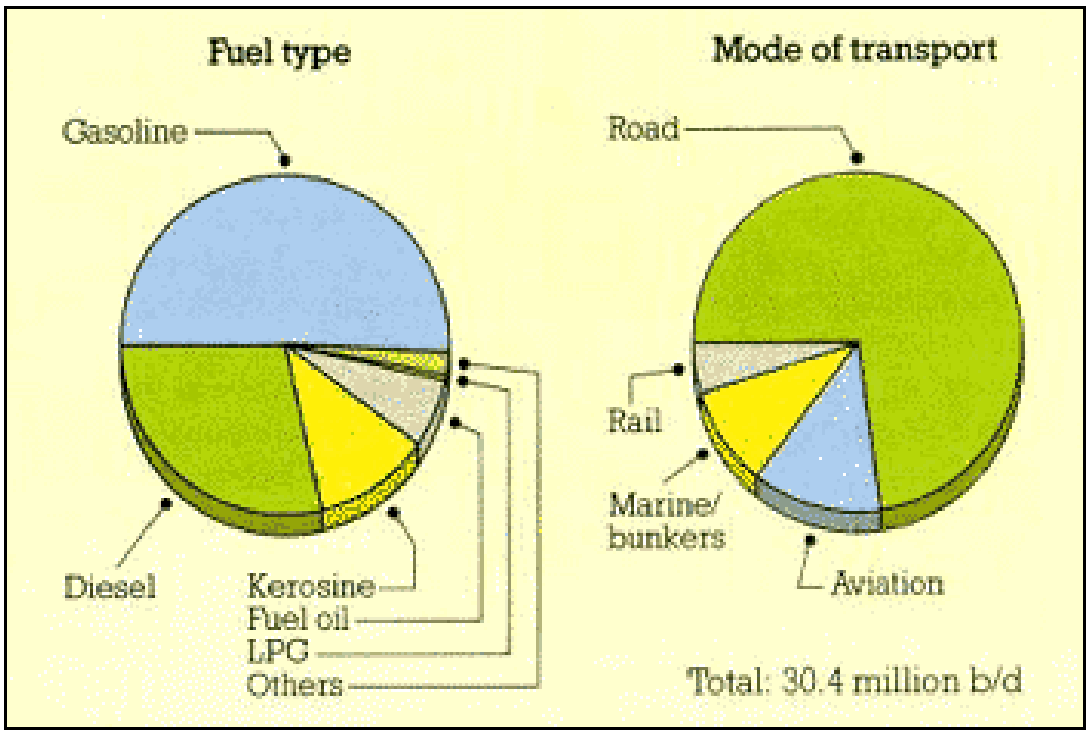

Figure 2.20 World Transportation Fuels Demand (Council 2014)

In regards to the future of internal combustion engine, this mobility solution is the best solution available for at least the next two decades. Traditional petroleum based fuels and other alternative fuels are expected to fuel these engines. Advances of hybridization, mechanical, electrical and hydraulic, will help in specific developments for applications with frequent start/stops and deceleration/accelerations. Alternatives solutions such as electrics cars have issues like limited range and lack of charge station, therefore mass use of such vehicles is not practical at the moment. Electric cars require renewable production of energy.

Presently, about 90% of electricity in the OECD countries is produced by non-renewable energy sources, and in Australia about 90% of the electricity is produced by burning of coal (Agency 2014). Hence the extra energy required to fuel the electric cars will be produced by burning coal or oil and this makes the solution presently unviable.

Petrol powered car discharge pollutant such as CO_2, water vapour, hydrocarbons, nitrogen oxides and CO which is harmful to the environmental.

Pollutant emissions from motor vehicles can be decreased by the use of alternative fuels. Alcohols such as methanol and ethanol are the two main alternatives to gasoline use in IC engine vehicles.

Liquefied Natural Gas (LPG), Compressed Natural Gas (CNG), and Liquefied Petroleum Gas (LPG) are alternative substitutes for fuel such as gasoline and diesel which are increasing in popularity. CNG, LNG, LPG are more environmentally friendly fuels which also enhance sustainability of transport, energy economy and energy security.

2.9.1 Hydrogen as a spark ignition engine fuel

Reviewing the results of alternative fuels for SI engine, Najjar (2009) concludes that hydrogen is the most environmental friendly alternative fuel as it potentially CO_2 free use. In addition, hydrogen improves the combustion process, as it has characteristic such as low ignition energy in air, wide flammability limits, high flame speed and high heating valve which favour the combustion properties. However, there are some limitations associated with hydrogen engine application. Hydrogen at atmospheric temperature has only approximately 5% of the energy of petrol of the same volume. This is a main barrier for road vehicle applications.

Table 2-5 lists some combustion properties of hydrogen as a fuel for engine applications and compared with corresponding values of methane and gasoline. It outlines that hydrogen has an outstanding wide flammable air/fuel mixture range which favour to the engine combustion properties to enable ultra-lean mixtures combustion. In addition, it has the lowest ignition energy and fastest laminar flame speed to travel through the combustion in comparison to methane and gasoline. However,

it shows that the adiabatic flame temperature and auto ignition temperatures are very close in comparison to methane and petrol.

Table 2-5 Some Comparative combustion properties of Hydrogen with Methane and Gasoline (Karim 2003)

Property	Hydrogen	Methane	Gasoline
Flammability Limits (%by volume)	4-75	5.3-15.0	1.2-6.0
Minimum Ignition Energy	0.02	0.28	0.25
Auto-ignition Temperature (K)	858	813	~500-750
Laminar Flame Speed at N.T.P. (m/s)	1.90	0.38	0.37-0.43
Adiabatic Flame Temp. (K)	2318	2190	~2470
Quenching Gap at NTP (mm)	0.64	2.03	~2.0

Table 2-6 shows some of the useful overall properties as an engine fuel of Hydrogen and compared to corresponding values of Methane and iso-octane. It is highlight that hydrogen has the lightest gaseous fuel for stoichiometric combustion and it requires the least amount of fuel to achieve stoichiometric combustion compare with methane and iso-octane. The heating value on mass basis is also the highest. However, combustion energy of stoichiometric mixture is one of the highest.

Table 2-6 Some Comparative Properties of Hydrogen, Methane and Iso-Octane (Karim 2003)

Property	Hydrogen	Methane	Iso-Octane
Density at1 ATM and 300K (Kg/m^3)	0.082	0.717	5.11
Stoichiometric Composition Air (% by Volume)	29.53	9.45	1.65
No. of Moles After Combustion to Before	0.85	1.00	1.058
Stoichiometric Fuel/Air Mass Ratio	0.029	0.058	0.0664
HEATING VALUES			
H.H.V. (MJ/kg)	141.7	52.68	48.29
L.H.V. (MJ/kg)	119.7	46.72	44.79
H.H.V. (MJ/m^3)	12.10	37.71	233.29
L.H.V. (MJ/m^3)	10.22	33.95	216.38
Thermal Conductivity At 300 (mW/mK)	182.0	34.0	11.2
Combustion Energy per kg of stoich mixt. (MJ)	3.37	2.56	2.79
Diffusion Coefficient Into Air at NTP (cm^2/s)	0.61	0.189	0.05
Kinematic Viscosity At 300K (mm^2/s)	110	17.2	1.18

Karim (Karim 2003) has conclude some of the unique features associated with hydrogen that make it outstandingly well suit to engine applications. Some of these most notable features are the following:

- Hydrogen has very high flame propagation rates ranges with the engine cylinder compares to other type of fuels. These rates stay adequately high even at leaner mixtures (Y.AI-ALousi 1982).
- The lean limit of hydrogen in a SI engine is much lower than other common fuels, as shown typically in Figure 2.21 for a range of compression ratios. This allows a lean mixture engine operation.

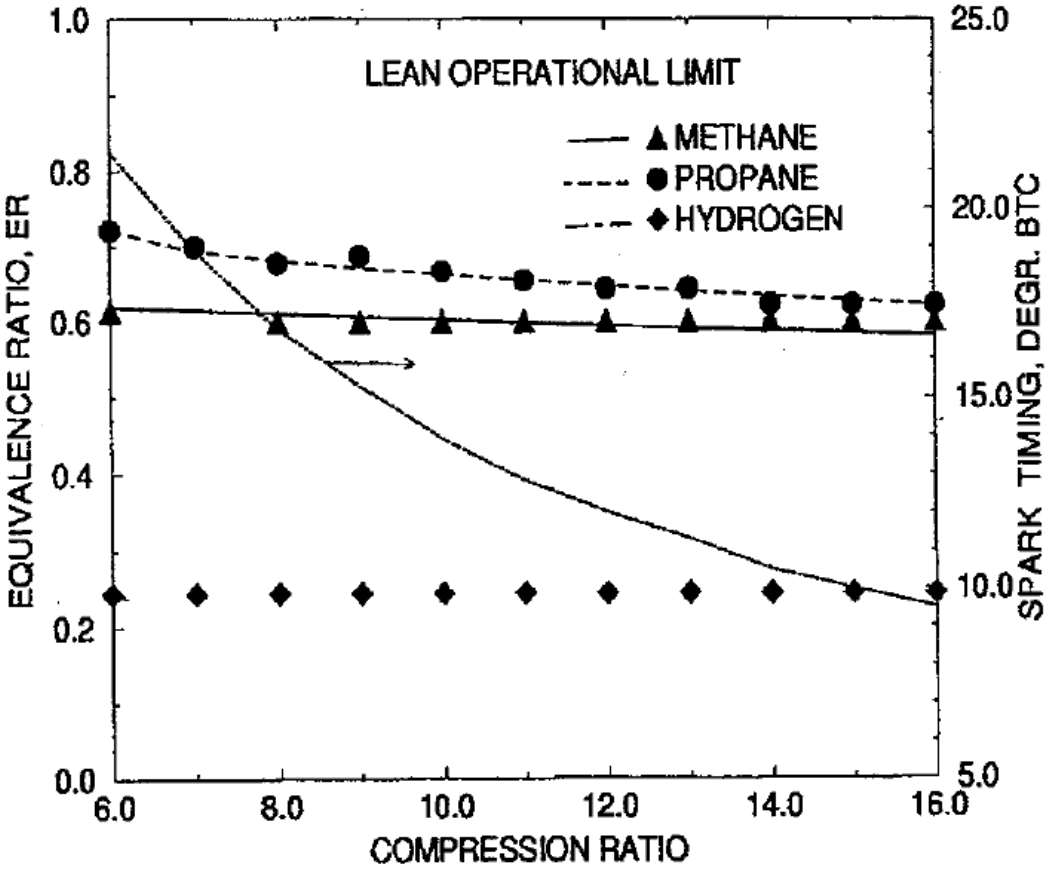

Figure 2.21 Variations of the lean operational limits with changes in compression ratio for different gaseous fuels at 900 rev/min (Karim 2003)

- Hydrogen associated with less undesirable exhaust emissions in comparison with other fuels. There are no unburned hydrocarbons, carbon monoxide, carbon dioxide, and oxides of sulphur, smoke or

particulates. In addition, with lean operation, the level of NO_x tends to be smaller than other fuels.

- The fast burning characteristics of hydrogen permit engine operate at much high-speed. This allows an increase in power output with a reduced penalty for lean mixture operation.

2.10 SUMMARY

This chapter, firstly, provides a literature review on background of two-stroke engines that is related to this thesis. Next, a review of two-stroke engine applications and background of different fuel injection as well as ignition systems are presented. Further, it follows with discussion on air-assist DI and non-assist DI systems. Lastly, a description of current and future fuels for SI engines is reviewed. Based on the literature review conducted during this research project it was found that no study has been done on the use of direct injection and jet ignition systems in 2-stroke IC engines which shows a clear gap in knowledge and provides justification for this study.

CHAPTER 3

3.SIMULATION MODEL AND METHODOLOGY

3.1 TWO-STROKE ENGINE DESIGN AND CAD MODELLING

3.1.1 Engine design

The engine design concepts are based on a non-air assist direct injection system and replaces the standard spark plug with a jet ignition device. This technology allows fuel to be directly injected into the combustion chamber as the piston is moving up and closing the exhaust port. The injector is positioned diagonally to the jet ignition device in the cylinder head, ensuring a complete burn for lower emissions and better fuel economy.

The engine uses a loop scavenging design as shown in Figure 3.1 for intake and exhaust port arrangement. All port timing events are symmetrical with respect to TDC and BDC. The piston port controls the exhaust and transfer process and the reed valve controls the inlet process.

This design is typical of racing engines where the exhaust is finely tuned to produce a pattern of pressure waves that maximize the removal of the exhaust gases. The present definition of the transfer port and exhaust port openings is not yet optimized. The exhaust and lamellar intake is not modeled in the CFD simulation.

The engine specification is shown in Table 3-1.

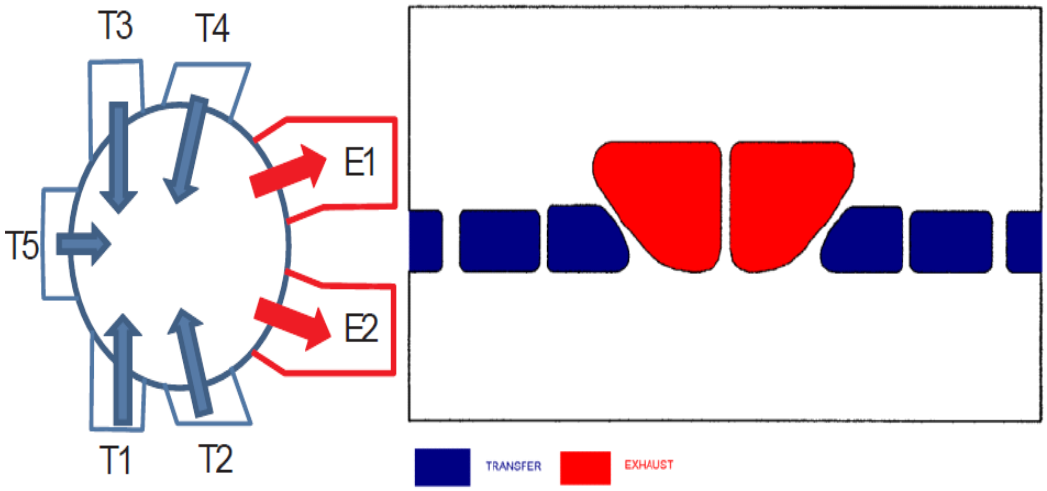

Figure 3.1 Loop scavenging (Fleck 2006)

Table 3-1 Specification of the Simulation Engine

Engine Type	direct injection, single cylinder two-stroke
Bore	82 mm
Bore / Stroke	1.083
Displacement	399.8 m^3
Effective CR (VC-TDC)	8.281
Rod Length	150 mm
Clearance Volume	0.2856E-4 m^3

The ports timing by the piston is symmetrical. The intake port opens at 115 CA degree BTDC, and closes at 244 CA degrees BTDC. The exhaust poet opens at 85 CA degrees BTDC, close at 244 CA degrees BTDC, and the valve effective area is shown in Figure 3.2.

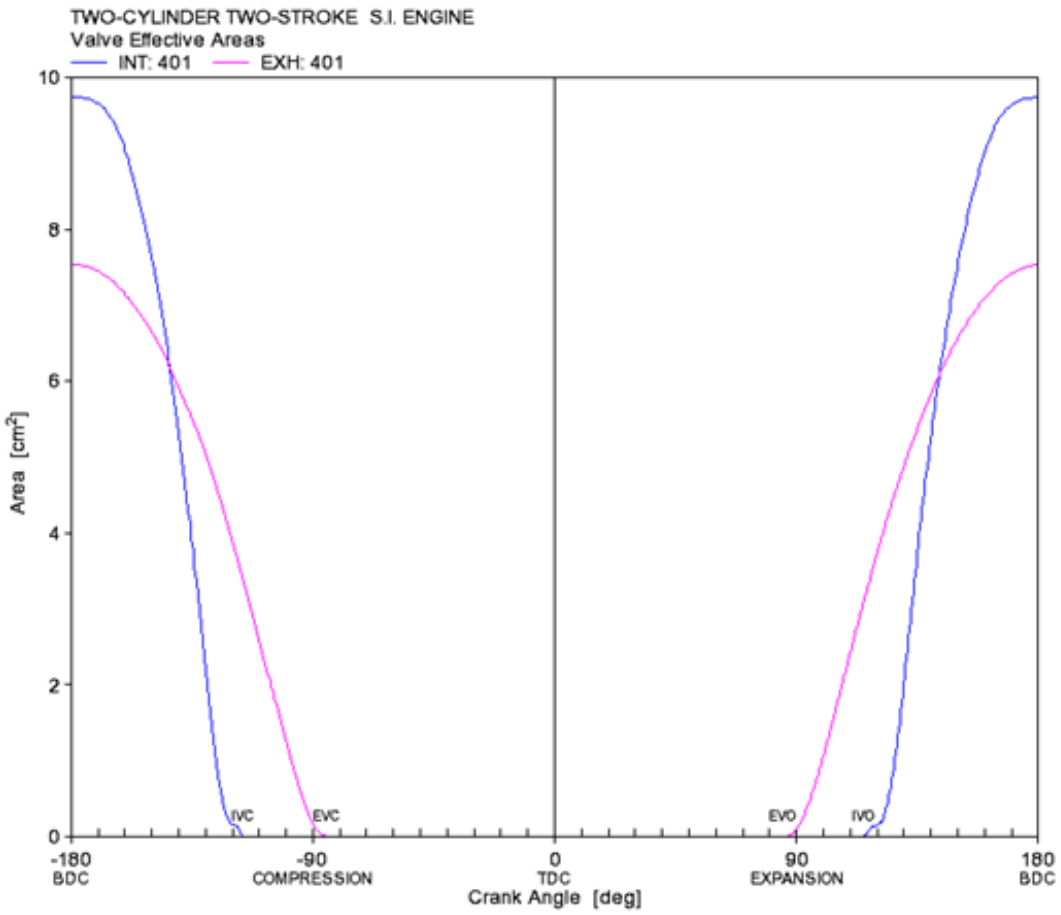

Figure 3.2 Engine vale effective port areas

The 3D CAD model of two-stroke engine and jet ignition device was designed in SolidWorks. SolidWorks is one of the most prominent computer-aided design (CAD) packages on the market today, and it is used by many top companies worldwide to design, engineer, and document their products in a variety of fields.

In SolidWorks, the 3D parts are from a series of simple 2D sketches and features including as extrude, revolve, fillets, cuts and holes, and creating 2D drawings from the 3D parts and assemblies.

Figure 3.3 to Figure 3.6 is the main engine components and Figure 3.7 presents the full design of the engine assembly.

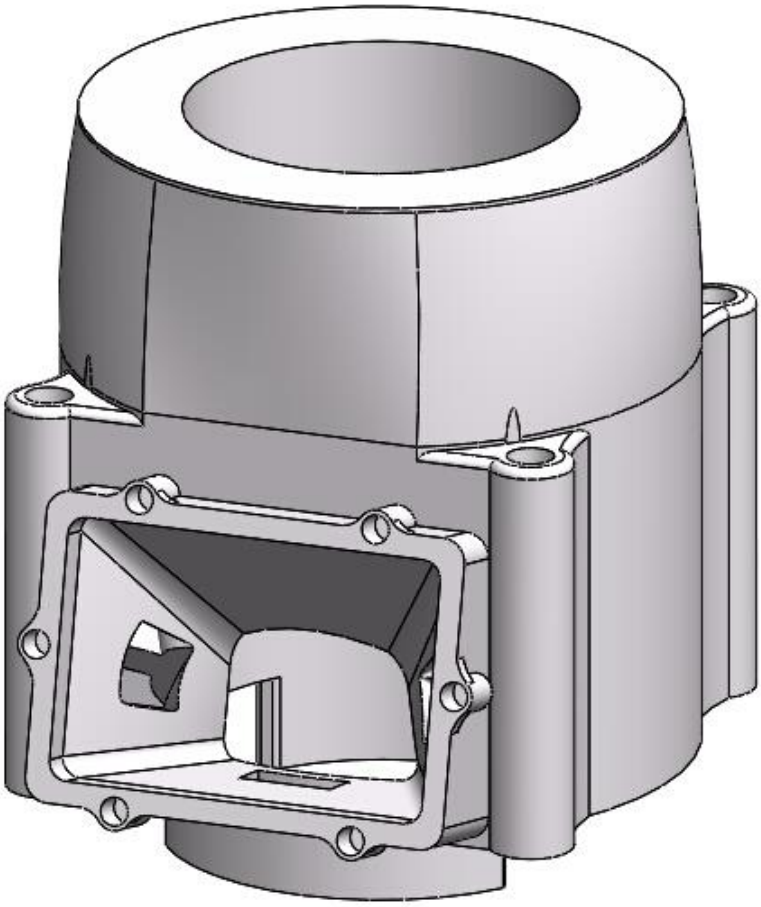

Figure 3.3 Engine Cylinder Bore

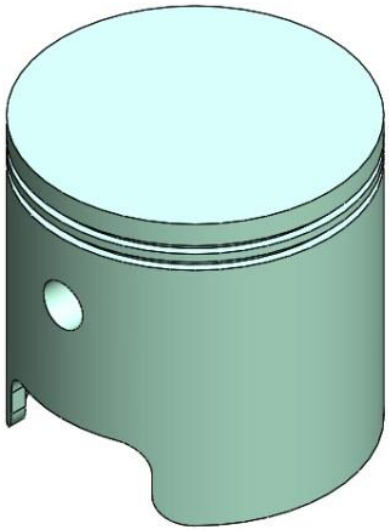

Figure 3.4 Piston

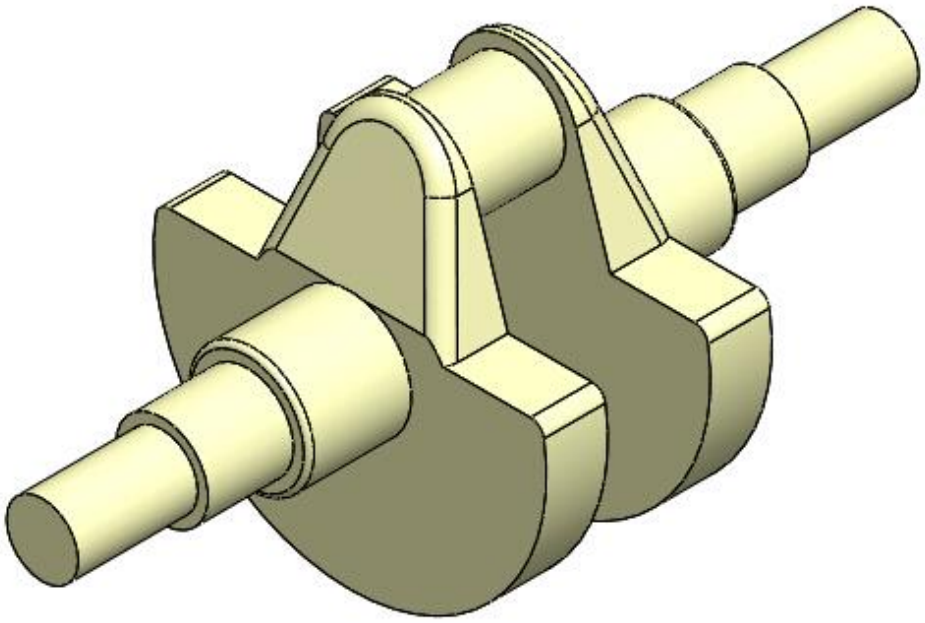

Figure 3.5 Crankshaft

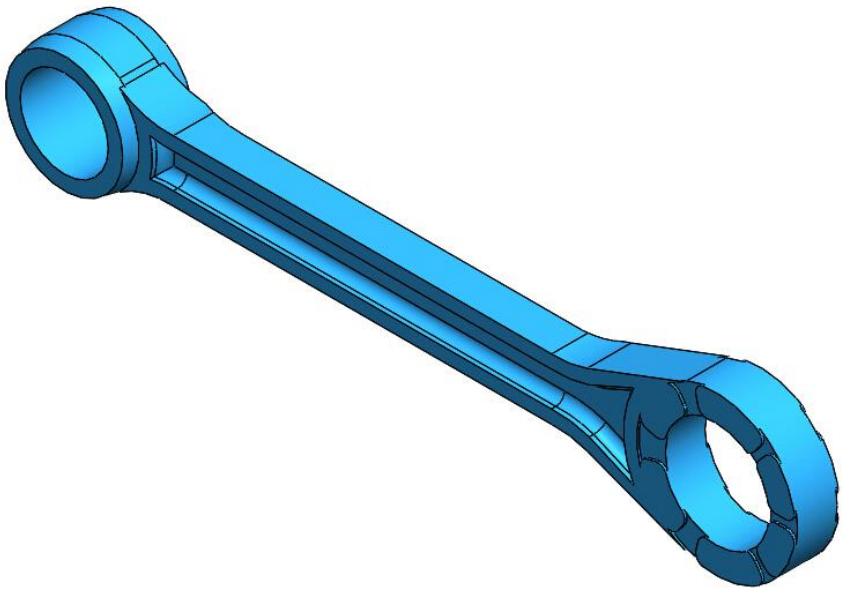

Figure 3.6 Connecting Rod

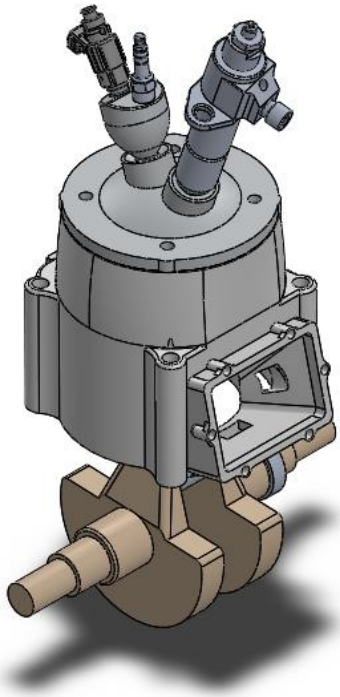

Figure 3.7 Two-stroke Engine Assembling

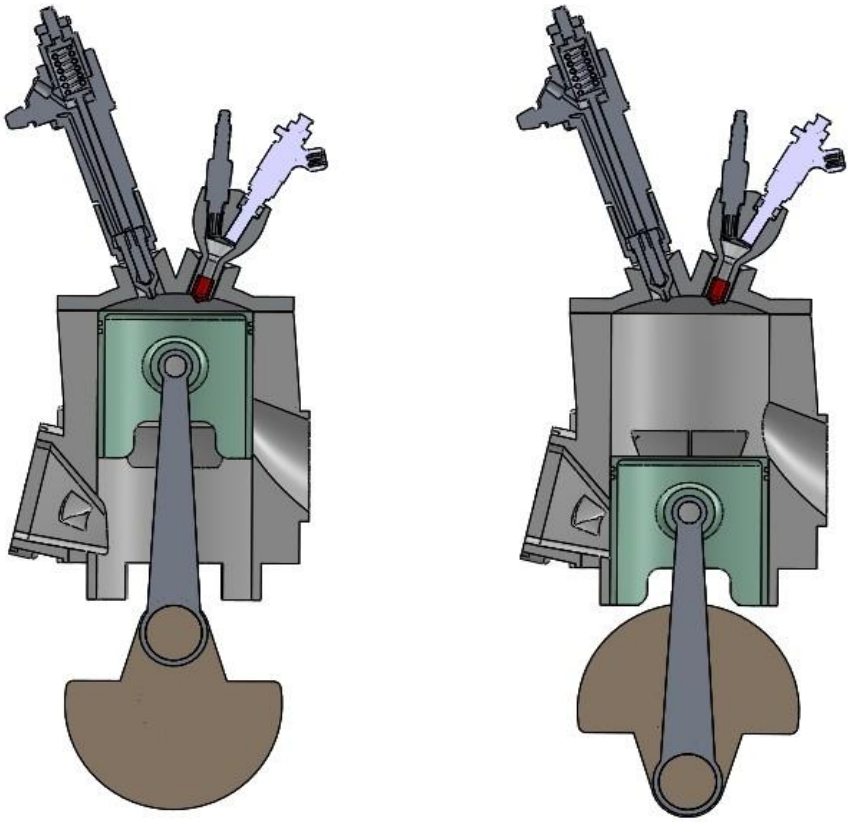

Figure 3.8 Two-stroke engine half section view

3.1.2 Injector and jet ignition device design

The design of the engine features one direct injector coupled with a jet ignition device, replacing the standard spark plug in a conventional two-stroke direct injection engine. The jet ignition device is coupled with another direct injector and an 8mm spark plug.

The main injector uses a prototype of the Westport Compressed Natural Gas Direct Injection (CNG-DI) injector, which uses gaseous fuels only (usually natural gas or hydrogen). The other injector uses the prototype of BOSCH EV12. The design of the injector and jet ignition device is shown in Figure 3.11 and Figure 3.12.

The combustion chamber is a flat-top piston combustion chamber. Small amounts of fuel are injected in the pre-chamber to create close stoichiometric condition and the mixture is ignited in the pre-chamber first. Hot combusted gaseous from pre-chamber are then distributed in the main chamber through its 6 nozzles. The main chamber consists of 16 nozzles and features fast actuation enabled multiple injections. A different mode of combustion is determined by fuel injected in the main combustion chamber relative to jet ignition event. The main chamber fuel is injected before the jet ignition event burns pre-mixed. Main chamber fuel injected after jet ignition event burns diffusion controlled. Fuel is injected in the gaseous phase and the load is controlled by the amount of fuel injected into the main chamber.

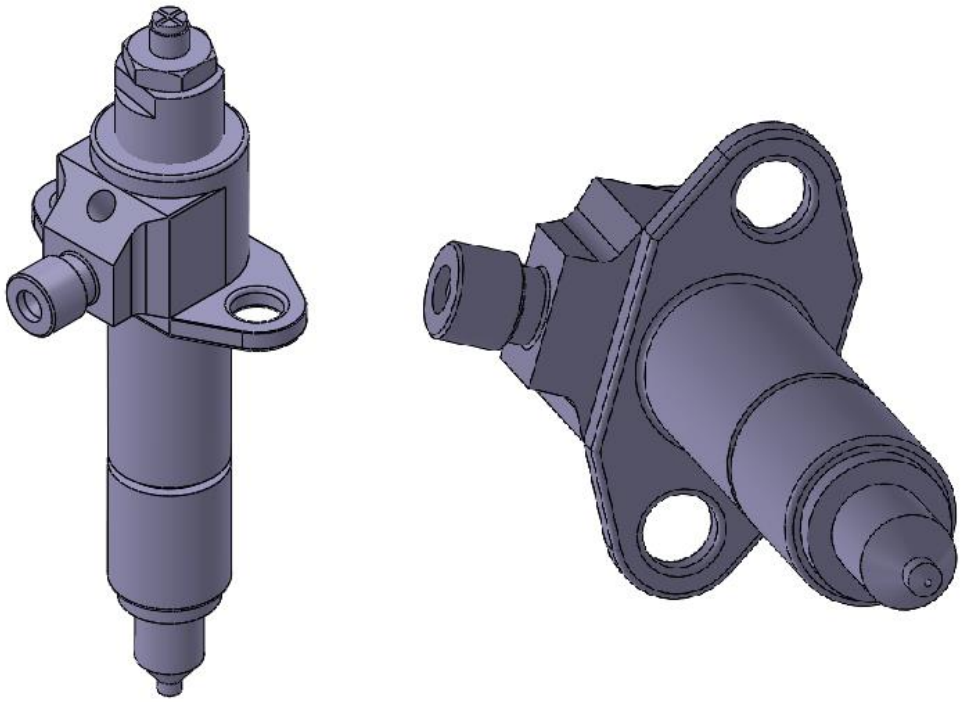

Figure 3.9 Main injector

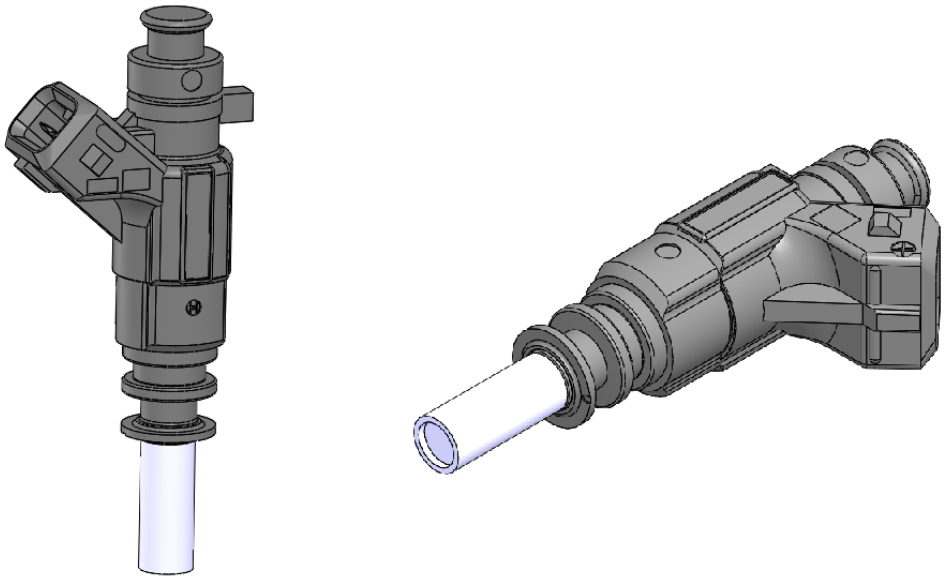

Figure 3.10 Pre-chamber injector

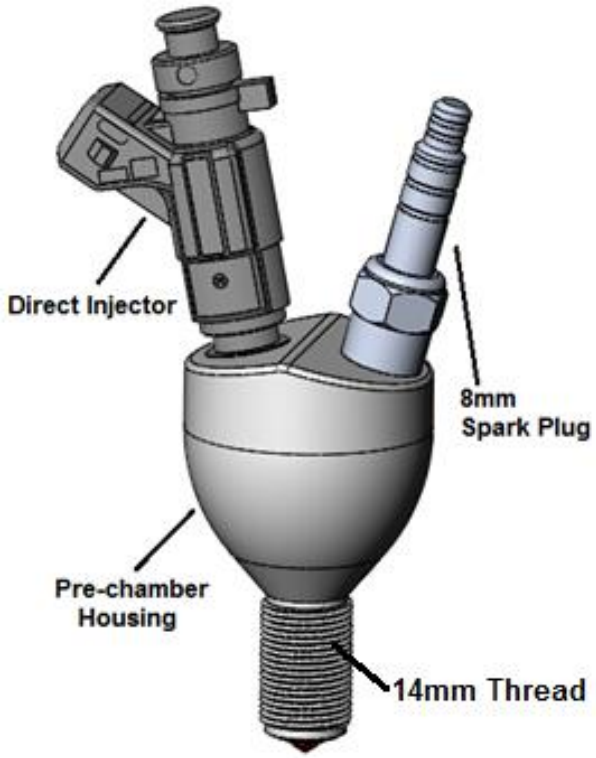

Figure 3.11 Jet Ignition design, replace with 14mm conventional spark plug

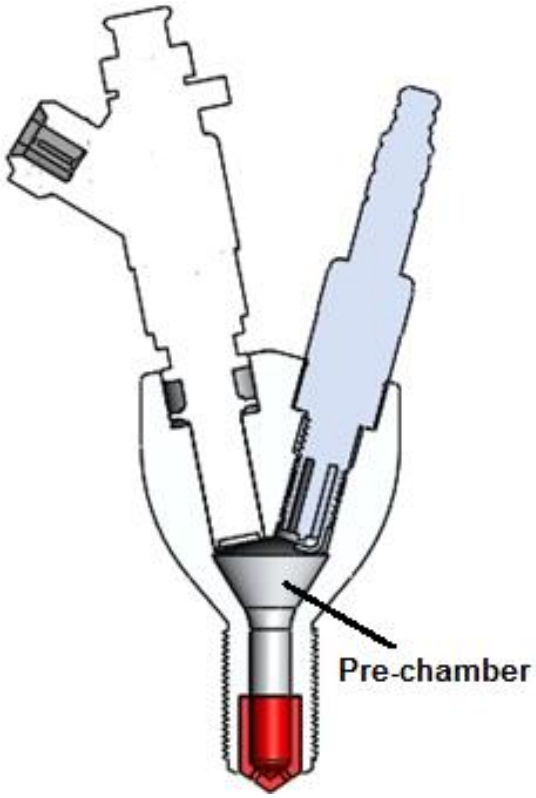

Figure 3.12 Jet Ignition pre-chamber half section view

3.2 TWO-STROKE ENGINE CFD MODELLING

The combustion chamber geometry of the engine was modelled in SolidWorks and imported to Star CCM+ to perform 3D combustion simulation. STAR-CCM+ (Computational Continuum Mechanics) is one of the Adapcao CD company's newly launched generation of CFD software. It uses the most advanced numerical computational continuum mechanics algorithms techniques, and is combined with modern software engineering to achieve excellent performance and high reliability. It is a powerful tool for thermal fluid analysis.

CFD simulations are performed to study the combustion mode with various injection timings to test the lean operation and the knock limit.

The two-stroke CFD model contains the combustion chamber with the jet ignition device and a main injector which is shown in Figure 3.14 at 100 ° BTDC.

3.2.1 Mesh Generation

Mesh generation is a significant factor in the accuracy of predictive CFD calculations. The computational mesh was generated by the Star CCM+. In order to implement the movement of the piston, the Prism Layer Mesher was used. Simulations were carried out with fine grid having 0.02m face spacing which contains 204,200 cells, 605,800 faces and 22,700 vertices with time step of 0.5, and it stretches and compresses as the piston moves between 0 ° to 360 ° (BTC to TDC) as shown in Figure 3.16. The computation is not grid nor model independent as no industrial flow involving complex separated reacting flows in complex geometries. This enhanced mesh has volume refinements outside the main chamber's direct injector's 16 holes, a cone downstream of each pre-chamber outlet, and internally for the pre-chamber. Combustion is initiated at 180 ° CA in the cells located at the spark plug electrodes (Figure 3.16).

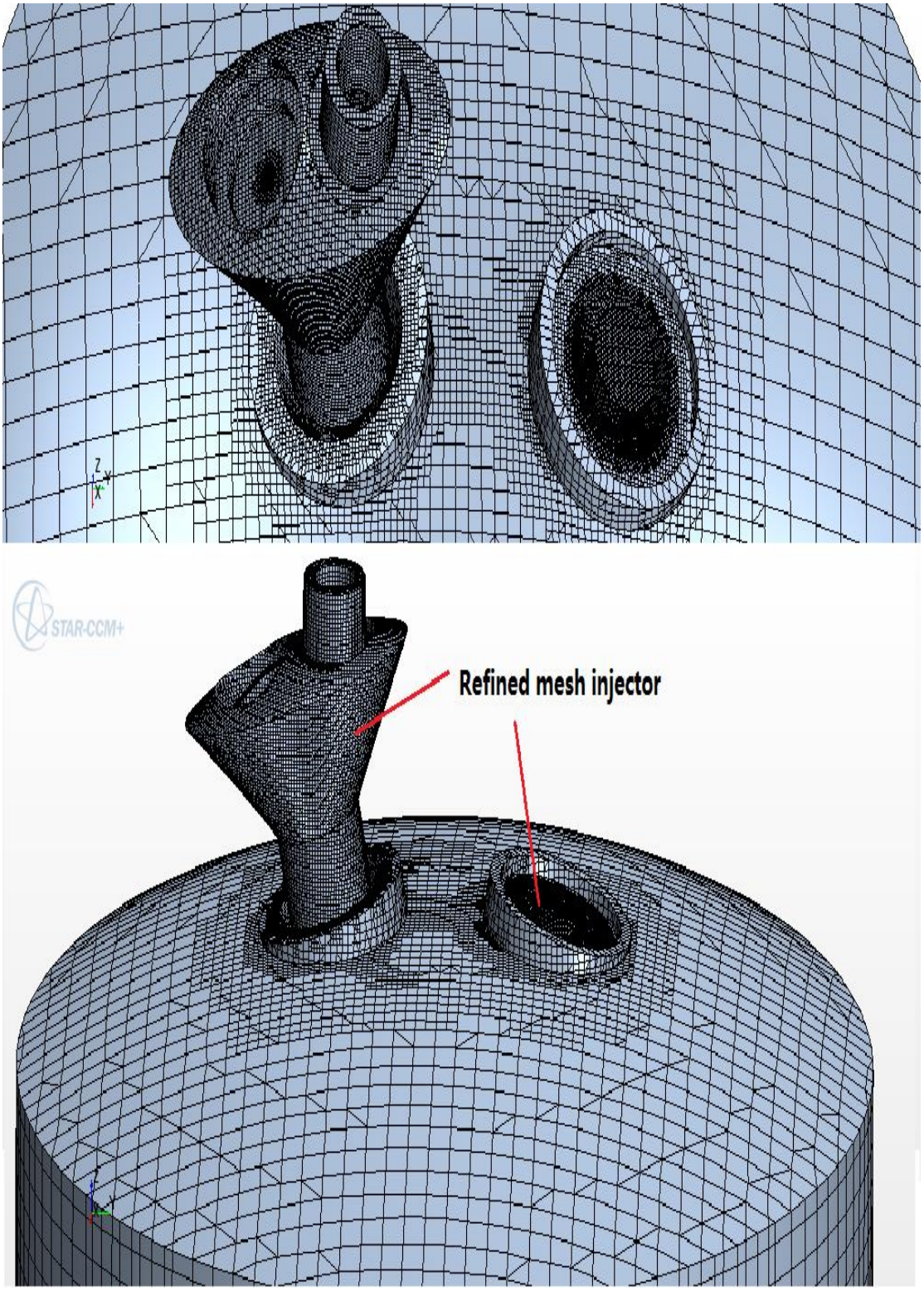

Figure 3.13 Computational meshes for CFD simulations

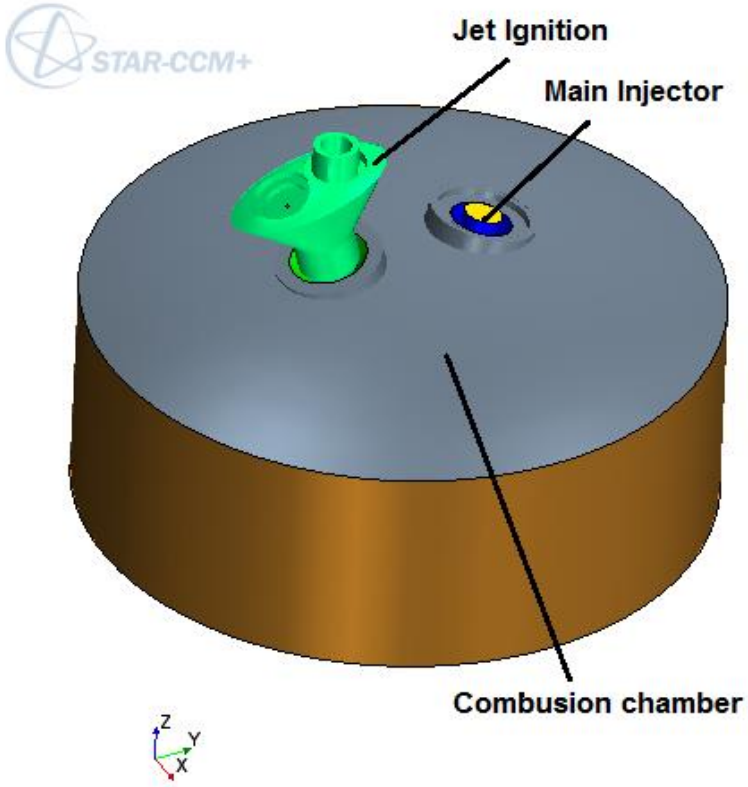

Figure 3.14 Two-stroke CFD model geometry

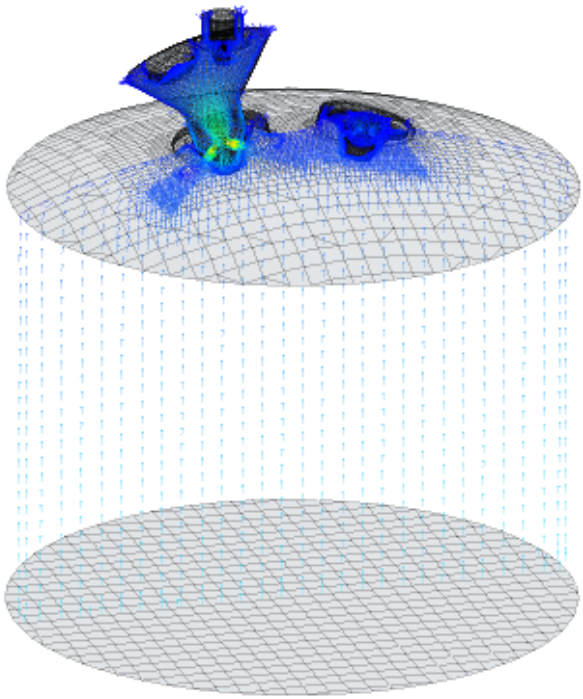

Figure 3.15 Two-stroke engine velocity diagram

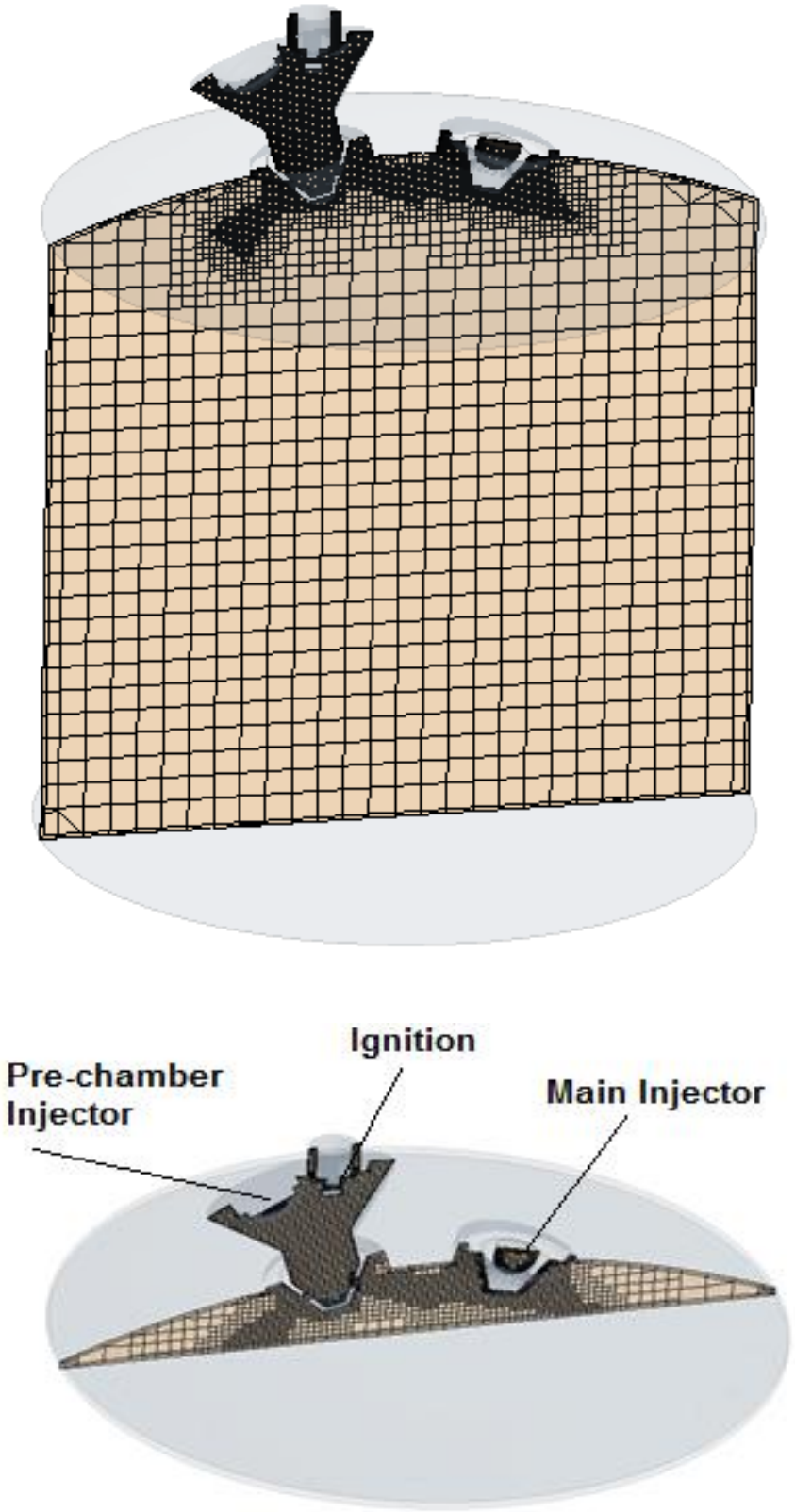

Figure 3.16 CFD mesh grid from BDC to TDC

3.2.2 Boundary Condition

It is critical that boundaries be appropriately separated and demarcated for both meshing and analysis. Two types of boundaries were used in this simulation, namely the wall boundary and mass flow inlet boundary.

The mass flow inlet boundary condition was applied at the jet ignition nozzle and the main injector nozzle. The quantity specified at the inlet was at a constant mass flow rate, which was obtained from the mass flow rate calculation. The turbulence intensity is set at 0.01 and turbulence viscosity ratio is 10. No-slip wall boundary conditions were applied to the cylinder wall, piston, head and valves. The physics condition of the cylinder wall is assumed to be smooth, impermeable and stationary. The surface of the piston top is a moving wall boundary (liner displacement).

Since this study is in the design stage, constant boundary conditions are selected for all the computational analysis. This model is focused on simulating combustion phasing and injection timing. The intake valve timing and exhaust valve timing were not simulated in the CFD model, and the intake and exhaust ports are assumed to be always closed during combustion. Boundary conditions such as initial pressure and temperature during CFD computation were obtained with RICARDO WAVE, while combustion analyses are obtained through STAR CCM+.

3.3 3D MODELLING METHODS

Coupled STAR-CCM and DARS-CFD simulations are performed with various injection timings. The engine works with direct injection of a gaseous fuel (H2) and jet ignition of a lean stratified mixture is made closer to stoichiometric in the central area below the jet ignition device.

3.3.1 Modelling Turbulence

The flow is turbulent and turbulence is modelled using a Reynolds-Averaged Navier-Stokes (RANS) turbulence model (Joel H. Ferziger 2002). To obtain the Reynolds-Averaged Navier-Stokes (RANS) equations, the Navier-Stokes equations for the instantaneous load and speed fields are deteriorated into a mean value and a fluctuating part. The averaging process may be thought of as time averaging for steady-state situations, and ensemble averaging for repeatable transient circumstance. The subsequent equations for the mean quantities are essentially identical to the original equations, other than an extra term now shows up in the momentum transport equation. This extra term is a tensor quantity, known as the Reynolds stress tensor, and has the following definition:

$$\mathbf{T}_t \equiv -\rho\overline{\mathbf{v}'\mathbf{v}'} = -\rho\begin{bmatrix}\overline{u'u'} & \overline{u'v'} & \overline{u'w'}\\ \overline{u'v'} & \overline{v'v'} & \overline{v'w'}\\ \overline{u'w'} & \overline{v'w'} & \overline{w'w'}\end{bmatrix}$$

Equation 3-1

Local turbulence is especially vital as it advances micro-scale mixing among the gas species. If the turbulence is too weak it would be impossible give fast mixing among the gas species, the micro-mixing process will intervene with the chemical kinetics. The turbulence intensity should influence combustion scaling reaction rates utilizing the Kong-Reitz model (Lumsden G. 1995):

$$s_i^{\,t} = s_i^{\,l} \frac{\tau_{kin}}{\tau_{kin} + f \cdot \tau_{turb}}$$

Equation 3-2

Where

$$\tau_{turb} = C \cdot \frac{K}{\varepsilon}$$

And

$$f = \frac{1 - \exp(-r)}{0.632}$$

$$r = \frac{m_{H_2O} + m_{H_2}}{1 - m_{N_2}}$$

It is broadly recognized that turbulence models are vague representations of the physical phenomena being simulated, and no single turbulence model is the best for each flow modelling. Consequently, it is necessary to provide a suite of models that reflect the current state of the art (CD-adapco 2013).

3.3.2 Modelling Combustion

Combustion is modelled by using homogeneous reactor models which serve as a placeholder for chemistry models. STAR-CCM+ provides the Dars-CFD Reaction model as the choice for complex chemistry. Star CD and STAR CCM+ are both very well-known CFD programmes and have been used for combustion analysis for more than 20 years (Allocca et al. 2005; Olmo & Thornton 2005).A detailed complex chemistry model is implemented in STAR-CCM+ with the Dars-CFD library. This library includes the stiff ODE (Ordinary Differential Equation) solver to integrate the chemical composition equations using gas mechanisms. General species transport equation is solved using chemistry ADI Algorithm(CD-adapco 2013).

The general species transport equation can be formulated as follows:

$$\frac{\partial}{\partial t}\rho Y_k + \frac{\partial}{\partial x_j}(\rho u_j Y_k + D_{k,j}) = \omega_k$$

Equation 3-3

Where $D_{k,j}$ is the diffusion flux component and source term ω_k is the rate of production of species k.

Within each time-step n, the fluid solver goes through a number of iterations. The current iteration is denoted with k. For steady-state simulations, n and k denote the same index.

Kinetics equations are obtained by using DARS-CFD (CD-adapco 2014). The kinetics equations use the A, n and E_a Arrhenius rate constants:

$$k = A \cdot T^n \cdot e^{-E_a / R \cdot T}$$

Equation 3-4

Where k is the rate coefficient, R is the gas constant, T is the temperature (K),E_a is the activiation energy and A is the pre-exponetial factor

STAR-CCM solves the Partial Differential Equations (PDEs) for energy and species conservation (Lehtiniemi 2007):

$$\frac{\partial}{\partial t}\rho Y_k + \frac{\partial}{\partial x_j}(\rho \cdot u_j \cdot Y_k + F_{k,j}) = 0$$

$$\frac{\partial}{\partial t}\rho h + \frac{\partial}{\partial x_j}(\rho \cdot u_j \cdot h + F_{h,j}) = \frac{\partial}{\partial t} p + u_j \cdot \frac{\partial}{\partial x_j} p + \tau_{i,j} \cdot \frac{\partial}{\partial x_j} u_i$$

Equation 3-5

While DARS-CFD solves the Ordinary Differential Equations (ODEs) for chemical kinetics (Lehtiniemi 2007):

$$\frac{\partial}{\partial t} Y_i = \frac{\omega_i \cdot W_i}{\rho}$$ Equation 3-6

Almost perfect mixing of products and reactants is normally accomplished when chemical kinetics is the constraining element of the reacting system under investigation, Nonetheless, regularly these mixing mechanisms have to depend on liquid motion or large-scale eddies and turbulence to provide the mixing.

Hydrogen combustion in air using a complex chemistry model of 9 species and 19 reversible reactions as detailed in the following equations:

Main Hydrogen Reactions (CD-adapco 2013):

1. $H_2+O_2 \rightarrow 2OH$
2. $H_2+OH \rightarrow H_2O+H$
3. $H+ O_2 \rightarrow OH+O$
4. $O+H_2 \rightarrow OH+H$
5. $H+O_2+M_1 \rightarrow HO_2+ M_1$
6. $H+2O_2 \rightarrow HO_2+O_2$
7. $H+ O_2+N_2 \rightarrow H O_{2+} N_2$
8. $OH+HO_2 \rightarrow H_2O+O_2$
9. $H+HO_2 \rightarrow 2OH$
10. $O+HO_2 \rightarrow O_2+OH$
11. $2OH \rightarrow O+H_2O$
12. $H_2+M_2 \rightarrow 2H+M_2$
13. $O_2+M \rightarrow 2O+M$
14. $H+OH+M_3 \rightarrow H_2O+M_3$
15. $H+ H_2O \rightarrow H_{2+} O_2$
16. $2H_2O \rightarrow H_2O_2+ O_2$
17. $H_2O_2+M \rightarrow 2OH+M$
18. $H_2O_2+H \rightarrow HO_2+H_2$
19. $H_2O_2+OH \rightarrow H_2O+HO_2$

Table 3-2 provided some important hydrogen chemical properties in engine combustion.

Table 3-2 Hydrogen combustion chemical properties

	H_2	O_2	H	O	OH	HO_2	H_2O	H_2O_2	N2
Molecular weights	2.01	32.0	1.005	16.0	17.005	35.005	18.01	24.01	28.0
For each species:									
Density	Ideal gas								
Molecular viscosity	1.76×10^{-5} Pa.s								
Specific heat	Determined via thermodynamic polynomial functions								
Thermal conductivity	Determined via the Lewis number								

A premixed mixture of hydrogen and air enters inlet at a pressure of 1 bar and a temperature of 1000K.

3.4 1D CAE MODEL IN WAVE

A CAE tool is used to define the engine operation in full cyclic. Computer-aided engineering simulations are modelled using Ricardo WAVE. Wave is CAE software to analyse the dynamics of mass flows, pressure waves, and energy losses in cylinder, injectors, orifices and ducts, and the intake and exhaust manifolds of various combustion modes

and engines. Wave Build allows simulations to be performed almost on any intake, exhaust and combustion system design.

Two 1D CAE models has been set up in WAVE. They are direct injection and non-direct injection two-stroke system as shown in Figure 3.17 and Figure 3.18. The aim of this simulation is to compare and improve the top load and part load engine efficiency in direct and non-direct system CAE models. Moreover, the combustion burn angle obtained from CFD simulation is translated into WAVE to investigate the extended lean limit of jet ignition, and compare engine efficiency map between jet ignition and conventional spark ignition.

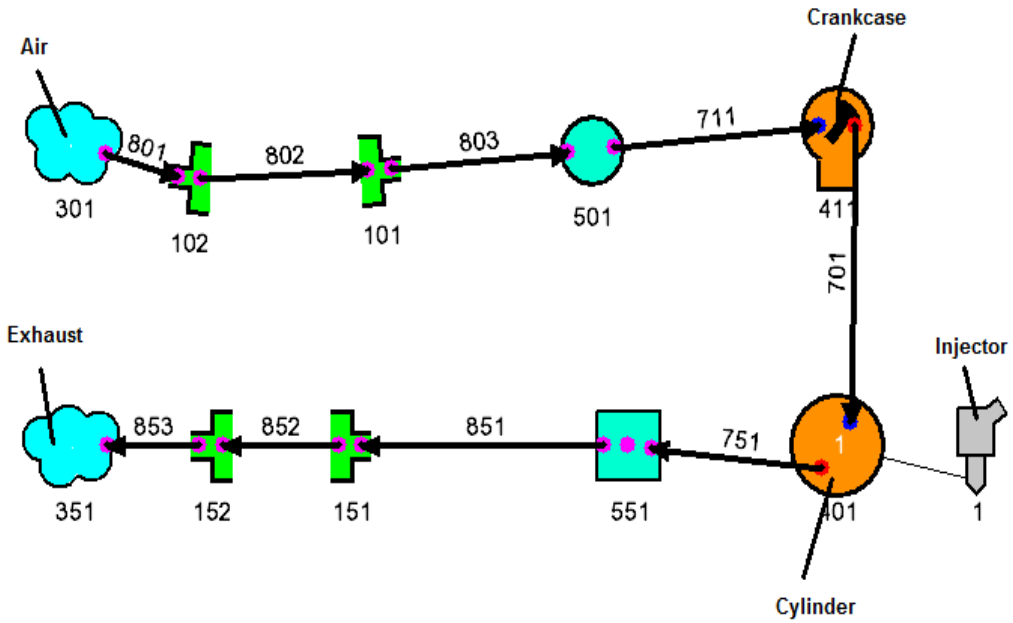

Figure 3.17 Single cylinder DI two-stroke engine in Ricardo WAVE

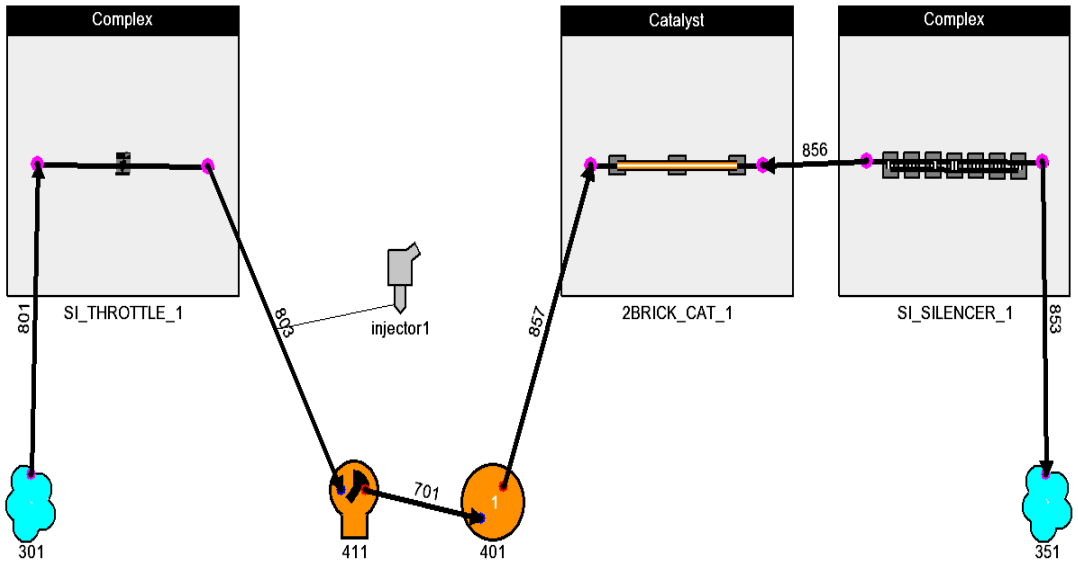

Figure 3.18 Single cylinder port fuel injection two-stroke engine in Ricardo WAVE

3.5 1D MODELLING METHODS

The WAVE solver is designed to read a model containing the geometry of the model network which contains flow and control elements, and initial conditions for the flow field and all control data for the run.

The mass flow calculations in the flow network are solved as one dimensional compressible flow equation governing the conservation of mass, speed and energy. The flow network is split into a number of small volumes and the governing equations are then written in a finite difference form for each of these elementary volumes.

The mass and energy equations are used to solve mesh system, and each volume and the momentum equation is used to solve each boundary between volumes. The equations are written as:

$$mass = \frac{dm}{dt} = \sum \dot{m}$$ Equation 3-7

$$energy = \frac{de_T}{dt} = \sum mh + sources$$ Equation 3-8

$$momentum = \frac{dmu}{dt} = -A\frac{dp}{dx}dx + \sum \dot{m}u - sources$$ Equation 3-9

The solution of the governing equations is obtained by the application of a finite difference technique utilizing the finite-volume approach to the discretization of the partial differential equations. The time-differencing is based on the explicit technique, with the time-step conducted by the Courant condition.

In terms of the geometry and governing the equations, this solution is better than the method of characteristics because it does not require the inaccurate and cumbersome ad hoc treatment.

These ad hoc treatments, which are inherent in the method of characteristics, introduce inaccuracies specifically in the areas of source terms such as heat transfer, friction, distributed losses, and boundary conditions at locations of abrupt area change, junctions of multiple ducts, and bends.

On the other hand, Ricardo Wave is able to solve these problems accurately, and with no special difficulty, due to its solution technique and basic formulation.(RicardoSoftware 2010)

The two-stroke engine combustion used the Weibe function model. The Wiebe function is widely used to predict the mass fraction and burn rate with various fuels and combustion systems in IC engines. These include traditional spark ignition engines and direct injection petrol engines, direct injection and indirect injection diesel engines, premixed charge compression ignition engines and homogeneous charge compression ignition engines. This relationship allows the independent input of function shape parameters and of burn duration. (Ghojel 2010)

The cumulative mass fraction burned (W) as a function of crank angle θ is shown below:

$$W = 1.0 - \exp\left(-AWI\left(\theta/BDUR\right)^{(WEXP+1)}\right)$$ Equation 3-10

where: *AWI* = Internally calculated parameter of end of combustion completeness level

θ = Degrees past start of combustion

BDUR = Total combustion duration

WEXP = User-entered exponent in Wiebe function

The simulation input parameters of burn profile can be adjusted to observe the effects of combustion duration. The entire combustion cure position can be moved forward or backward by setting 50% burn point profile. The total combustion duration can be extended longer or compressed shorter by setting the 10%-90% duration profile. The Wiebe exponent is controlling the shape of the Wiebe curve.

By default, Spark-Ignited combustion models in WAVE follow a constant combustion air/fuel ratio under the assumption that the fuel-air mixture is fully premixed.

3.6 OPERATION CONDITION

The computational starts at the intake valve closure and ends at the exhaust valve opening. The initial condition is set by CAE simulation results with temperature is 450K and pressure is 1.5bar. The simulation runs one revolution starting at BDC as 0^0 CA and ending at BDC as 360^0 CA. Computational mesh at bottom and top dead centres are shown in Figure 3.16. The model consists of 200,000 polyhedral cells for minimized memory and computational time. Piston moves present compression and power strokes, with the computational domain made up of the in cylinder volume contract or expends accordingly. Morphing motion in STAR CCM+ redistributes mesh vertices according to the variable in- cylinder space by changing the grid density while maintaining the shape and size of the elements. The spark discharge in the pre-chamber is simulated with a small sphere in between the electrode and acts as pulse temperature igniter, rising the temperature up to 2500K at specific spark duration. Simulations have been performed neglecting scavenging and residual gases within the cylinder and pre-chamber during intake valve closure.

Table 3-3 shows the operating condition for the engine in STAR CCM+.

Table 3-3 Engine Operating boundary Condition

Engine speed	7500 rpm
Compression ratio	15
Exhaust Port Open	85 °CAD BTDC
Exhaust Port Close	275 CAD BTDC
Intake Port Open	115 CAD BTDC
Intake Port Close	244 CAD BTDC
Pre-chamber injection timing	175 – 185 CAD BTDC
Pre-chamber spark ignition timing	180 – 185 CAD BTDC
Early injection timing	140 – 160 CAD BTDC
Stratified injection timing	150 – 170 CAD BTDC
Diffusion injection timing	160 – 180 CAD BTDC
Fuel type	Hydrogen, H_2

3.7 HOMOGENEOUS REACTOR SIMULATIONS

Other simulations have been performed exploring the different opportunities available to work low loads in high compression ratio, high turbocharging environment.

DARS-CFD homogeneous reactor simulations are performed for the auto-ignition of a homogeneous H_2-air mixture.

Close to HCCI combustion efficiency may be achieved working with fuel-to-air ratios smaller than the HCCI values for top dead centre (TDC) auto-ignition, and then using the jet ignition to start the very rapid combustion process making stable an otherwise unstable process.

In homogeneous charge spark ignition system, the fuel and oxidizer are premixed. However, rather than using a spark plug electric discharge to ignite a small portion of the mixture in the pre-chamber and start a flame burning the mixture travelling towards the boundaries of the combustion chamber, the temperature and pressure of the air/fuel mixture are increased during compression process until the entire mixture reacts spontaneously and simultaneously. Because there is no direct initiator of combustion, HCCI is extremely challenging to control, reasons why this combustion mode is not practically used in any production engine.

The use of bulk ignition by jet ignition of partially burned hot combustion gases may produce a controlled-HCCI operation with mixtures controlled to have auto-ignition at top dead center or slightly later with a relatively wide range of gas parameters rather than the difficult HCCI-operation with very narrow oscillations of the gas parameters about the necessary values. HCCI is producing a nearly isochoric combustion that from a thermodynamic point of view delivers the maximum piston work for a given amount of fuel energy introduced within the cylinder. To keep peak pressures within reasonable limit, the fuel to air equivalence ratio Φ has to be kept low, or the air to fuel equivalent ratio $\lambda = 1/\Phi$ has to be kept high, very far from stoichiometric.

Direct injection of the fuel coupled to jet ignition or Diesel ignition is the way to achieve a pressure limited cycle where the top dead center isochoric combustion of the premixed mixture from early is followed by the ideally constant pressure diffusion controlled combustion of late injection. High speeds of actuation of the direct fuel injector and high flow rates are prerequisite of the HCCI controlled operation modulating premixed and diffusion combustion processes. The auto ignition of

premixed air hydrogen mixtures in Diesel-like conditions is studied here with a Stochastic Reactor Model.

DARS (2014) is a program to analysis of complex chemistry in combustion engine applications. It includes chemical kinetic models tailored for specific conditions and handles the gas phase chemistry. DARS consist of many reactor tools for use with the chemical models such as the Stochastic Reactor Model (SRM). The idea behind the SRM is that the assumption of homogeneity within the combustion chamber is replaced by statistical homogeneity, with physical quantities described by Probability Density Functions (PDF) distributions. This is realized by dividing the mass into a random number of virtual particles. Each particle has a chemical composition, a temperature and a mass, and is able to mix with other particles and exchange heat with the cylinder walls. Since the model is 0-dimensional, no information is provided on the position of the particles. Initial conditions of the gas properties are defined at intake valve closure (IVC). Development of the in-cylinder combustion then follows a time integration in which the volume changes doe to the piston motion and events such as turbulent mixing, heat transfer and chemical reactions are solved. Even though there is no strict position in space for the particles, there is a distribution of the particle properties that mimics the phase-space variations of the cylinder contents giving the SRM a more realistic behaviour than a homogeneous model. The heat transfer model is based on the Woschni correlation and the mass fraction burned is ultimately controlled by the chemical kinetics. This model may provide reasonable results given that the model parameters are well calibrated vs. experiments and the number of particles is high. The SRM calculates over time the in-cylinder conditions such as species concentrations, density, pressure, temperature, cylinder volume, heat release, heat transfer. Combustion duration and auto-ignition timing can be determined through SRM simulations.

3.8 WHY HYDROGEN FUEL?

The simulations have been performed with hydrogen fuel. The reasons are because hydrogen has simpler chemistry when compared to other fuel sources (CNG, petrol etc.), and it also reduces the simulation time and requires less calculation time.

Hydrogen is the lightest element in the universe. The complete combustion of hydrogen is clean and H_2 is much simpler than the detailed chemistry of CH_4 or $C_3 H_8$. In addition, hydrogen is reducing the simulation time as it is simple chemistry. CH_4 or $C_3 H_8$ need more simulation time to calculate the generated equations.

3.9 MASS FLOW RATE CALCULATION

The engine speed is 7500 RPM, while the air-to-fuel equivalent ratio of the hydrogen fuelled engine is λ =2. Spark is advanced with reference to top dead center position to allow combustion initiation. Kinetics is important in the early stage of combustion. The combustion started as soon as the pre chamber is fully initiated, then the products are quickly spread all over the main chamber to burn the rest of fuel within a short time. Ignition starts the combustion that propagates quickly to the pre-chamber and then to the main chamber.

Injector boundary conditions are set up to achieve sonic flow conditions at the main injector holes. Injection pressure is 300 bar for the main injector. The total flow area is 0.7 mm^2. The main injector is made of 16 nozzles of 0.25 mm diameter each. With H_2, the speed of sound is 1290 m/s. Pre-chamber injector is single hole and jet ignition is made of 12 nozzle of 0.20mm diameter each.

3.9.1 Main Chamber

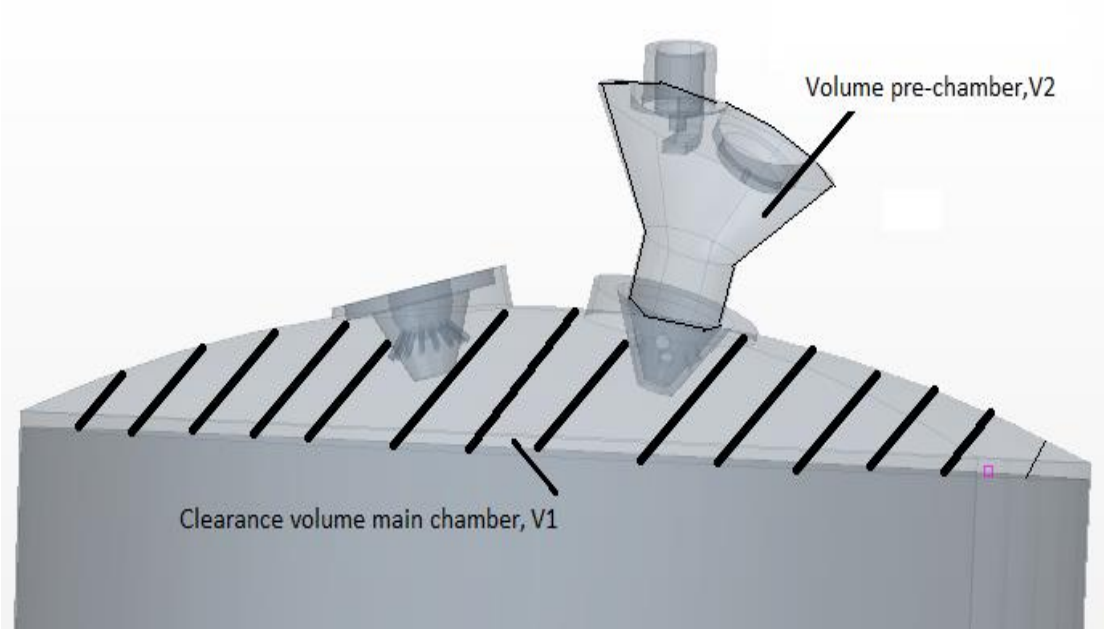

Figure 3.19 Combustion volume

Initial conditions are at bottom dead centre (BDC). Temperature is 450K. Pressure is 1.5bar. Composition is all air.

Mass of air = 0.195g

$\lambda = 2$

Thus, Mass of fuel (Hydrogen),

$$m_{(main,H2)} = \frac{0.195/34.3}{2} = 0.0028426g$$

$$M = \Delta t \cdot \rho \cdot v \cdot A \qquad \text{Equation 3-11}$$

$$\dot{m} = \frac{M}{\Delta t} \qquad \text{Equation 3-12}$$

$\Delta t = 20^0\, CA$

$$In\ time = \frac{20}{6N} = \frac{20}{6 * 7500} = 4.44444 \times 10^{-4} s$$

Thus, $\dot{m} = \frac{0.0028426/1000}{4.44444 \times 10^{-4}} = 0.00639585$

3.9.2 Pre-Chamber

Clearance volume, $V_1 = 28555\, mm^3$

Pre-chamber volume, $V_2 = 1442\, mm^3$

Mass of air in pre-chamber,

$m_{(pre-chamber,air)} = 0.195 * 0.05 = 0.00975g$

Mass of Hydrogen in pre-chamber,

$m_{(pre-chamber,H2)} = \frac{0.195 * 0.05}{34.3} = 0.0002842566g$

$M = \Delta t \cdot \rho \cdot v \cdot A$

$\dot{m} = \frac{M}{\Delta t}$

$\Delta t = 10^0\, CA$

$In\ time = \frac{10}{6N} = \frac{10}{6 * 7500} = 2.22222 \times 10^{-4} s$

Thus, $\dot{m} = \frac{0.00028426}{2.22222 \times 10^{-4}} = 0.0012791547$

3.10 INJECTION STRATEGIES

For each injection strategy, the same amount of fuel is injected in the main and pre-chambers for all strategies and are kept constant.

For early injection, fuel in main chamber is injected during compression and premixed with air to create homogeneous mixture in the main

chamber. Fuel is injected close to TDC to create a cloud of fuel close to the jet ignition nozzles to create charge stratification, while fuel in the main chamber is injected before TDC up to TDC producing diffusion-like charge. However, early injection is more likely to "knock".

For stratified injection, the fuel is injected into the cylinder just before ignition. This allows a leaner air/fuel ratio combustion and avoids engine knock when operating at higher compression ratios. Figure 3.20 presents the H_2 mass fraction at firing top dead center below the cylinder head evidencing charge stratification.

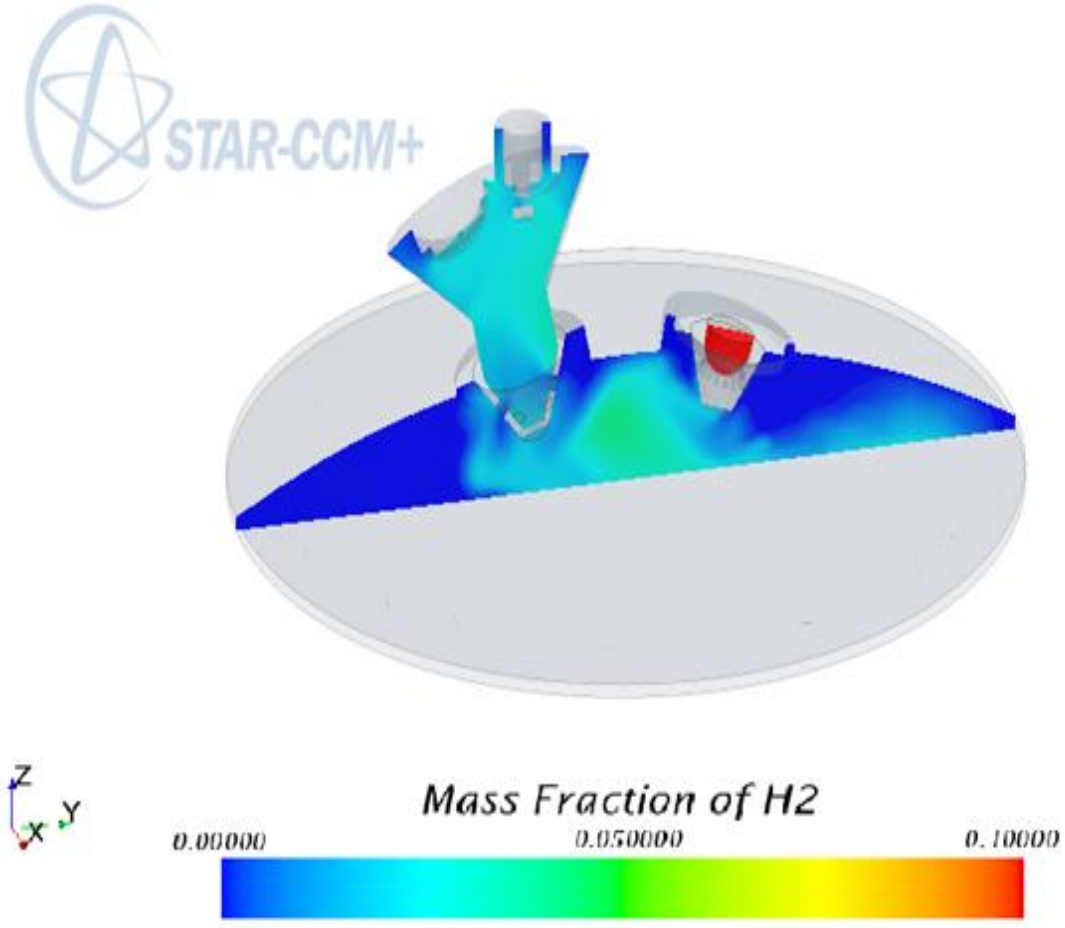

Figure 3.20 Mass fraction of H_2 near TDC

For diffusion injection, the fuel is injected very close to TDC. This reduces the pollutant emission and improving pumping loss, and the mechanical efficiency and the fuel economy of the engine are improved.

3.11 SUMMARY

This chapter first presented two-stroke engine design approach and CAD modelling methodologies. In addition, a summary of 1D CAE model and CFD combustion modelling that was completed during this study, including explanation of the software packages occupied, was provided. Followed by this is a discussion of using hydrogen as a single fuel sources in this simulation. Moreover, necessary calculation of mass flow rate was provided. Lastly, descriptions of different injection strategies, along with simulation data are provided.

CHAPTER 4

4.SIMULATION RESULTS

4.1 CFD SIMULATION RESULTS

The combustion efficiency of jet ignition coupled with direct injection in two-stroke engine was observed through 3D CFD computational software, Star CCM. The goal of this study is to compare the various combustion modes and optimise the injection timing, spark plug timing and combustion duration.

4.1.1 Effect of Injection Timing

Fuel injection timing plays an important role in the air/fuel mixing process. Three runs (early, Stratified and diffusion) were completed with different injection timing as can be seen in Table 4-1. The same amount of fuel is injected in the main chamber and pre-chamber for all strategies. The spark plug is set to retard from 180 to 185 CA degrees for all combustion modes.

Table 4-1Three combustion modes operation condition

Spark ignition timing	180 - 185 CAD BTDC
Pre-chamber injection timing	175 - 185 CAD BTDC
Pre-chamber spark ignition timing	180 - 185 CAD BTDC
Early injection timing	140 - 160 CAD BTDC
Stratified injection timing	150 - 170 CAD BTDC
Diffusion injection timing	160 - 180 CAD BTDC
Fuel type	Hydrogen, H_2

Figure 4.1 and Figure 4.3 shows the average cylinder temperature and pressure plots in the combustion chamber over crank angle. The range plotted is the significant degree crank angle in the combustion process of two-stroke engine. Based on the plots, all three modes of combustion show a similar trend with the early mode having the highest peak temperature at about TDC. The stratified mode has peak temperature at 186 crank angle degrees and illustrates a good pattern in combustion chamber while the diffusion mode shows the lowest peak temperature. In early injection, pressure is building up earlier than the start of combustion in pre-chamber due to the mixture pre-ignited in the combustion chamber. As expected from the temperature plot, stratified mode experiences peak pressure during power stroke while diffusion produces the lowest peak in-cylinder pressure.

IMEP was calculated numerically and each injection strategies are compared in Table 4-2.

Table 4-2 IMEP values for each injection strategies

Injection strategy	Early	Stratified	Diffusion
IMEP (bar)	5.01	4.55	4.69

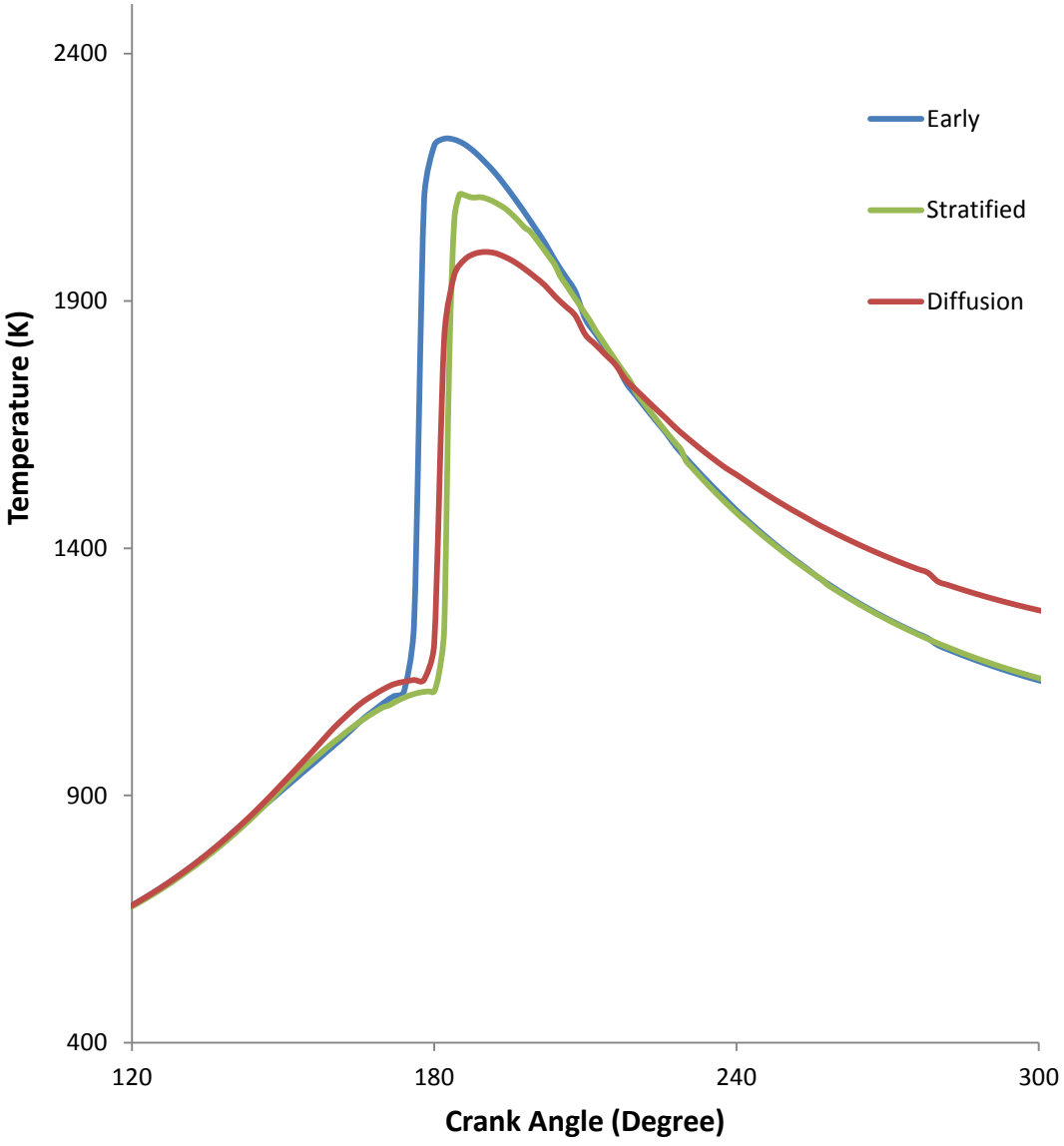

Figure 4.1 Temperature vs. Crank Angle at different combustion modes

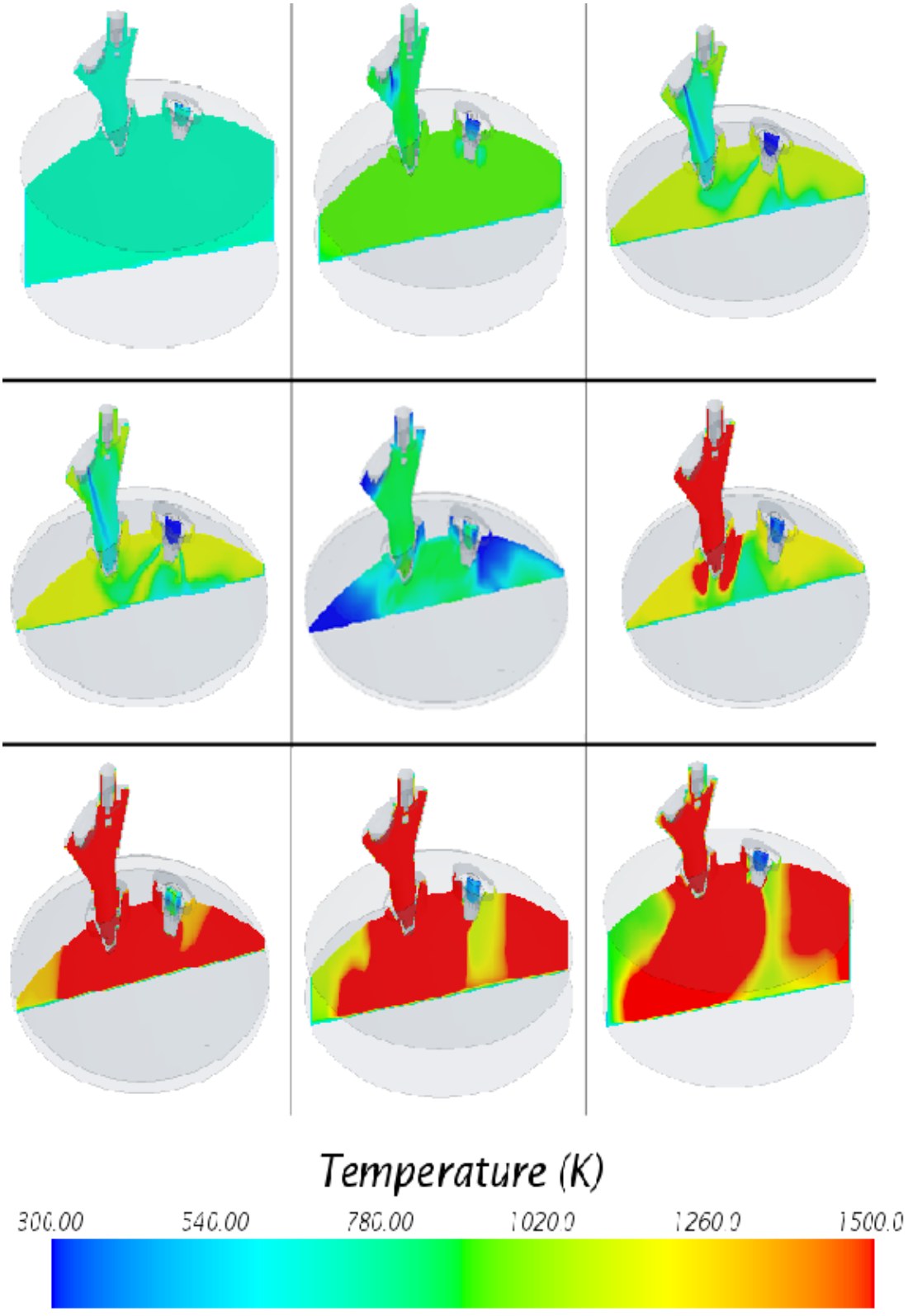

Figure 4.2 Temperature from 130 to 230 CA degrees in stratified combustion mode

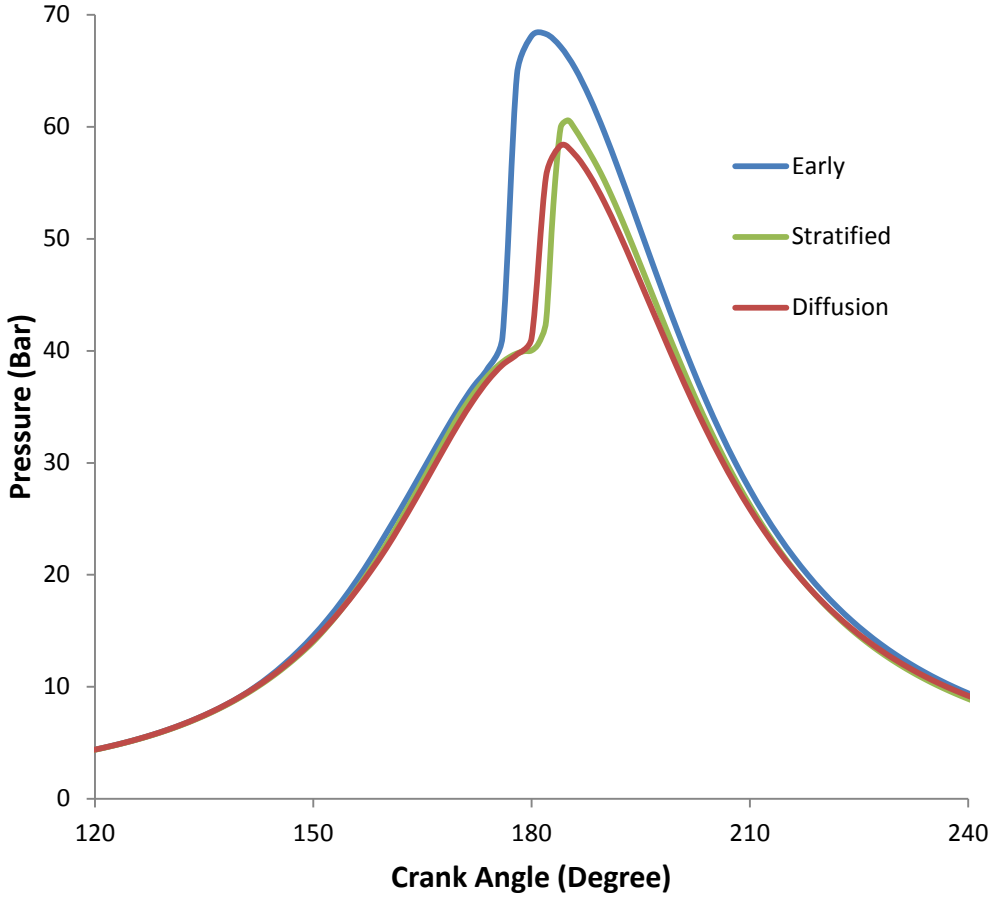

Figure 4.3 Pressure vs. Crank Angle at different combustion modes

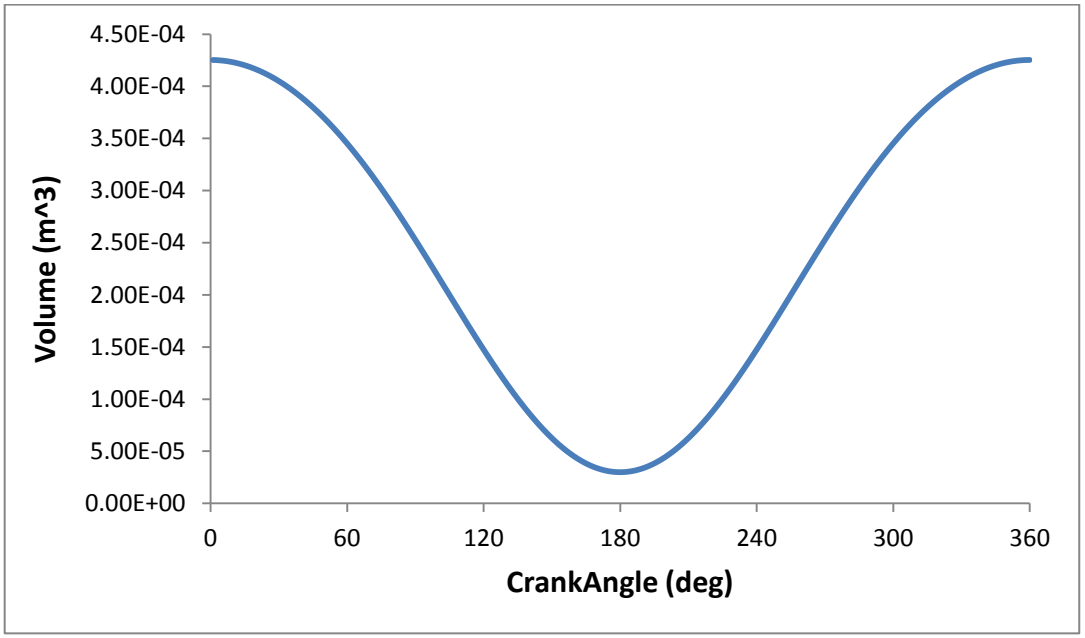

Figure 4.4 Volume vs. Crank Angle

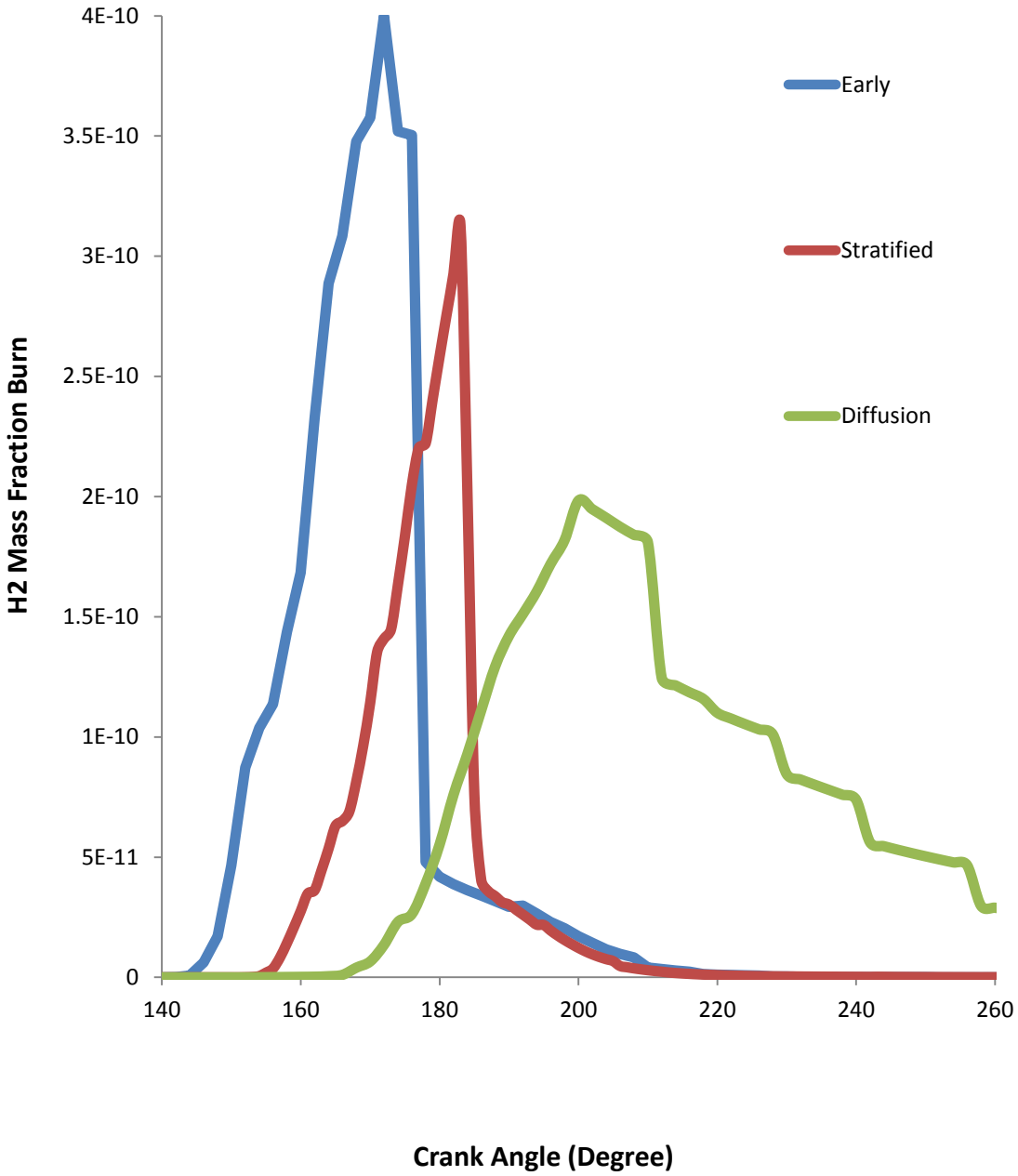

Figure 4.5 Fuel mass fraction with constant total fuel injected at different combustion modes

The analysis of the mass fraction burn (MFB) angles is shown in Figure 4.5 for all the combustion strategies. The 10-90% burn duration which indicates the mixture ability to propagate a flame is the main interest in

this study. It is noted that different combustion strategies were tested with the same amount of fuel to control the energy input for combustion.

In early combustion, the fuel injection is from 140 – 160 degree. The 10-90% burn duration for early combustion is the shortest which gets burned within 6 degrees CA. However, the energy produced during the combustion was subtracted by the compression movement of the piston. It is noted that for early combustion, pre-ignition occurred at 175 degrees (Figure 4.7); 5 degrees before TDC. Fuel that is injected during compression provides nimiety times for the fuel and air to fully mix when associated with increase of in-cylinder pressure reacting to self-ignite. In addition, hydrogen in oxygen has the lowest MIE (minimum ignition energy), which leads to uncontrolled pre-ignition problems.

For stratified combustion, the fuel is injected at 150 – 170 degrees CA to create a cloud of fuel (high concentration of in fuel respect to air in combustion chamber) underneath the jet ignition nozzle as shown in Figure 4.8. The 10-90% mass burned duration is short and gets burned within 8 degrees CA and 50% fuel burdened within 3.5 degrees CA (Figure 4.6) due to well pre-mixed fuel and air, which burned instantaneously with most of the combustion energy translated to power stroke. Stratified charge results in significantly increased burn rates, with faster flame initiation and hence propagation with constant total fuel injected (Attard et al. 2011). Hot gases through the jet ignition nozzle ignite the high concentration of fuel almost instantaneously. However, it can be seen that the combustion is not fully complete due to some of the fuel being distributed far from jet ignition and distributed close to the combustion chamber wall that is cold. This reduces heat transfer from the burned to unburned mixture.

	A	B	C	E	
1	CrankAngle	H2 mass fraction			
2	1	3.10E-63	3.129E-10	Maximum	
3	2	3.52E-63	2.81624E-10	90%	
4	3	4.47E-63	1.56458E-10	50%	
5	4	5.87E-63	3.12915E-11	10%	
6	5	7.44E-63			
7	6	8.99E-63			
8	7	1.04E-62			
9	8	1.16E-62			
10	9	1.26E-62			
11	10	1.34E-62			
181	180	2.76E-10			
182	181	2.93E-10			
183	182	3.13E-10	max fuel	2.82E-10	10% MFB
184	183	2.02E-10			
185	184	7.62E-11		1.56E-10	50% 'MFB
186	185	4.04E-11			
187	186	3.59E-11			
188	187	3.38E-11			
189	188	3.13E-11			
190	189	3.03E-11			
191	190	2.81E-11	90% mfb		
192	191	2.61E-11			
193	192	2.40E-11			

Figure 4.6 10-90% burn duration results for stratified combustion.

In diffusion combustion, the fuel injection is from 160 – 180 crank angle degree. It produces slow combustion as shown in Figure 4.9. This is because when fuel is injected from 160 to TDC, there is not enough time for the fuel to mix with air. Consequently, it took almost 70 Crank angle degrees to burn 90% fuel as shown in Figure 4.5.

Stratified combustion proved to be the best combustion mode for application of a jet ignition device and direct injection in a two-stroke engine. Jet ignition pre-chamber has the ability to control the combustion mixture and combustion strategy. However to further benefits from this advantage, some optimizations are required. The jet ignition nozzle angle needs to be aligned with the main injector nozzle for the hot product of combustion from pre-chamber to ignite the main chamber mixture.

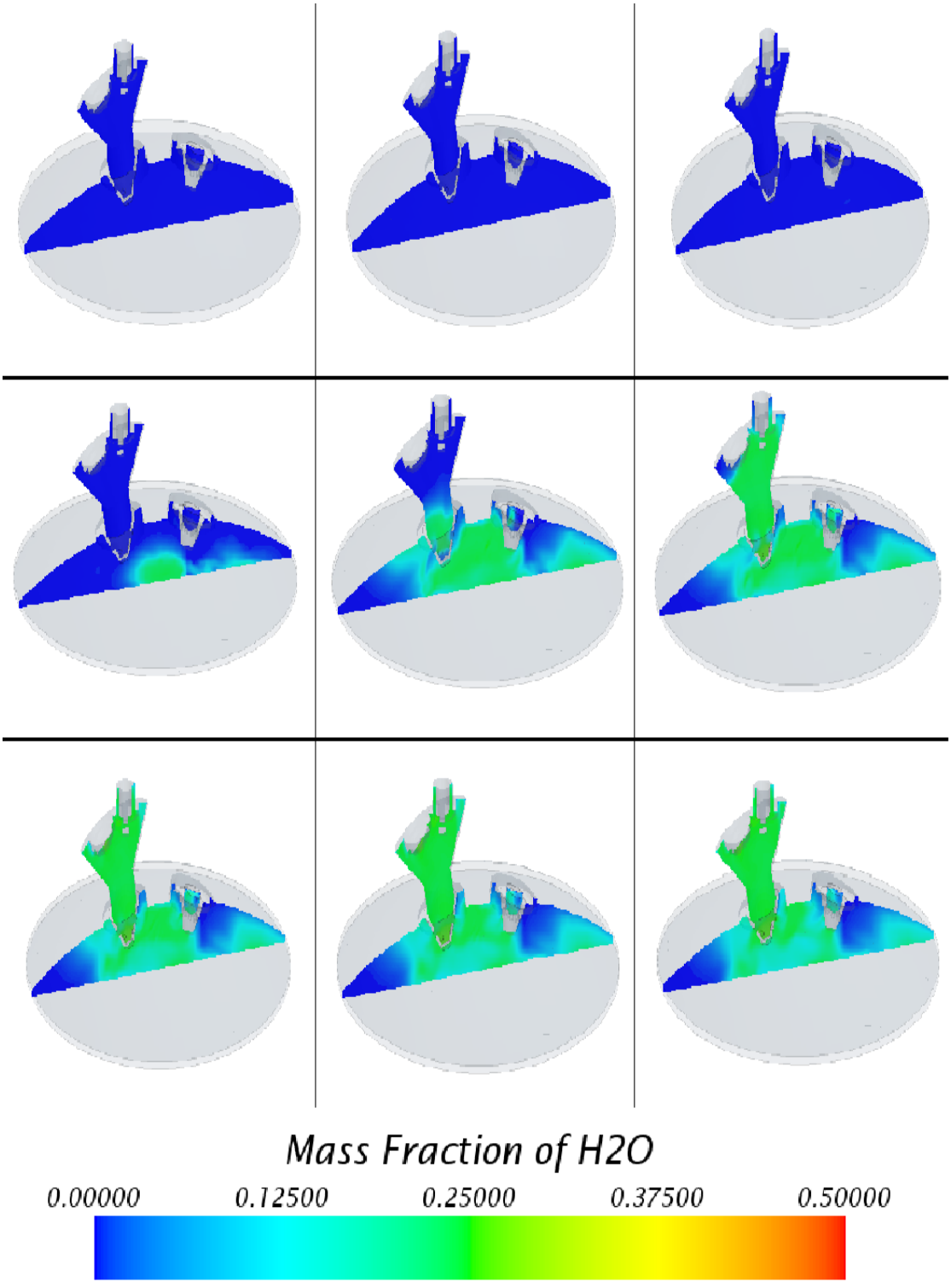

Figure 4.7 Pre-ignition occurred in early combustion mode around 175 CA degrees

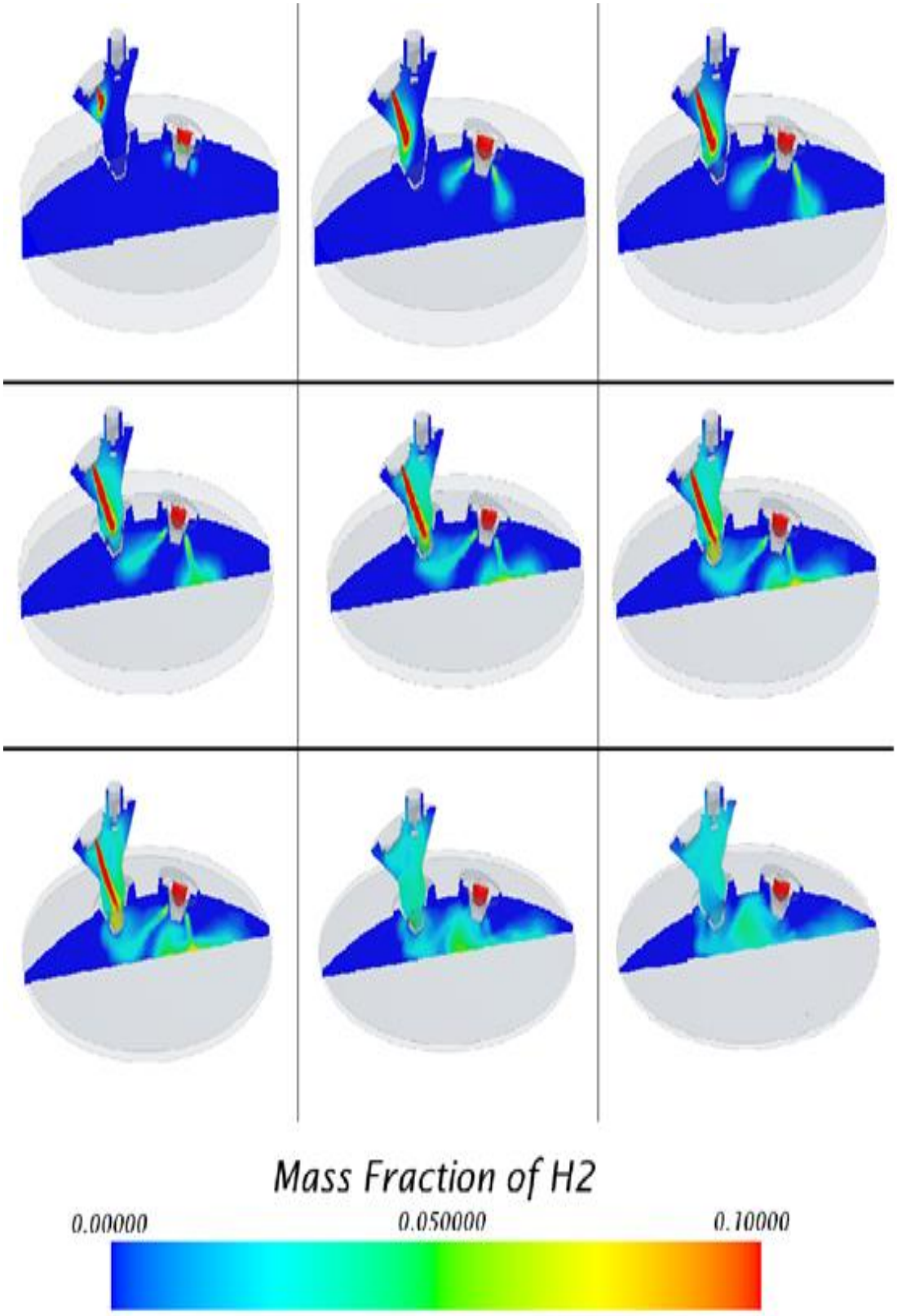

Figure 4.8 Cloud underneath injector nozzle from 150 to 180 CA degrees and achieved Stoichiometric mixture on stratified combustion

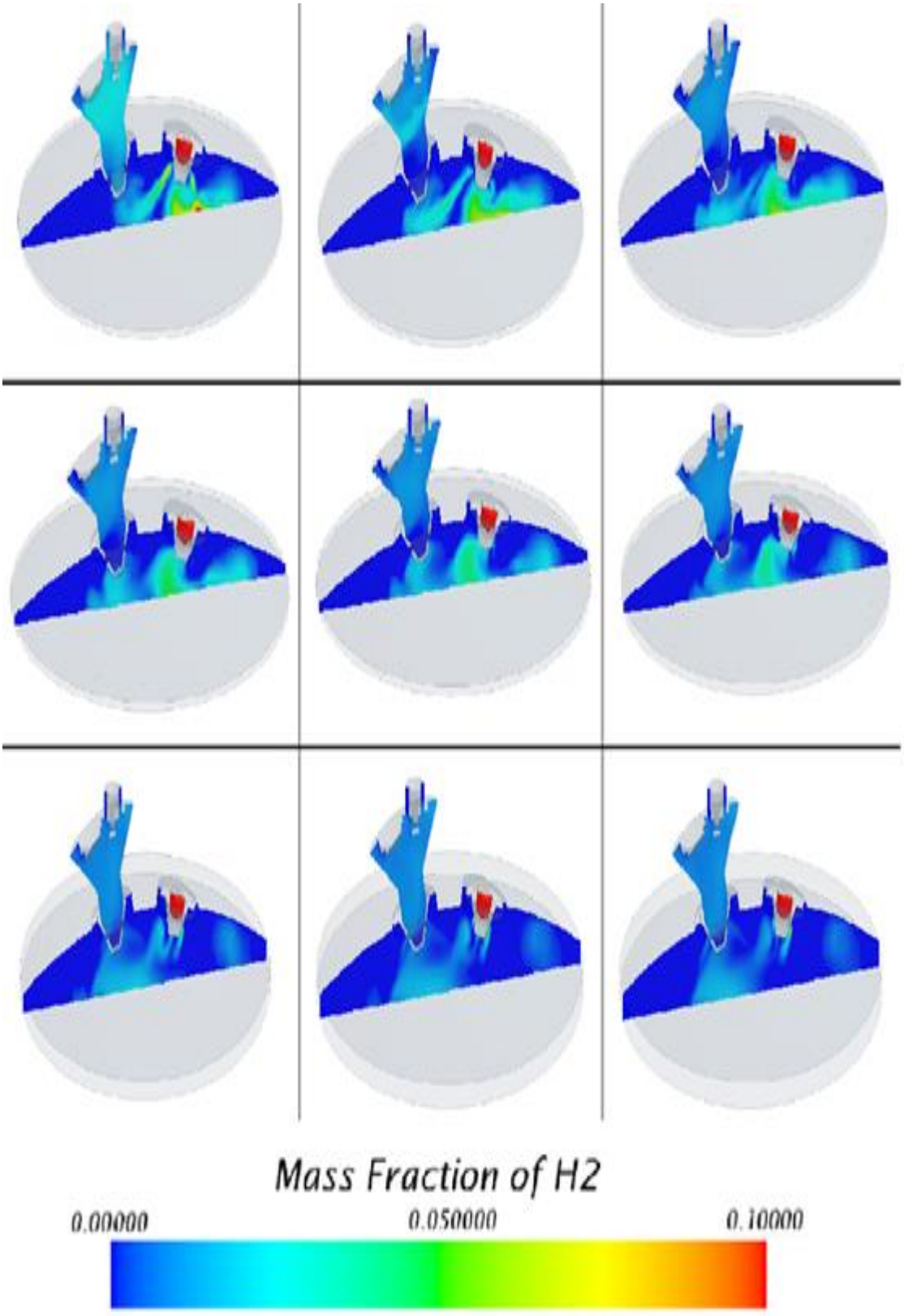

Figure 4.9 the unburned hydrogen fuel in combustion chamber after TDC in diffusion combustion

4.2 VALIDATION WITH PREVIOUS RESULTS

The major advantage of jet ignition system is to allow the combustion process to be completed faster. This is due to ignition system producing multiple, distributed ignition sites which charge the main combustion chamber rapidly. This has been numerically simulated and experimental validated by GM (1975), Toulson (2008) and MAHLE powertrain (William P. Attard 2012). The numerical results obtained from the current study were validated against published experiments and modelling data, to establish whether modelling results are reliable and a good indication of what occurs during the combustion process. These data were obtained from a previous investigation on a single cylinder coupled with hydrogen assisted jet ignition CFR engine by Toulson (2008).

A single cylinder coupled with hydrogen assisted jet ignition CFR engine was used for the Toulson (2008) experimental test. The CFD modelling was done in STAR/KINetics. STAR CCM plus detailed chemical kinetic model has been validated for internal combustion engines test cases (Binjuwair & Ibrahim 2013; Riegler & Bargende 2002).

Figure 4.10 shows a comparison of the H_2- Gasoline modelling and experimental results for MFB at $\lambda = 1.7$ with CFR engine in Toulson (2008) report.

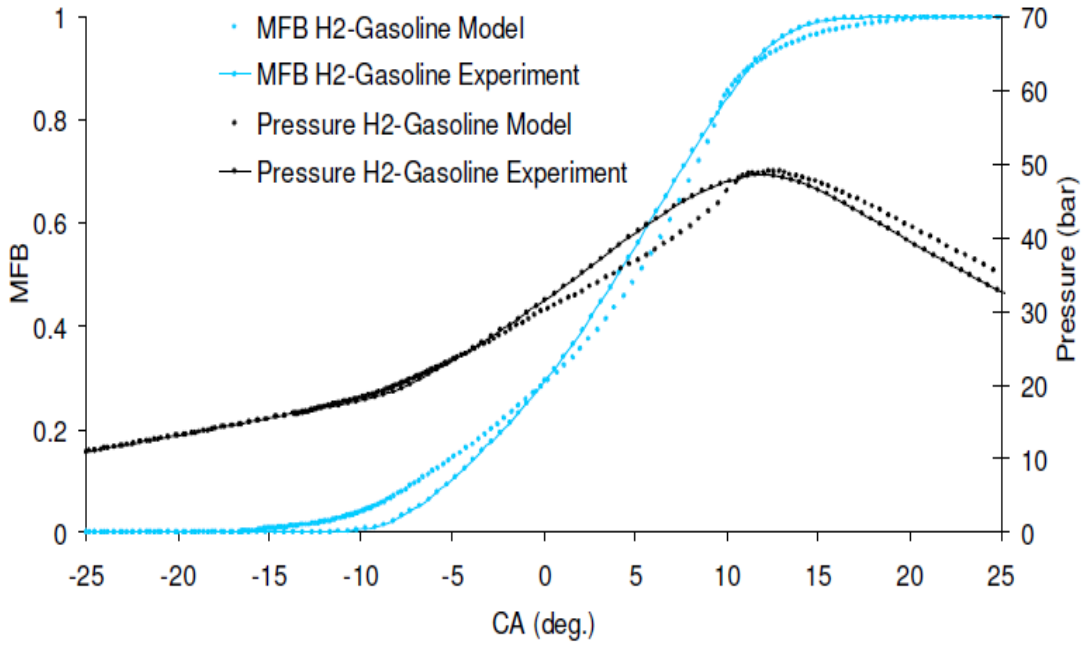

Figure 4.10 Experimental and modelling comparison of H2-Gasoline (λ=1.7, 1200 rev/min, CR=11 and WOT) (Toulson 2008)

The MFB data shown in Figure 4.10 indicates that 90% of fuel gets burned within 10 CA degrees. The comparison shows that CFD simulation results are very close to experimental results.

4.3 1D CAE Simulation Results

The 1D simulation was performed with WAVE. Wiebe function is used as a primary combustion model and it was applied on all engine cylinder elements. The mass fraction and burn rate results were obtained from previous CFD simulation with stratified injection.

4.3.1 1D CAE Two-stroke Engine with Direct Injection and Jet Ignition Simulation Results

The baseline two-stroke direct injection engine model was delivering top efficiencies in the mid 30% range sharply decreasing with load. The new engine shows the ability, thanks to the higher compression ratio (from 12 to 15). But more than that, thanks to the coupled direct injection and jet ignition of the gaseous fuel permitting fast combustion rates and load

control throttle-less to achieve high 20% and above 30% efficiencies over a significant portion of the speed and load range.

Worthy of note, combustion is modelled with a Wiebe function of the same 50% mass fuel burned 5 degrees crank angle after top dead center and combustion duration 10-90% of 7.5 degrees crank angle for all the operating points. Properly developed jet ignition well coupled to direct injection may produce even shorter combustion durations of bulk confined premixed mixtures.

The advantages of precise lubrication (no oil premixed with the fuel, no oil burning in the combustion chamber), in terms of combustion speed and friction mean effective pressure reductions are disregarded.

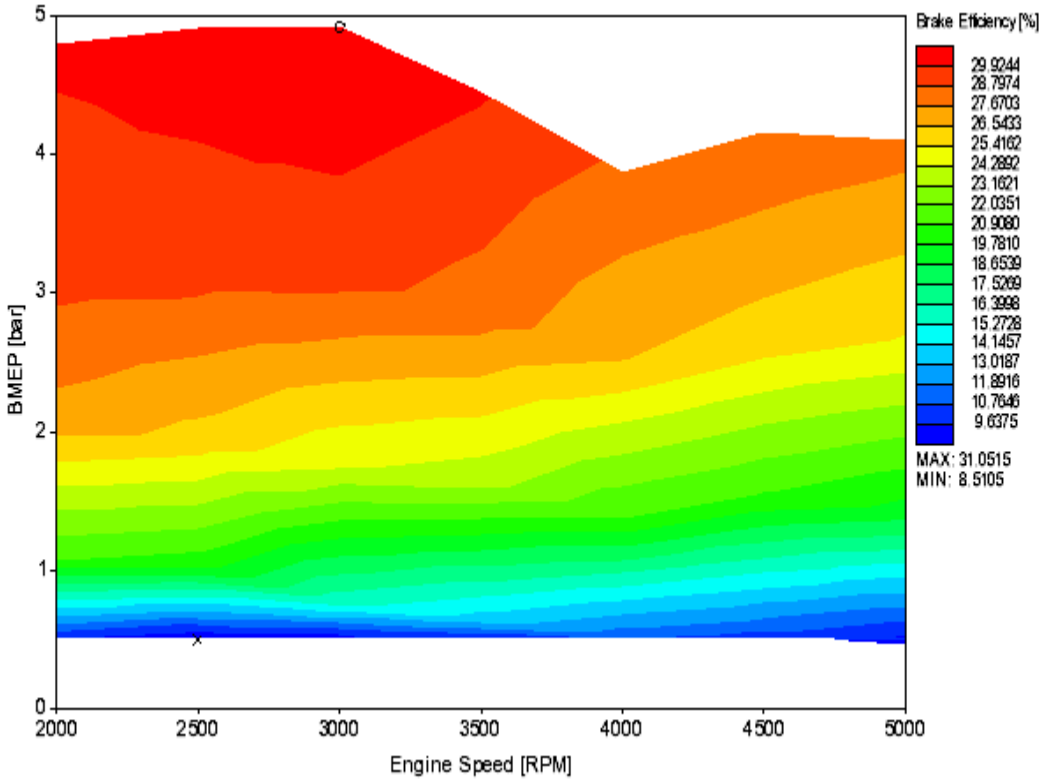

Figure 4.11 Computed brake efficiency vs. the brake mean effective pressure and engine speed.

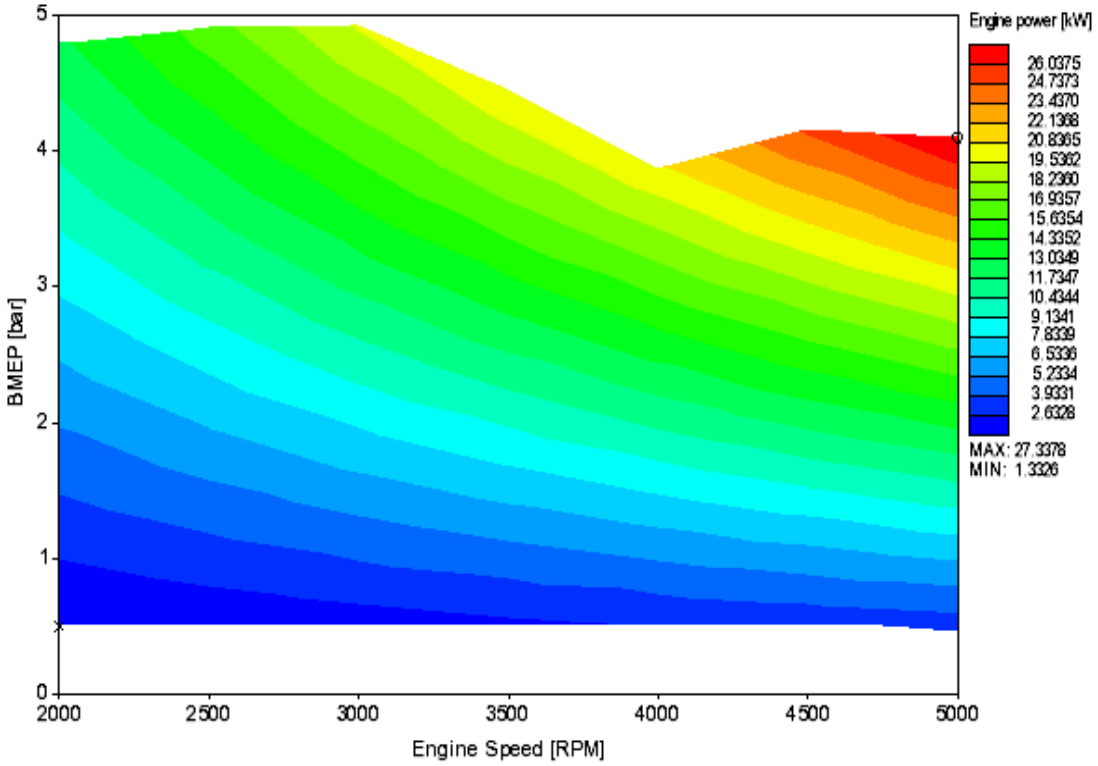

Figure 4.12 Computed brake power vs. the brake mean effective pressure and engine speed

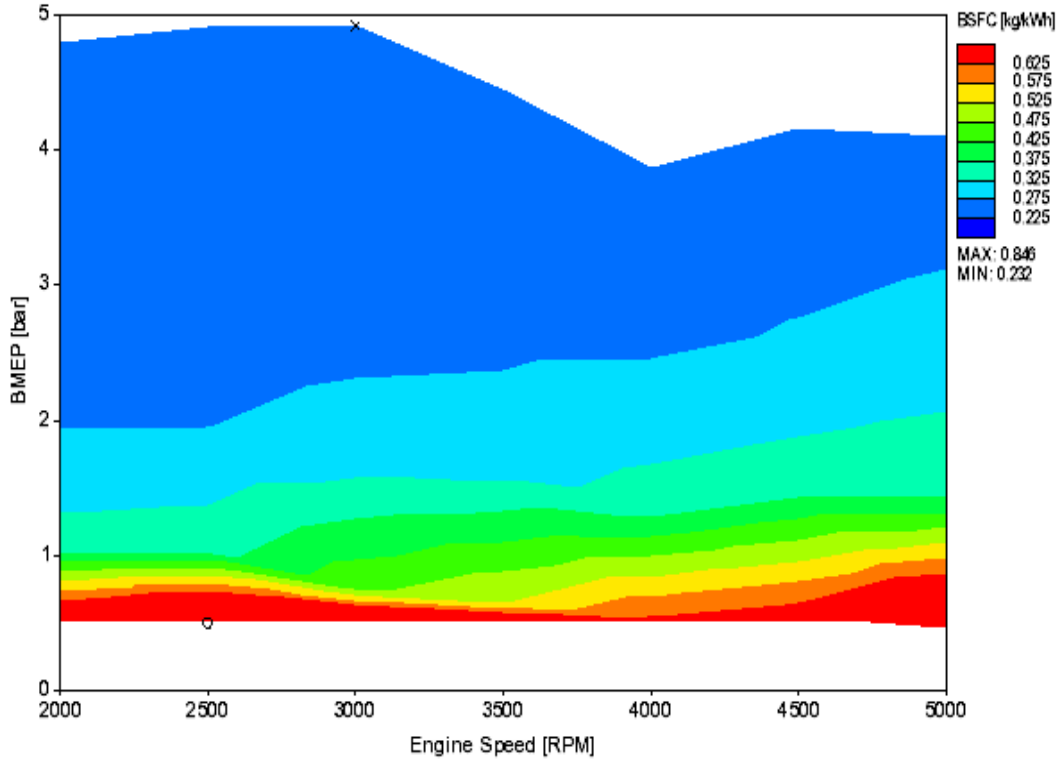

Figure 4.13 Computed brake specific fuel consumption vs. the brake mean effective pressure and engine speed.

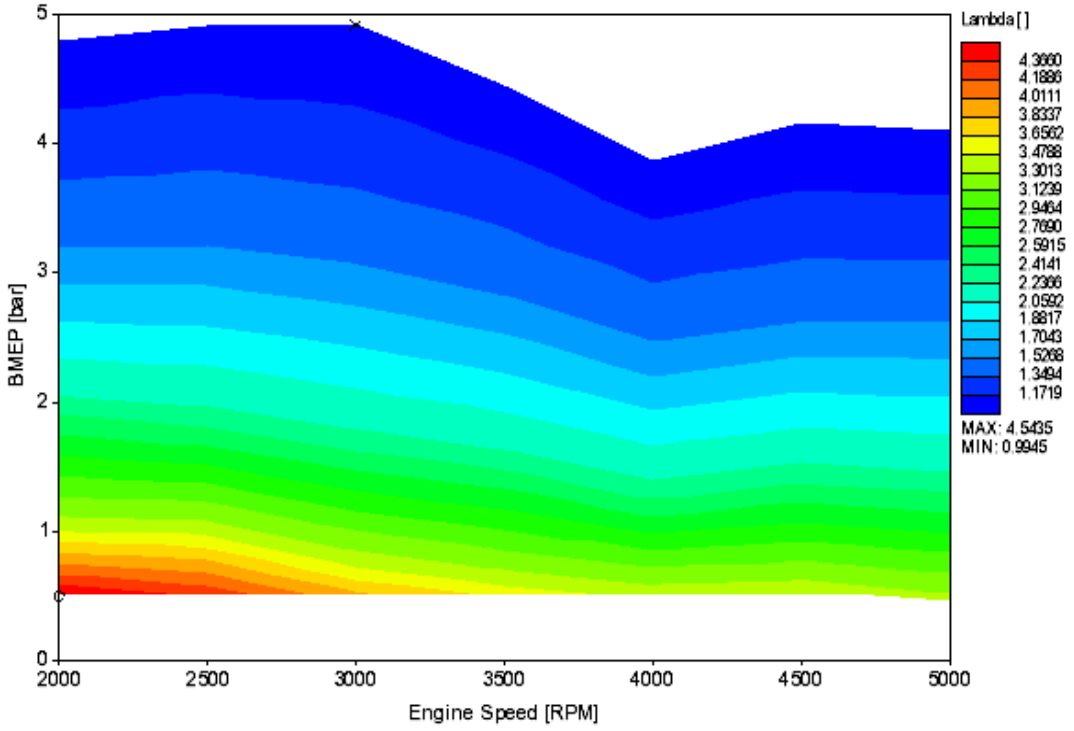

Figure 4.14 Computed lambda vs. the brake mean effective pressure and different engine speed.

4.3.2 Comparison between Direct and Port Fuel Injection in Two-Stroke Engine

As previously described in chapter 3.4 1D CAE Model in Wave, two CAE mode has been set up to compare engine performance between direct injection and port injection in two-stroke engine.

The comparison between direct and port fuel injection at different engine speed has been performed at full load engine condition with hydrogen fuel. The air fuel ratio is constant at 0.0292, which is equal to the stoichiometric value. Brake thermal engine efficiency, indicated torque and power versus different engine speed are presented in Figure 4.15, Figure 4.16 and Figure 4.17, for both direct and port fuel injection.

In Figure 4.15, results show that the maximum brake thermal efficiency of the direct injection mode is 30.1% at 3000 RPM compared to port fuel injection engine mode is 12.8% at 4000 RPM. This is due to short circuiting

losses in the port fuel injection system, and incomplete combustion inside the combustion chamber at higher RPM range.

In addition, the expansion chamber is not modelled in this simulation, which leads to a greater thermal brake engine efficiency loss in non-direct injection. In conventional two-stroke engines, the expansion chamber forces unburned fuel air mixture back into the cylinder through the exhaust port and its volumetric efficiency. In contrast to direct injection, the unburned fuel mixture is impossible to escape from the exhaust port as the fuel is only injected after the exhaust port closes.

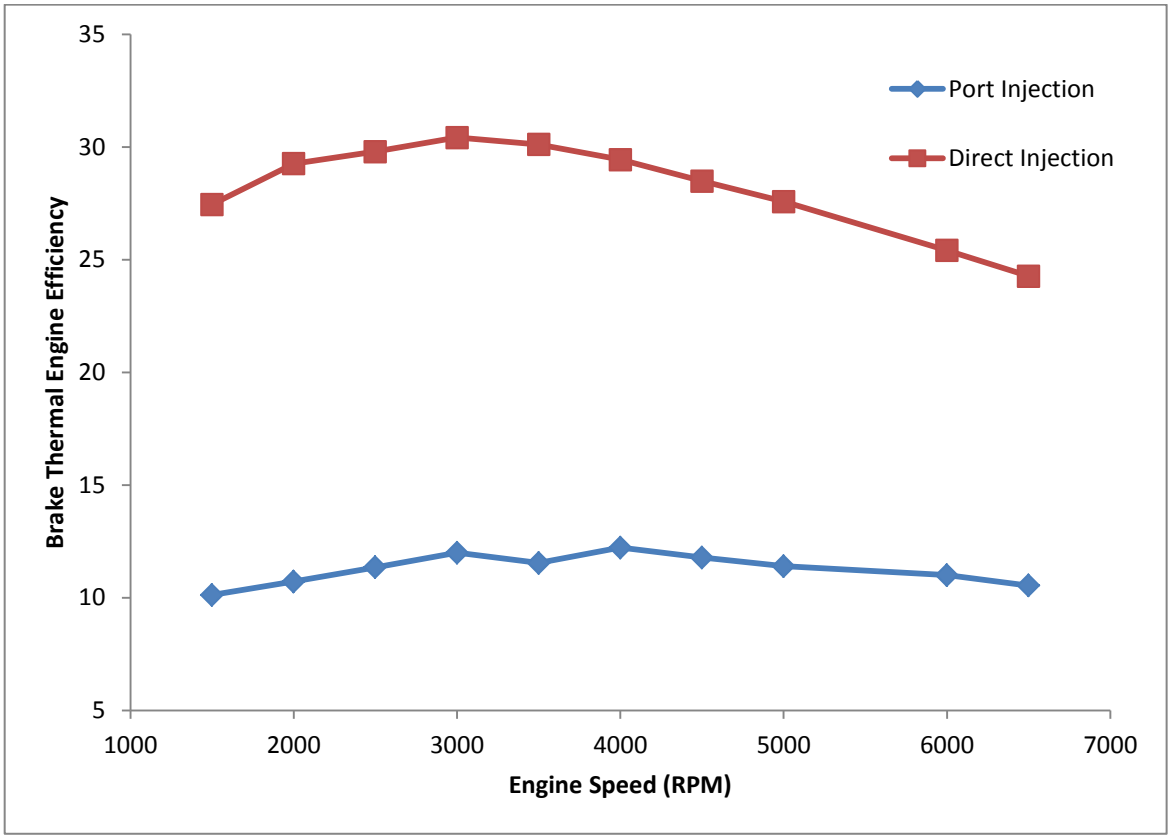

Figure 4.15 Brake thermal engine efficiency versus engine speed

The indicated power of direct injection is about 20% greater than the port fuel injection, and the indicated torque is about 30% greater than the port fuel injection over the whole tested RPM range, which presented in Figure 4.16 and Figure 4.17.

This is achieved because in direct injection system, the fuel is directly injected into the combustion after the port close. It also indicates that direct injection system engine can operate in leaner air-fuel ratios without loss of power.

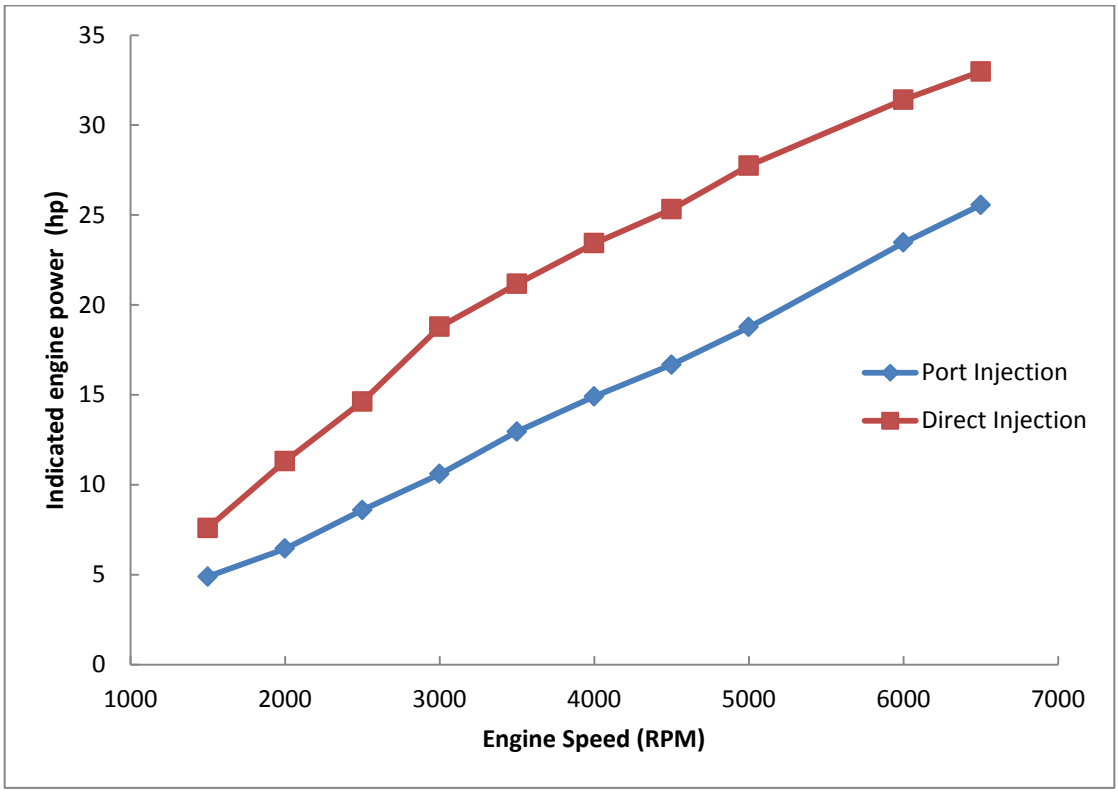

Figure 4.16 Indicated Power versus engine speed

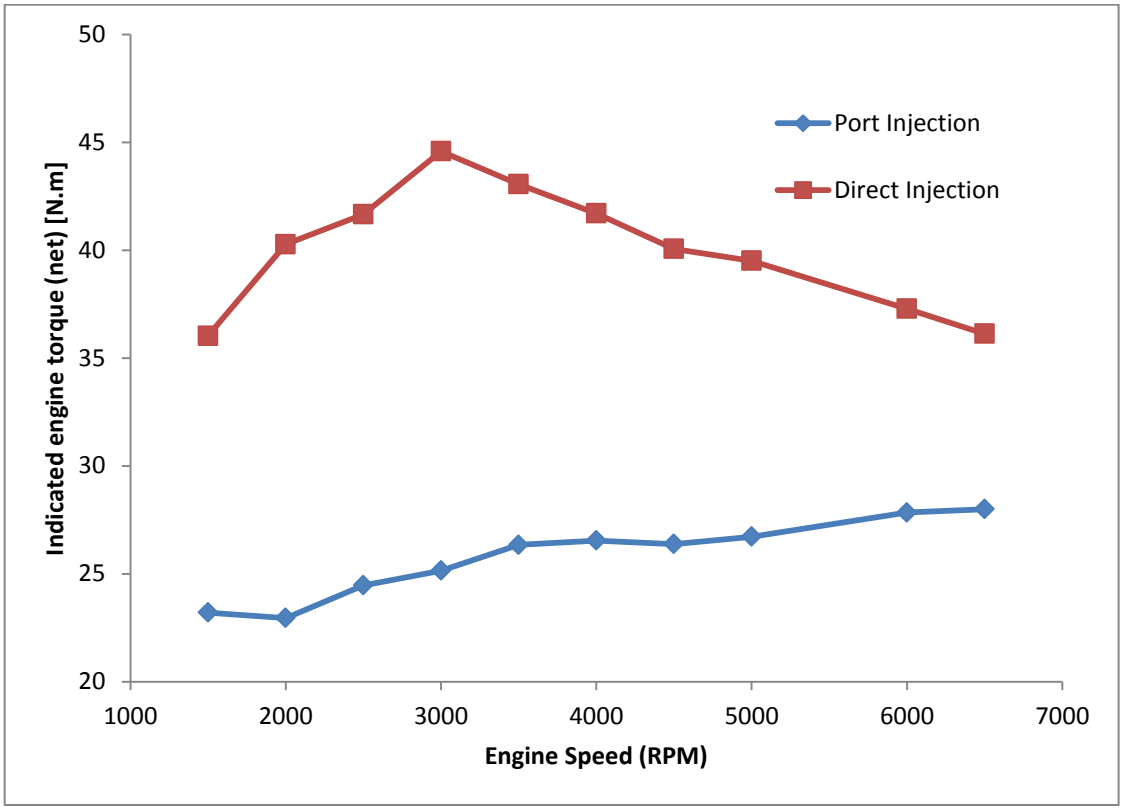

Figure 4.17 Indicated engine torque (net) versus engine speed

4.3.3 Comparison between Spark Ignition and Jet Ignition in Two-Stroke Engine

The coupling of a 3D-CFD program (STAR-CCM) with a 1D program (Ricardo Wave) is done by integration of the 3D-grid of the engine component as parameter of the 1D computational model of a complete engine. From the input of combustion rates obtained from CFD simulation for throttle less jet ignition and standard spark plug, efficiency maps are plotted.

The comparison between spark ignition and jet ignition at different air fuel ratio has been performed in 1D engine & gas dynamics simulation software WAVE. From the results, the lean limit of spark ignition and jet ignition is shown in Figure 4.18. It can be seen that jet ignition which is independent to the combustion mixture permits a leaner combustion compared to spark ignition. This leads to a higher thermal engine

efficiency with further improvements expected after optimizing the jet ignition device.

The significant level of tolerance with a jet ignition system is related to a manageable fast burn rate that provides multiple ignition sites and burns the combustion mixture almost instantaneously without spark delay such as experienced in spark ignition. With jet ignition system that permit extended lean limit, the variability in the initial flame development was reduced relative to the conventional spark ignition system. Jet ignition also improves combustion stability and can be limited in spark ignition due to chemical composition and local cyclic turbulence in the vicinity of the spark plug (Toulson et al. 2012).

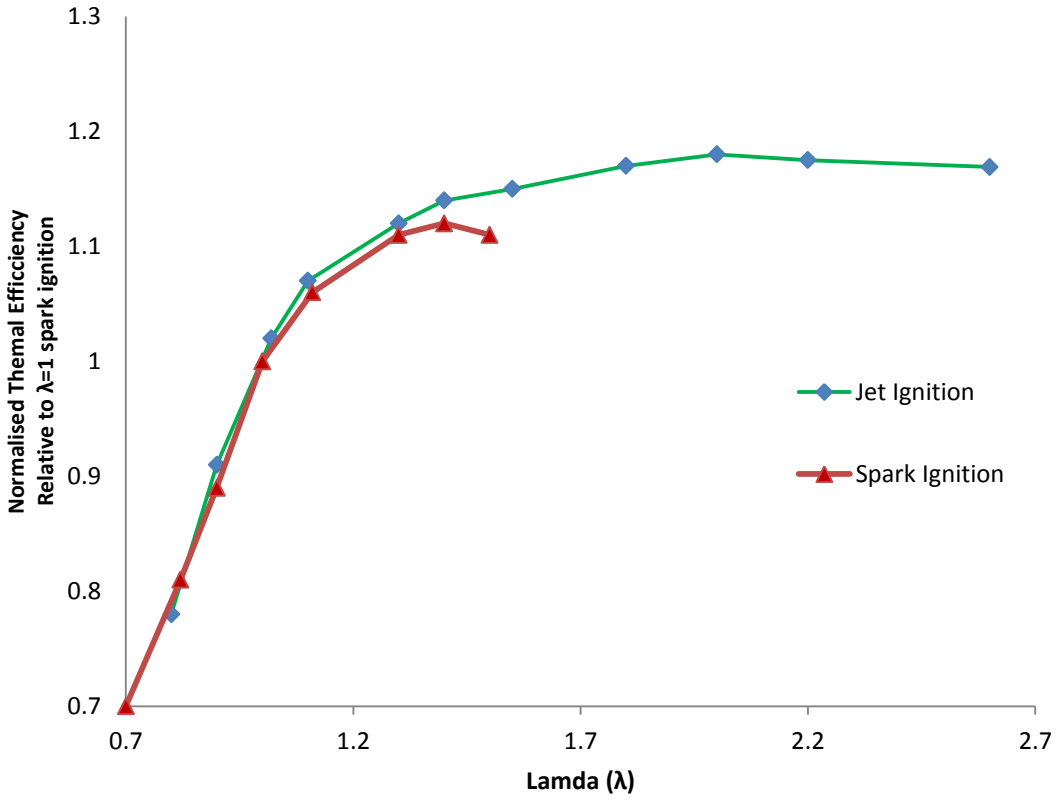

Figure 4.18 Spark Ignition vs. Jet Ignition lean limit

The comparison between spark ignition and jet ignition at different load conditions also has been performed in 1D engine & gas dynamics simulation software WAVE. BMEP and brake thermal engine efficiency vs different RPM are presented in Figure 4.19 and Figure 4.20, for both jet ignition and spark ignition.

Under part load condition, results highlight that the jet ignition combustion system has notable benefit over conventional spark plug. An approximately 2 – 5% improvement in break mean effective pressure was observed. This is achieved because of the faster burn rate and precise timing in the pre chamber fuel injection system. This demonstrates jet ignition can operate in leaner air-fuel ratios without loss of power.

Under full load condition, the maximum brake thermal efficiency of jet ignition is 30.30% at 3000 RPM where as in spark ignition is 28.9% at 3000 RPM. It can be seen that there is an insignificant improvement in jet ignition compared to spark ignition. The efficiency improvements are associated with a combination of combustion improvements, reduced engine throttling and reduced heat losses. Coupling jet ignition and direct injection is proved to perform better than conventional spark ignition with optimum injection strategy.

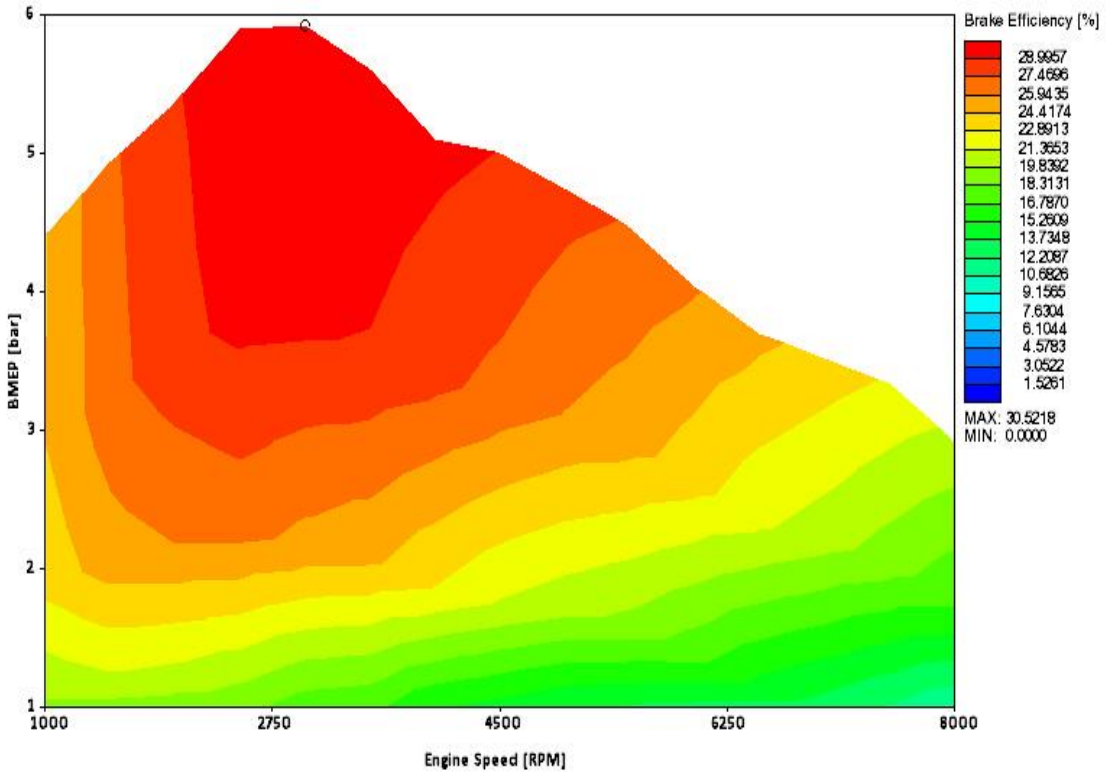

Figure 4.19 Jet ignition brake efficiency vs. the brake mean effective pressure and engine speed

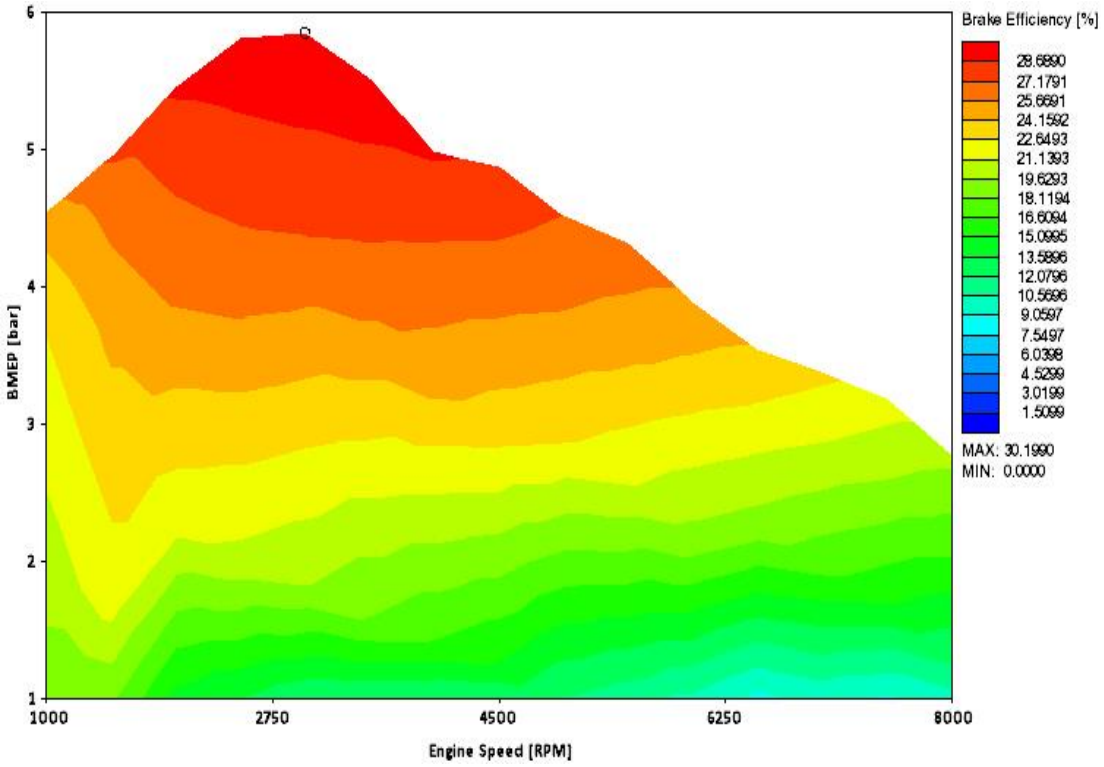

Figure 4.20 Spark ignition brake efficiency vs. the brake mean effective pressure and engine speed

4.4 SUMMARY

This chapter examined the CFD combustion modelling results attained using Star CCM+. First, different injection times in the main injector were analysed and through pressure, temperature and mass burn fraction plot, it was determined that stratified combustion proved to be the best combustion mode for application of jet ignition device and direct injection in two stroke engine. 90% fuel in the combustion chamber gets burned almost instantaneously and within 7.5 crank angle degrees.

Next, the combustion burn rate obtained from the CFD simulation was transferred into 1D software to examine the two-stroke engine performance. The results showed the baseline two-stroke direct injection engine model was delivering top efficiencies in the mid 30% sharply decreasing with load. The new engine coupled with direct injection and jet ignition with hydrogen fuel shows the ability to achieve high 20% and above 30% efficiencies over a significant portion of the speed and load range.

Following this, a comparison between direct injection and port fuel injection were examined through brake efficiency, power and torque versus different engine speed range plot. The results indicate direct injection have higher torque and power over port injection. This is due to overcome the short circuiting losses issues in port fuel injection and faster mass burn rate.

Lastly, a comparison between spark ignition and jet ignition in two-stroke engine are examined in 1D software WAVE. The results proven that jet ignition is able to run a much leaner mixture compared to spark ignition. It also indicate that jet ignition combustion system has remarkable benefit under part load engine operation condition over spark ignition, approximately 2 – 5% improvement in break mean effective pressure was observed under part load operating condition.

CHAPTER 5

5.CONCLUSION

5.1 RESEARCH ACHIEVEMENT

The primary objectives of this research were to investigate the performance of two-stroke IC engines with direct injection and jet ignition system and conduct a comparative study on using direct injection and jet ignition system at two-stroke IC engines instead of conventional fuel injection and ignition systems. These objectives were studied through 3D CFD simulation and 1D CAE simulation.

5.1.1 3D CFD Simulation

The CFD simulation has presented one of the latest concepts for the combustion systems and has being considered for hydrogen fuel based engines. The combustion system uses a flat type piston combustion chamber with direct injection and a jet ignition with hydrogen fuel. Combustion is always started by the jet ignition. The concept may be applied to low compression ratio/naturally aspirated engines as well as high compression ratio/high turbocharged engines.

The combustion and turbulence modelling has been investigated under high compression ratio and naturally aspirated environment with hydrogen fuel by using CFD. Detailed chemical kinetics was developed by use of STAR-CCM and DARS. The computed burning rates were comparatively fast, even with lean mixtures that are made stratified close

to the jet ignition nozzles. In addition, hydrogen assisted jet ignition indicates that it is possible to operate at high compression ratio with leaner mixture which increases efficiency and power output.

The influence of combustion evolution was studied stimulatingly in CFD simulation. Two-stroke engine coupled with direct injection and jet ignition provides opportunities to run the engine premixed stoichiometric and lean premixed, diffusion or mixed premixed/diffusion, depending on the timing of the jet ignition and the main chamber injection. The effectiveness of the different opportunities depends on the application, such as gasoline-like low compression ratio, naturally aspirated or diesel-like high compression ratio and turbocharged.

From the analysis of various injection timing, the major findings can be summarized as follows:

- Stratified mixture is the best combustion mode for this particular engine as it produces a cloud of fuel underneath the jet ignition nozzle that allows the mixture to burn almost instantaneously.

- Fuel injected earlier than 150 degree increases the occurrence of pre-ignition, as it provides excessive time for the fuel and air to mix.

- With fuel injection after 160 degrees, fuel has less time to mix with air, resulting in large amounts of unburned fuel left in the combustion chamber.

From the CFD simulation results, it is proved that jet ignition has the ability to run the engine throttle-less and have extended lean mixture limit, thanks to the multiple sites of hot gases from combustion in the jet ignition nozzles which allow the fuel to burn almost instantaneously.

5.1.2 1D CAE Simulation

The two-stroke engine, coupled with direct injection and jet ignition, has presented a novel combustion system being considered for two- stroke engine design. The 1D CAE model has reported on the preliminary design of the jet ignition device and the selection of the direct injector. The main chamber injector is to be used for the prototype of a two-stroke gasoline engine converted to hydrogen.

1D CAE results of engine simulations show the ability to run the engine throttle less by changing the load through the quantity of fuel injected. This achieves improved top fuel conversion efficiencies and reduced penalties changing the load or the speed.

Direct injection coupled with jet ignition has shown evident performance improvement when compared to port fuel injection, especially in the high speed range. A comparison between the two different injection systems has been made at full-load and stoichiometric air fuel ratio with hydrogen fuel, in a RPM range from 1500 to 6500 with 1000 increments. Thanks to direct injection, the fuel is only injected after the exhaust port closes to prevent fuel loss during the scavenging process. As a result, evident improvement of brake efficiency has been found.

Comparisons between spark ignition and jet ignition in two-stroke engines are examined in 1D software WAVE. The results prove that jet ignition is able to run a much leaner mixture when compared to spark ignition. It also indicates that jet ignition combustion systems have remarkable benefits under part load engine operation condition over spark ignition. An approximately a 2 – 5% improvement in break mean effective pressure was observed under partial load operating condition.

In direct injection systems, the crankcase is only pumping air during the compression process, instead of a pre-mixed air-fuel mixture as in a conventional two-stroke engine. The lubrication oil is only injected

where needed, such as in the crankcase and main bearings. There is only a small amount of oil burned during the combustion process and that basically can be negligible and therefore less polluting.

5.2 CONCLUSIONS OF RESEARCH

The main goal of this research was to facilitate traditional two-stroke engines by overcoming issues associated with short-circuit scavenging, poor engine efficiency and lubrication. These issues were addressed in the three previously posed research questions which involved the use of direct injection systems with jet ignition. Answers to the research questions are presented.

1. Is there any option to improve the top brake thermal engine efficiencies of two-stroke engine for transport applications?

Direct injection two-stroke engine - in the DI system, the fuel is directly injected to the combustion chamber after the port is closed. This drastically improves engine efficiency and overcomes the short circuit scavenging problem.

Comparison between direct injection and port fuel injection results show that direct injection improved approximately 10% brake thermal engine efficiency over port fuel injection at full load condition.

2. Is there any option to improve the part load efficiency of two-stroke engine for transport applications?

Load has to be changed diesel like (throttle less) by quantity of fuel injected (less load = less fuel injected). This requires an always lean burn combustion system which can be achieved by using jet ignition.

Comparison between direct injection and spark injection results show that jet injection has remarkable benefits under part load engine operating conditions versus spark ignition. Approximately 2 – 5%

improvement in break mean effective pressure was observed under part load operating conditions.

3. Is it possible to reduce the emissions of pollutants and the smoke of two-stroke engines for transport applications?

The oil does not need to be premixed with fuel, and the fuel is not escaping combustion through the exhaust. Fast completion combustion at different loads, air fuel ratios, and residual ratio. These can be achieved by using direct injection coupled with jet ignition.

In direct injection systems, the oil is not mixed with fuel. The oil is only injected where needed, such as in the main bearing and crankcase. There are only minimal amounts of oil burned during the combustion process. Thereby, non-premixed oil reduces emission pollutants. In addition, with jet ignition, it enables faster burn rates and reduces the short circuiting issues in two-stroke engines.

5.3 RECOMMENDATIONS FOR FUTURE WORK

During this research, a range of two-stroke engine parameters and data space have been tested and modelled. However, the engine design may be further optimized for increased efficiency and power density.
Suggestions for further modelling work include:

- Supercharging and asymmetric port timings may further improve both engine efficiency and power density.

- The jet ignition device has to be optimised to match the various fuel and application requirements. The system may be used for small to large engines with strongly variable power density and rpm range.

- The assembly and the components (injector and spark) need further development.

LIST OF REFERENCES

Agency, Ie 2014, Monthly Electricity Statistics, 01/03/2014, <WWW.IEA.ORG/STATS/SURVEYS/MES.XLS >.

Allocca, L, Auriemma, M, Corcione, FE, Valentino, G, Fontanesi, S, Gagliardi, V, Malaguti, S & Riganti, G 2005, 'Investigation of Mixture Formation Process in a HDDI Diesel Engine by CFD and Imaging Technique', <http://dx.doi.org/10.4271/2005-01-1918>.

Attard, WP, Bassett, M, Parsons, P & Blaxill, H 2011, 'A New Combustion System Achieving High Drive Cycle Fuel Economy Improvements in a Modern Vehicle Powertrain', <http://dx.doi.org/10.4271/2011-01-0664>.

Balduzzi, F, Vichi, G, Romani, L, Ferrara, G, Trassi, P, Fiaschi, J & Tozzi, F 2015, 'Development of a Low Pressure Direct Injection System for a Small 2S Engine. Part I - CFD Analysis of the Injection Process', SAE Int. J. Engines, vol. 8, no. 4.

Bartolini, CM, Caresana, F & Vincenzi, G 2001, 'EXPERIMENTAL ANALYSIS OF A TWO-STROKE DIRECT INJECTION ENGINE PROTOTYPE', <http://dx.doi.org/10.4271/2001-01-1840>.

Binjuwair, S & Ibrahim, S 2013, 'Numerical Analysis of Flow Structure inside a Single Cylinder of a 4 Valve Head under Steady-State Condition', <http://dx.doi.org/10.4271/2013-24-0186>.

Blair, GP 1989, Advances in Two-stroke Cycle Engine Technology (Progress in Technology), Society of Automotive Engineers Inc.

Boretti, AA 2012, 'Stochastic reactor modelling of multi modes combustion with diesel direct injection or hydrogen jet ignition start of combustion', Int J Hydrogen Energy, vol. 37, no. 18, pp. 13555-63.

Boretti, AA & Watson, HC 2009a, 'Enhanced combustion by jet ignition in a turbocharged cryogenic port fuel injected hydrogen engine', Int J Hydrogen Energy, vol. 34, no. 6, pp. 2511-6.

---- 2009b, 'The lean burn direct injection jet ignition gas engine', Int J Hydrogen Energy, vol. 34, no. 18, pp. 7835-41.

---- 2009c, 'Numerical Study of a Turbocharged, Jet Ignited, Cryogenic, Port Injected, Hydrogen Engine', <http://dx.doi.org/10.4271/2009-01-1425>.

BOSCH 2015, Gasoline Fuel-Injection System K-jetronic, viewed 15/07/2015 2015, <http://vwts.ru/injector/k-jetronic/gasoline_fuel_injection_system_k-jetronic_eng.pdf>.

CD-adapco 2013, STAR-CCM+9.02 user manual.

---- 2014, A comprehensive toolkit for reaction modeling, viewed 15/05/2014 <http://www.cd-adapco.com/products/star-ccm%C2%AE/dars>.

CIMAC 2006, Recent Developments in 4 Stroke Engines, <www.cimac.com/cimac_cms/uploads/explorer/events_2006/6_Developments_in_4_Stroke_Diesel_Engines_Niven_Nerheim.pdf>.

Council, WP 2014, Alternative Transport Fuels - Courtesy of AIP, viewed 15/05/14 <http://www.world-petroleum.org/index.php?/Technology/alternative-transport-fuels-courtesy-of-aip.html>.

Crazymechanical 2015, Fuel Injection System on Petrol Engine, viewed 15/07/2015 2015, <http://www.crazymechanical.com/notes/automobile-engineering/fuel-injection-system-on-petrol-engine/>.

eBay 2014, What Are the Different Types of Fuel Injection?, viewed 15/07/2015 <http://www.ebay.com.au/gds/What-Are-the-Different-Types-of-Fuel-Injection-/10000000177633624/g.html>.

Fleck, B, Fleck, R., Kee, R.J., Hu, X., Foley, L. and Yavuz, I. 2006, 'CFD Simulation and Validation of the Scavenging Process in a 125cc 2-Stroke Racing Engine.', SAE Technical Paper, vol. 32, no. 0061.

Ghojel, JI 2010, 'Review of the development and applications of the Wiebe function: a tribute to the contribution of Ivan Wiebe to engine research', Int. J. Engine Res, vol. 11, pp. 297-312.

Gitano-Briggs, H & Willson, B 2004, 'Development of a Compression Pressurized Direct Fuel Injection System for Retrofit to Two-Stroke Engines', <http://dx.doi.org/10.4271/2004-32-0062>.

Gupta, RB 1999, Auto Design, Satya Prakashan, New Delhi.

Hannu Jääskeläinen, MKK 2014, Engine Fundamentals, viewed 05/05/14 <https://www.dieselnet.com/tech/diesel_fundamentals.php>.

Inchley, WD 2008, The Theory of Heat Engines, Lindemann Press.

Joel H. Ferziger, MP 2002, Computational Methods for Fluid Dynamics, Third edn, Springer, Berlin.

Karim, GA 2003, 'Hydrogen as a spark ignition engine', International Journal of Hydrogen Engine, vol. 28, no. 6, pp. 569-77.

Lehtiniemi, H 2007, Efficient Engine CFD with Detailed Chemistry, <https://www.erc.wisc.edu/documents/symp07-Lehtiniemi.pdf>.

Leighton, S & Ahern, S 2003, 'Fuel Economy Advantages on Indian 2-stroke and 4-stroke Motorcycles Fitted with Direct Fuel Injection', <http://dx.doi.org/10.4271/2003-26-0019>.

Lumsden G., WHC, Glasson N., Chow C., Chalko T 1995, 'Observations of Hydrogen Assisted Jet Ignition', paper presented to Proceedings of Hydrogen Power Thermal & Electrochemical Systems International Symposium, Italy.

M. Badami, MRM, F. Millo and P. Nuccio 1999, 'Comparison Between Direct and Indirect Fuel Injection in an S.I. Two-Stroke Engine', paper presented to Proceedings of the 1999 SAE Small Engine Technology Conference, Madison, Wisconsin.

Marine Engine Digest 2013, Two-stroke versus four-stroke outboard motors, viewed 10/03/2013 <http://www.marineenginedigest.com/specialreports/2versus4stroke.htm>.

MSD 2014, SetYourTiming, viewed 20/08/2014 <http://www.setyourtiming.com/faq.html>.

Najjar, YSH 2009, 'Alternative Fuels for Spark Ignition Engines', The Open Fuels & Energy Science Journal, vol. 2, no. 1, pp. 1-9.

Olmo, L & Thornton, J 2005, 'CFD Analysis of Mixture Formation and Combustion Process for High Performance DI Gasoline Engine', <http://dx.doi.org/10.4271/2005-01-0214>.

Oswald, R, Ebner, A & Kirchberger, R 2010, 'High Efficient 125- 250 cm3 LPDI Two-Stroke Engines, a Cheap and Robust Alternative to Four-Stroke Solutions?', <http://dx.doi.org/10.4271/2010-32-0019>.

Pattakon 2014, Asymmetric Timing in the two-stroke engines, viewed 02/9/2014 <http://www.pattakon.com/pattakonPatAT.htm>.

RicardoSoftware 2010, WAVE 8.0 User's Manual.

Riegler, UG & Bargende, M 2002, 'Direct Coupled 1D/3D-CFD-Computation (GT-Power/Star-CD) of the Flow in the Switch-Over Intake System of an 8-Cylinder SI Engine with External Exhaust Gas Recirculation', <http://dx.doi.org/10.4271/2002-01-0901>.

Roth, AC 2004, Small Gas Engines, 8 edn, Goodheart Wilcox Publisher.

S. Kumarappa a & Prabhukumar, GP 2008, 'Improving the Performance of Two Stroke Spark Ignition Engine by Direct Electronic CNG Injection', Jordan Journal of Mechanical and Industrial Engineering, vol. 2, no. 4, pp. 169-74.

Ski-doo 2009, 2009 Ski-Doo Press Kit: E-TEC Backgrounder, <http://www.brp.com/sites/default/files/Resources/en-CA/Media.Center/PDF/2007_01_31_E-TEC_backgrounder.pdf>.

---- 2014, ROTAX 800R E-TEC, viewed 11/05/2014 2014, <http://www.ski-doo.com/technologies/engine-technologies/2-strokes>.

Stone, R 1999, Introduction to Internal Combustion Engine, Society of Automotive Engineers, Inc., Warrendale.

Thipse, SS 2008, Internal Combustion Engine, JAICO PUBLISHING HOUSE, DELHI.

Toulson, E 2008, 'APPLYING ALTERNATIVE FUELS IN PLACE OF HYDROGEN TO THE JET IGNITION PROCESS', The University of Melbourne

Toulson, E, Huisjen, A, Chen, X, Squibb, C, Zhu, G, Schock, H & Attard, WP 2012, 'Visualization of Propane and Natural Gas Spark Ignition and Turbulent Jet Ignition Combustion', SAE Int. J. Engines, vol. 5, no. 4, pp. 1821-35.

TUM 2013, Investigation of a novel pre-chamber concept to improve ignition and combustion of lean premixed natural-gas-air mixtures in gas motors, <www.td.mw.tum.de/tum-td/en/de/forschung/themen/pgi_gasmotor>.

EPA 2001, Final Report of the Small Business Advocacy Review Panel on Control of Emissions from Nonroad Large Spark Ignition Engines, Recreational Engines (Marine and Land-based), and Highway Motorcycles. , United States Environmental Protection Agency.

William P. Attard, HB 2011, 'A Single Fuel Pre-Chamber Jet Ignition Powertrain Achieving High Load, High Efficiency and Near Zero NOx Emissions', SAE Int. J. Engines, vol. 5, no. 3, pp. 734-46.

Wyczalek, F, Harned, J, Maksymiuk, S & Blevins, J 1975, 'EFI Prechamber Torch Ignition of Lean Mixtures', SAE Technical Paper, vol. 750351.

Y.AI-ALousi 1982, 'Examniation of the combusion processes and performance of a spark ignition engine using a data aquisition system', University of Calgary.

Yamaha 2013, Two Stroke HPDI ® : Benefits, viewed 10/03/2013 <http://www.yamahaoutboards.com/outboards/2-Stroke-HPDI/benefits>

LIST OF PUBLICATIONS

Following is a list of publications during the course of this master program.

Boretti, A, Mazlan, **Jiang, S.**, "Advanced Two Stroke Engine with Direct Injection and Jet Ignition," F2014-CET-010, FISITA Congress 2014.

Boretti, A, Mazlan, S. K., **Jiang, S.** & Bing, J. Z., "Numerical Analysis of Mixture Formation and Combustion Evaluation in Direct Injection Jet Ignition Gas Engines," F2014-CET-013, FISITA Congress 2014.

Boretti, A, **Jiang, S.** 2014, "Development of a two stroke direct injection jet ignition compressed natural gas engine", Journal of Power Technologies, vol. 94, no. 3.

Boretti, A, **Jiang, S.** & Scalzo, J., "A Novel Wankel Engine Featuring Jet Ignition and Port or Direct Injection for Faster and More Complete Combustion Especially Designed for Gaseous Fuels", 2015-01-0007, 18th Asia pacific automotive engineering conference, Melbourne, Australia.

Boretti, A, **Jiang, S.** & Scalzo, J., "A Naturally Aspirated Four Stroke Racing Engine with One Intake and One Exhaust Horizontal Rotary Valve per Cylinder and Central Direct Injection and Ignition by Spark or Jet" , 2015-01-0006, 18th Asia pacific automotive engineering conference, Melbourne, Australia.

Bing, J. Z , Boretti, A, Mazlan, S. K. & **Jiang, S.**, "Numerical investigation of dual fuel diesel-CNG combustion on engine performance and emission", 2015-01-0009, 18th Asia pacific automotive engineering conference, Melbourne.

Boretti, A, **Jiang, S.**, "Two Stroke Direct Injection Jet Ignition Engines for Unmanned Aerial Vehicles", 2015-01-2424, SAE 2015 AeroTech Congress & Exhibition.

APPENDIX A

A.FURTHER STAR CCM+ MODELING RESULTS

This appendix provides published paper work “Numerical Analysis of Mixture Formation and Combustion Evaluation in Direct Injection Jet Ignition Gas Engines” which on a four-stroke engine with jet ignition modelling results.

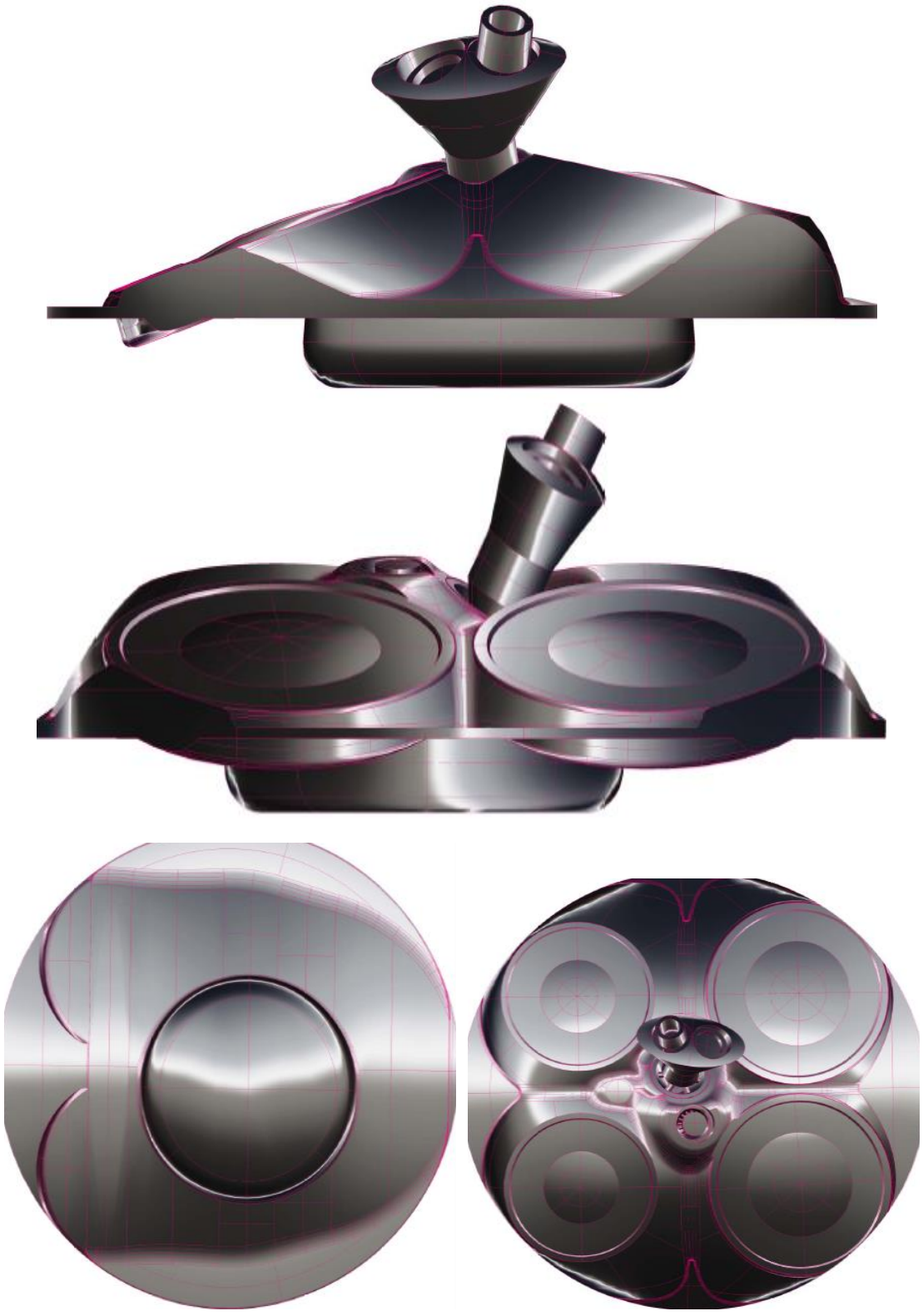

Figure A.1– Direct injection jet ignition combustion system.

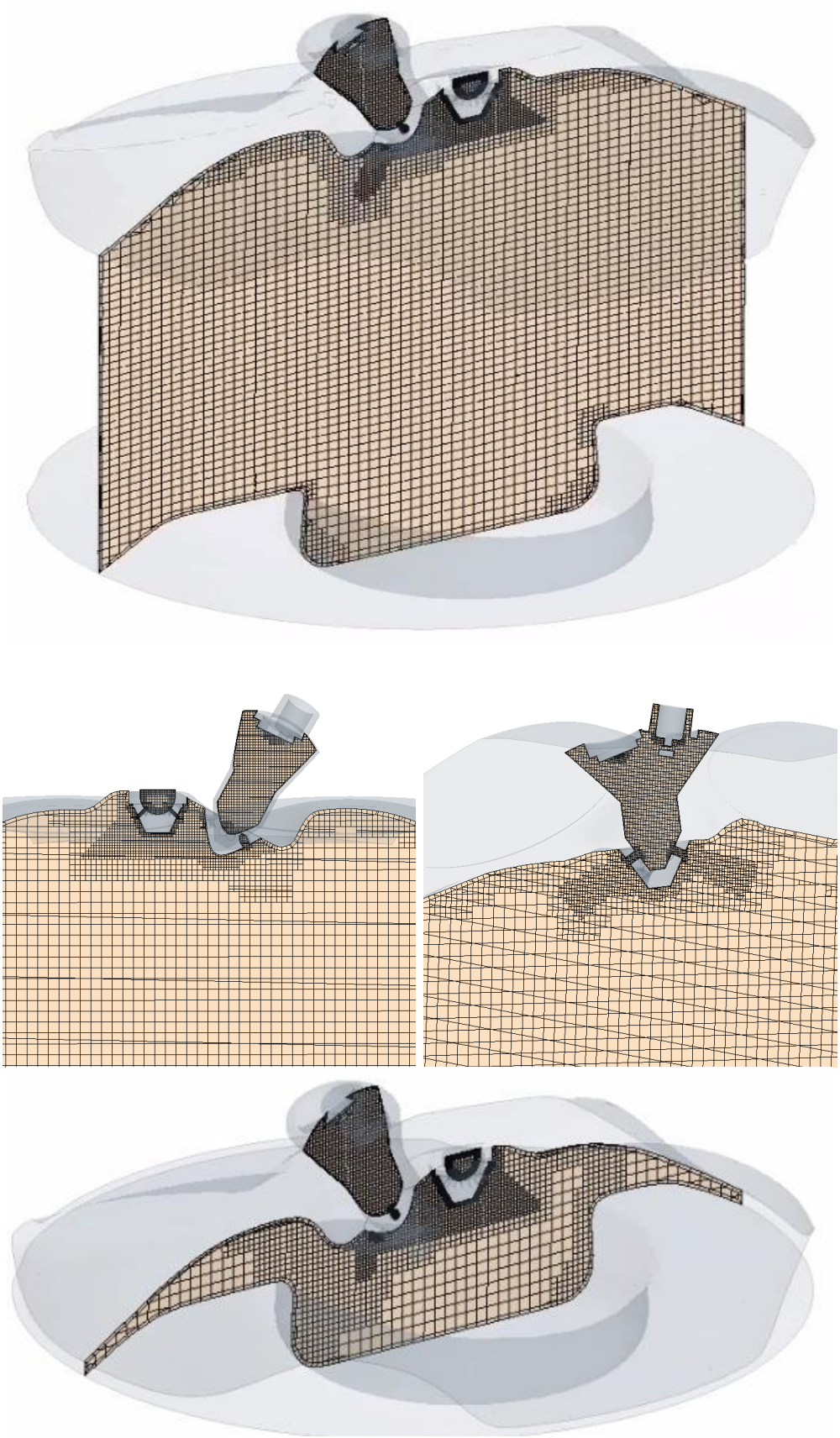

Figure A.2 Computational mesh at bottom and top dead centers.

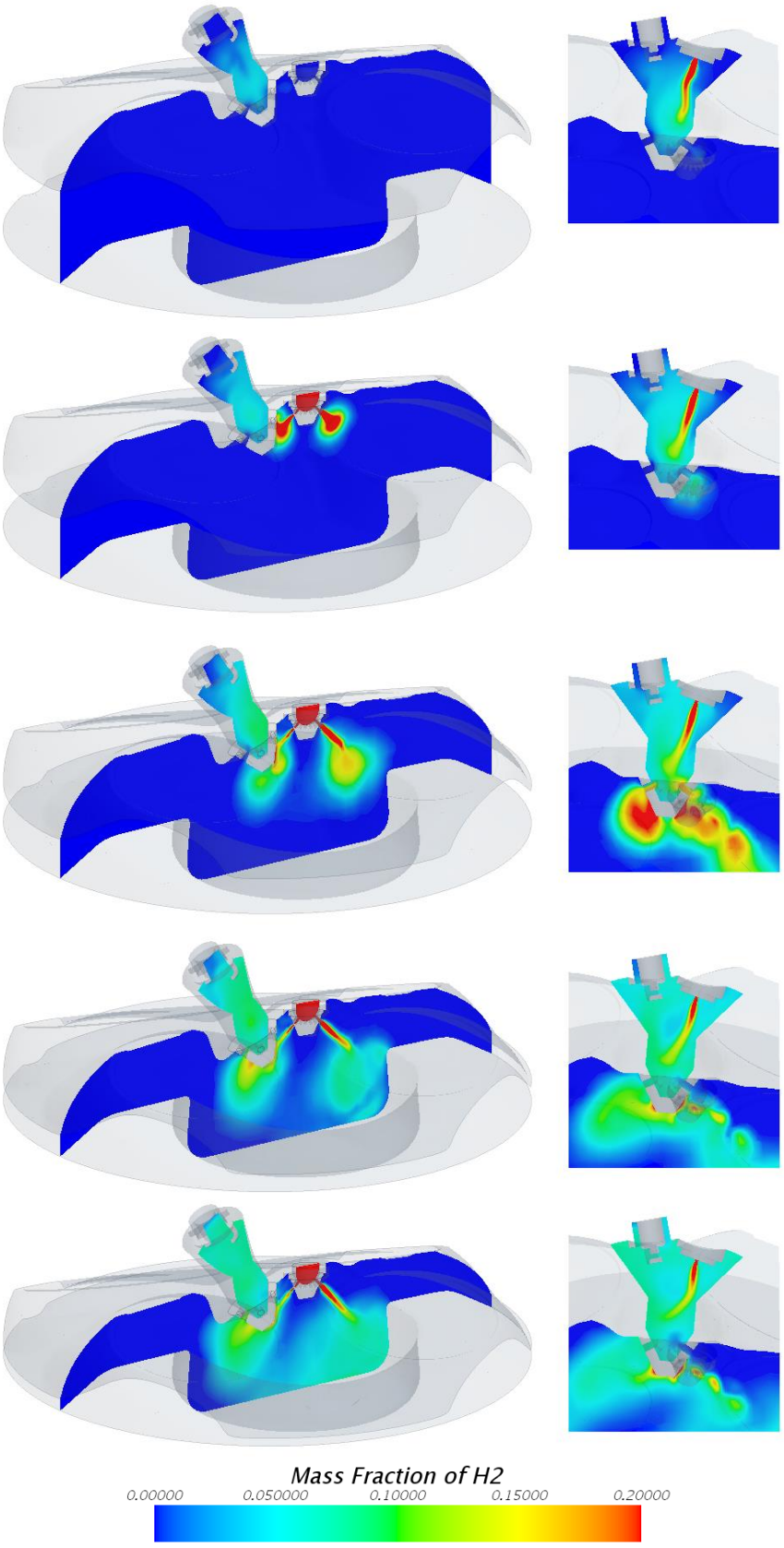

Figure A.3 Top to bottom: H2 mass fraction at 314, 324, 334, 344 and 354 degrees crank angle (firing top dead center is 360 degrees crank angle)

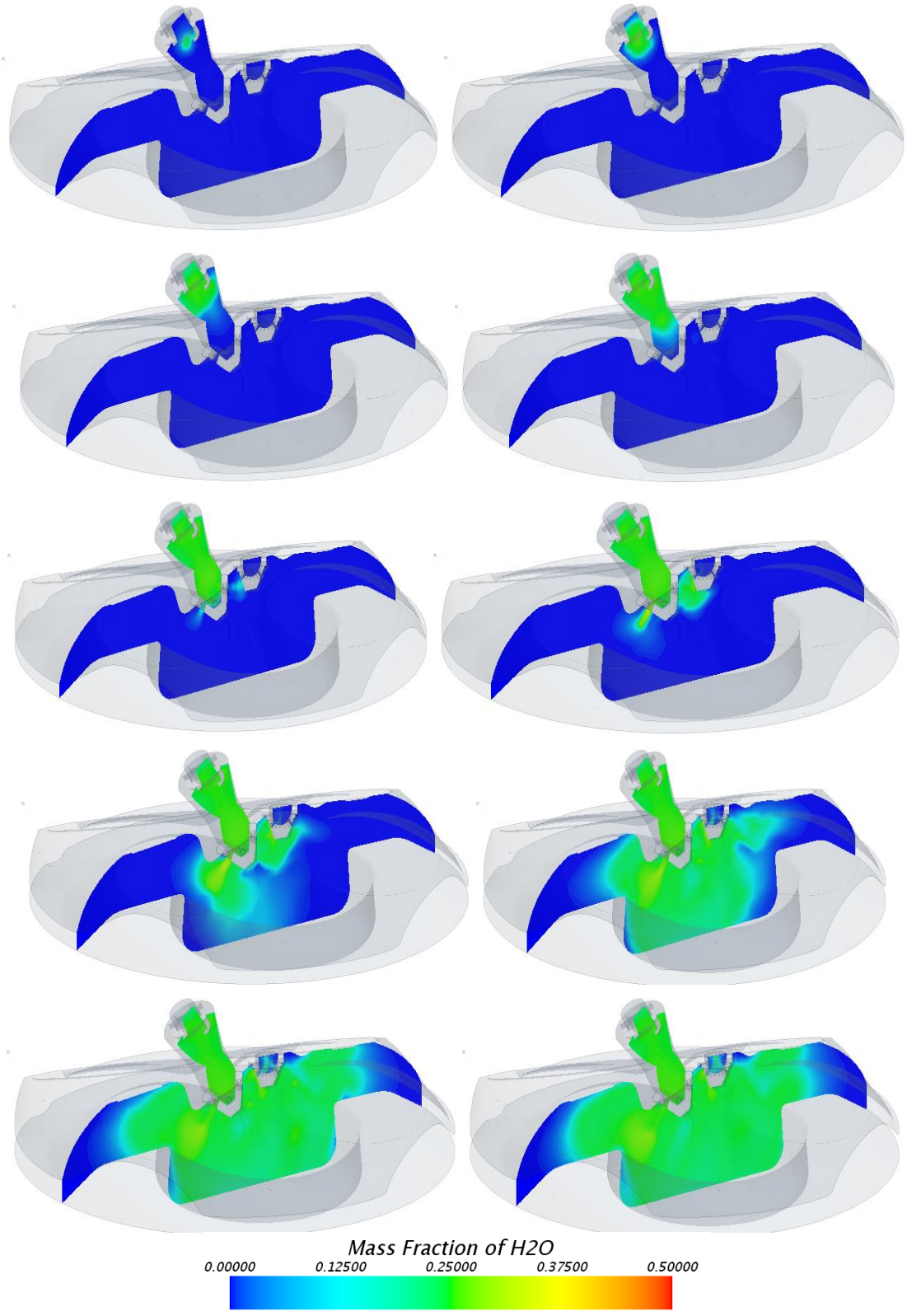

Figure A.4 Left to right, top to bottom: H_2O mass fraction at 362, 364, 366, 368, 370, 372, 374, 376, 378 and 380 degrees crank angle (firing top dead center is 360 degrees crank angle)

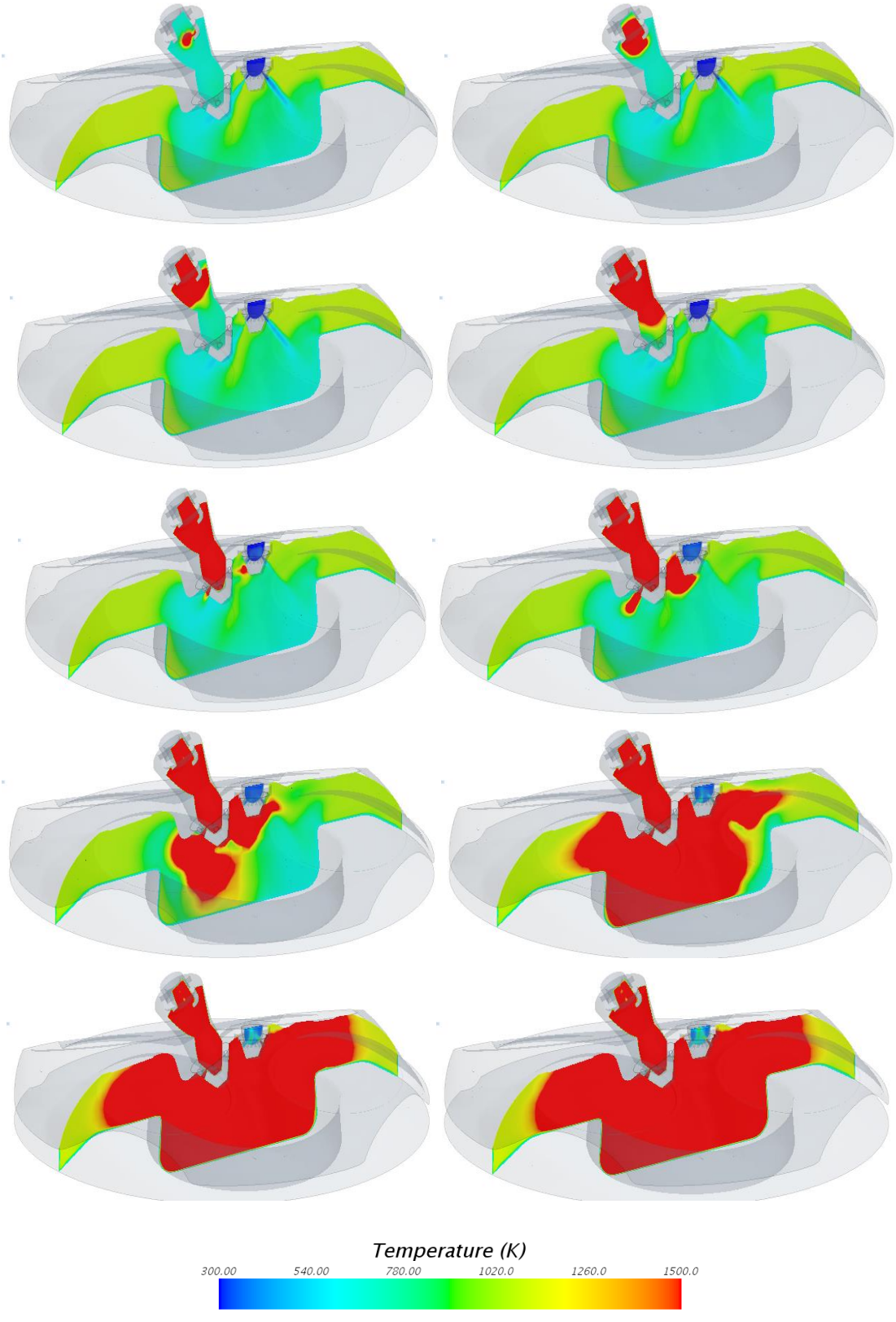

Figure A.5 Left to right, top to bottom: Temperatures at 362, 364, 366, 368, 370, 372, 374, 376, 378 and 380 degrees crank angle (firing top dead center is 360 degrees crank angle)

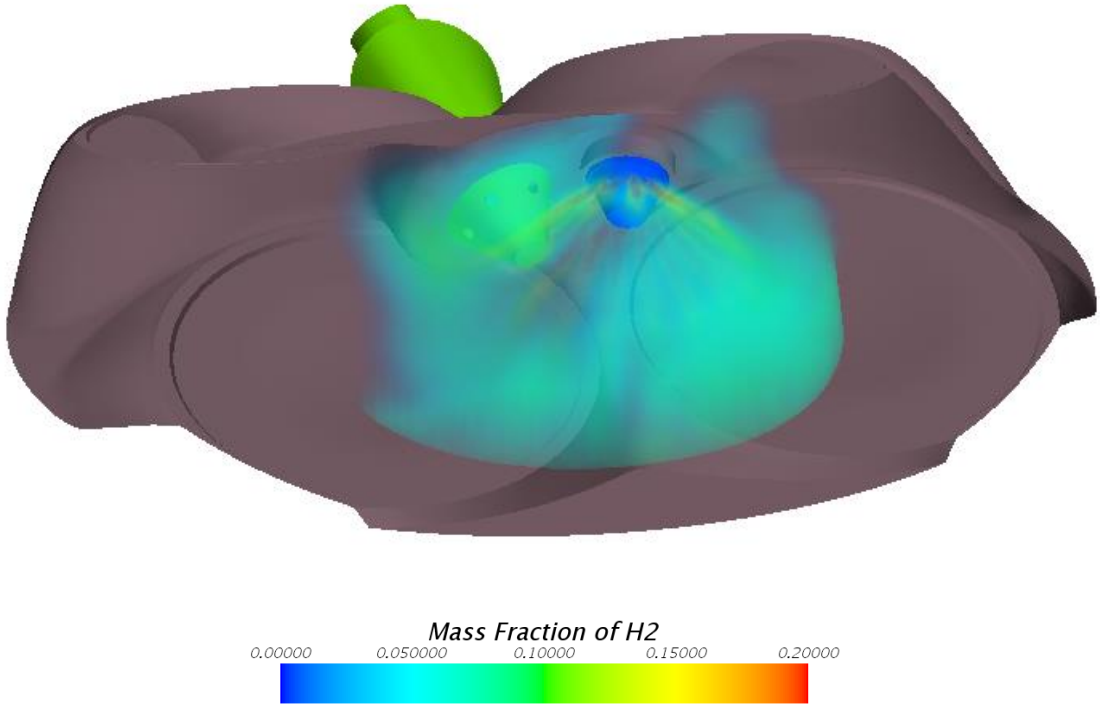

Figure A.6 H_2 mass fraction at firing top dead center below the cylinder head evidencing charge stratification.

APPENDIX B

B. CHEMICAL KINETIC MECHANISMS

The Dars-CFD reaction was imported into Star-CCM+ and shown below in Dars-CFD format.

```
DARS Preprocessor Version 1.0
! Preprocessor name and version number
harry
! Name Of Author  dars_1
! ProjectName 23-08-2007
! Date 2
! Number of reactive Species (1, 1, 1)
(1, 1, 2)   9
! Number of Equilibrium Species (1, 1,
3)   (1, 1, 2) (1, 1, 5) (1, 1, 6) (1,
1, 8) (1, 1, 1) (1, 1, 7) (1, 1, 4) (1,
1, 9) 1 0
! Number of mechanisms HYDROGENAIR
! Name of gas phase mechanism 38
! Number of reactions
r1f:H2+O2=2OH
2 1
! Number of reactant species / product
species
(1, 1, 1)   1
! Reactant species index and
stoichiometric coefficent
(1, 1, 2)   1
! Reactant species index and
stoichiometric coefficent
(1, 1, 5)   2
+1.700000E13  +0.000000E00
+1.999115E02
! Arrhenius coefficients
r1b:H2+O2=2OH
1 2
(1, 1, 5)    2
(1, 1, 1)    1
(1, 1, 2)    1
+2.223307E10  +3.876773E-01
+1.201605E02
r2f:H2+OH=H2O+H
2 2
! Number of reactant species / product
species
(1, 1, 1)   1
! Reactant species index and
stoichiometric coefficent
(1, 1, 5)   1
! Reactant species index and
stoichiometric coefficent
(1, 1, 7)   1
(1, 1, 3)   1
+1.170000E09  +1.300000E00
+1.517118E01
! Arrhenius coefficients
r2b:H2+OH=H2O+H
2 2
(1, 1, 7)    1
(1, 1, 3)    1
(1, 1, 1)    1
(1, 1, 5)    1
+7.979974E10  +9.726424E-01
+8.200486E01
r3f:H+O2=OH+O
2 2
! Number of reactant species / product
species
(1, 1, 3)   1
! Reactant species index and
stoichiometric coefficent
(1, 1, 2)   1
! Reactant species index and
stoichiometric coefficent
(1, 1, 5)   1
(1, 1, 4)   1
+2.000000E14  +0.000000E00
+7.029120E01
! Arrhenius coefficients
r3b:H+O2=OH+O
2 2
(1, 1, 5)    1
(1, 1, 4)    1
(1, 1, 3)    1
(1, 1, 2)    1
+6.712336E11  +3.741675E-01  -
1.190344E00
r4f:O+H2=OH+H
2 2
! Number of reactant species / product
species
```

```
(1, 1, 4)    1
! Reactant species index and
stoichiometric coefficent
(1, 1, 1)    1
! Reactant species index and
stoichiometric coefficent
(1, 1, 5)    1
(1, 1, 3)    1
+1.800000E10  +1.000000E00
+3.692798E01
! Arrhenius coefficients
r4b:O+H2=OH+H
2 2
(1, 1, 5)    1
(1, 1, 3)    1
(1, 1, 4)    1
(1, 1, 1)    1
+7.014220E09  +1.013510E00
+2.865851E01
r5f:H+O2+M1=HO2+M1
2 1
! Number of reactant species / product
species
(1, 1, 3)    1
! Reactant species index and
stoichiometric coefficent
(1, 1, 2)    1
! Reactant species index and
stoichiometric coefficent
(1, 1, 6)    1
+2.100000E18  -1.000000E00
+0.000000E00
! Arrhenius coefficients
r5b:H+O2+M1=HO2+M1
1 2
(1, 1, 6)    1
(1, 1, 3)    1
(1, 1, 2)    1
+6.275937E20  -1.659502E00
+2.142224E02
r6f:H+2O2=HO2+O2
2 2
! Number of reactant species / product
species
(1, 1, 3)    1
! Reactant species index and
stoichiometric coefficent
(1, 1, 2)    2
! Reactant species index and
stoichiometric coefficent
(1, 1, 6)    1
(1, 1, 2)    1
+6.700000E19  -1.420000E00
+0.000000E00
! Arrhenius coefficients
r6b:H+2O2=HO2+O2
2 2
(1, 1, 6)    1
(1, 1, 2)    1
(1, 1, 3)    1
(1, 1, 2)    2
+2.002323E22  -2.079502E00
+2.142224E02
r7f:H+O2+N2=HO2+N2
3 2
! Number of reactant species / product
species
(1, 1, 3)    1
! Reactant species index and
stoichiometric coefficent
(1, 1, 2)    1
! Reactant species index and
stoichiometric coefficent
(1, 1, 9)    1
! Reactant species index and
stoichiometric coefficent
(1, 1, 6)    1
(1, 1, 9)    1
+6.700000E19  -1.420000E00
+0.000000E00
! Arrhenius coefficients
r7b:H+O2+N2=HO2+N2
2 3
(1, 1, 6)    1
(1, 1, 9)    1
(1, 1, 3)    1
(1, 1, 2)    1
(1, 1, 9)    1
+2.002323E22  -2.079502E00
+2.142224E02
r8f:OH+HO2=H2O+O2
2 2
! Number of reactant species / product
species
(1, 1, 5)    1
! Reactant species index and
stoichiometric coefficent
(1, 1, 6)    1
! Reactant species index and
stoichiometric coefficent
(1, 1, 7)    1
(1, 1, 2)    1
+5.000000E13  +0.000000E00
+4.184000E00
! Arrhenius coefficients
r8b:OH+HO2=H2O+O2
2 2
(1, 1, 7)    1
(1, 1, 2)    1
(1, 1, 5)    1
(1, 1, 6)    1
+4.032871E14  +7.798494E-02
+2.972482E02
r9f:H+HO2=2OH
2 1
! Number of reactant species / product
species
(1, 1, 3)    1
! Reactant species index and
stoichiometric coefficent
(1, 1, 6)    1
! Reactant species index and
stoichiometric coefficent
(1, 1, 5)    2
+2.500000E14  +0.000000E00
+7.949600E00
! Arrhenius coefficients
r9b:H+HO2=2OH
1 2
(1, 1, 5)    2
(1, 1, 3)    1
```

```
(1, 1, 6)    1
+3.866511E10  +7.930199E-01
+1.544291E02
r10f:O+HO2=O2+OH
2 2
! Number of reactant species / product
species
(1, 1, 4)   1
! Reactant species index and
stoichiometric coefficent
(1, 1, 6)   1
! Reactant species index and
stoichiometric coefficent
(1, 1, 2)   1
(1, 1, 5)   1
+4.800000E13  +0.000000E00
+4.184000E00
! Arrhenius coefficients
r10b:O+HO2=O2+OH
2 2
(1, 1, 2)    1
(1, 1, 5)    1
(1, 1, 4)    1
(1, 1, 6)    1
+2.211958E12  +4.188524E-01
+2.221450E02
r11f:2OH=O+H2O
1 2
! Number of reactant species / product
species
(1, 1, 5)   2
! Reactant species index and
stoichiometric coefficent
(1, 1, 4)   1
(1, 1, 7)   1
+6.000000E08  +1.300000E00
+0.000000E00
! Arrhenius coefficients
r11b:2OH=O+H2O
2 1
(1, 1, 4)    1
(1, 1, 7)    1
(1, 1, 5)    2
+1.050171E11  +9.591325E-01
+7.510315E01
r12f:H2+M2=2H+M2
1 1
! Number of reactant species / product
species
(1, 1, 1)   1
! Reactant species index and
stoichiometric coefficent
(1, 1, 3)   2
+2.230000E12  +5.000000E-01
+3.874384E02
! Arrhenius coefficients
r12b:H2+M2=2H+M2
1 1
(1, 1, 3)    2
(1, 1, 1)    1
+6.309819E10  +7.541591E-01  -
5.301452E01
r13f:O2+M=2O+M
1 1
! Number of reactant species / product
species
(1, 1, 2)   1
! Reactant species index and
stoichiometric coefficent
(1, 1, 4)   2
+1.850000E11  +5.000000E-01
+3.998230E02
! Arrhenius coefficients
r13b:O2+M=2O+M
1 1
(1, 1, 4)    2
(1, 1, 2)    1
+4.508381E07  +1.114817E00  -
1.038420E02
r14f:H+OH+M3=H2O+M3
2 1
! Number of reactant species / product
species
(1, 1, 3)   1
! Reactant species index and
stoichiometric coefficent
(1, 1, 5)   1
! Reactant species index and
stoichiometric coefficent
(1, 1, 7)   1
+7.500000E23  -2.600000E00
+0.000000E00
! Arrhenius coefficients
r14b:H+OH+M3=H2O+M3
1 2
(1, 1, 7)    1
(1, 1, 3)    1
(1, 1, 5)    1
+1.807860E27  -3.181517E00
+5.072866E02
r15f:H+HO2=H2+O2
2 2
! Number of reactant species / product
species
(1, 1, 3)   1
! Reactant species index and
stoichiometric coefficent
(1, 1, 6)   1
! Reactant species index and
stoichiometric coefficent
(1, 1, 1)   1
(1, 1, 2)   1
+2.500000E13  +0.000000E00
+2.928800E00
! Arrhenius coefficients
r15b:H+HO2=H2+O2
2 2
(1, 1, 1)    1
(1, 1, 2)    1
(1, 1, 3)    1
(1, 1, 6)    1
+2.956437E12  +4.053425E-01
+2.291593E02
r16f:2HO2=H2O2+O2
1 2
! Number of reactant species / product
species
(1, 1, 6)   2
! Reactant species index and
stoichiometric coefficent
(1, 1, 8)   1
(1, 1, 2)   1
```

```
+2.000000E12  +0.000000E00
+0.000000E00
! Arrhenius coefficients
r16b:2HO2=H2O2+O2
2 1
(1, 1, 8)    1
(1, 1, 2)    1
(1, 1, 6)    2
+5.131339E13  -1.775678E-01
+1.553091E02
r17f:H2O2+M=2OH+M
1 1
! Number of reactant species / product
species
(1, 1, 8)   1
! Reactant species index and
stoichiometric coefficent
(1, 1, 5)   2
+1.300000E17  +0.000000E00
+1.903720E02
! Arrhenius coefficients
r17b:H2O2+M=2OH+M
1 1
(1, 1, 5)    2
(1, 1, 8)    1
+2.622180E09  +1.630089E00  -
3.268004E01
r18f:H2O2+H=HO2+H2
2 2
! Number of reactant species / product
species
(1, 1, 8)   1
! Reactant species index and
stoichiometric coefficent
(1, 1, 3)   1
! Reactant species index and
stoichiometric coefficent
(1, 1, 6)   1
(1, 1, 1)   1
+1.600000E12  +0.000000E00
+1.589920E01
! Arrhenius coefficients
r18b:H2O2+H=HO2+H2
2 2
(1, 1, 6)    1
(1, 1, 1)    1
(1, 1, 8)    1
(1, 1, 3)    1
+7.374760E09  +5.829103E-01
+8.682062E01
r19f:H2O2+OH=H2O+HO2
2 2
! Number of reactant species / product
species
(1, 1, 8)   1
! Reactant species index and
stoichiometric coefficent
(1, 1, 5)   1
! Reactant species index and
stoichiometric coefficent
(1, 1, 7)   1
(1, 1, 6)   1
+1.000000E13  +0.000000E00
+7.531200E00
! Arrhenius coefficients
r19b:H2O2+OH=H2O+HO2
2 2
(1, 1, 7)    1
(1, 1, 6)    1
(1, 1, 8)    1
(1, 1, 5)    1
+3.143718E12  +2.555527E-01
+1.452863E02
19
! Reverse reactions list1 2 3 4 5 6 7 8
9 10 11 12 13 14 15 16 17 18 19 20 21
22 23 24 25 26 27 28 29 30 31 32 33 34
35 36 37 38 0
! Number of FORD/RORD reactions
 4
! Number of third body species
M3
1
(1, 1, 7)    20
M2
3
(1, 1, 3)    2
(1, 1, 1)    3
(1, 1, 7)    6
M1
4
(1, 1, 1)    3.3
(1, 1, 9)    0.0
(1, 1, 7)    21
(1, 1, 2)    0.0
M
0
 10
! Number of third body reactions
9   (1,1,3)
10   (1,1,3)
23   (1,1,2)
24   (1,1,2)
25   (1,1,4)
26   (1,1,4)
27   (1,1,1)
28   (1,1,1)
33   (1,1,4)
34   (1,1,4)
 0
! Pressure dependent reactions
```